



Mechanical, Materials and Aerospace Engineering Department  
Illinois Institute of Technology  
3300 South State Street  
Chicago, Illinois

*Master's Comprehensive Thesis Defense*

May 12<sup>th</sup>, 2003

10 A.M.

Steve Talbot



# Hot Tensile Ductility Testing of a Modified 410 Stainless Steel and the Effects of Varying Sulfur Content on Workability

Mr. Bill Michaud  
*Scot Forge*

Dr. Philip Nash  
*Thermal Processing Technology Center*



# Background

- **Objective.**
  - Determine the effect of sulfur content in 2 separate batches of a modified 410 Stainless Steel.
- **Strategy.**
  - Hot ductility tensile tests in Gleeble 3500 thermo-mechanical tester.
  - Data analysis with percent reduction in area (%RA) and true strain-at-fracture ( $\epsilon_f$ ) values.
  - Sample analysis with L.O.M., S.E.M. and E.D.S.
- **Tensile Samples.**
  - Material donated by Scot Forge.
  - Sample produced in IIT machine shop and at Scot Forge to modified Gleeble 3500 specifications.
  - Over 120 samples tested.

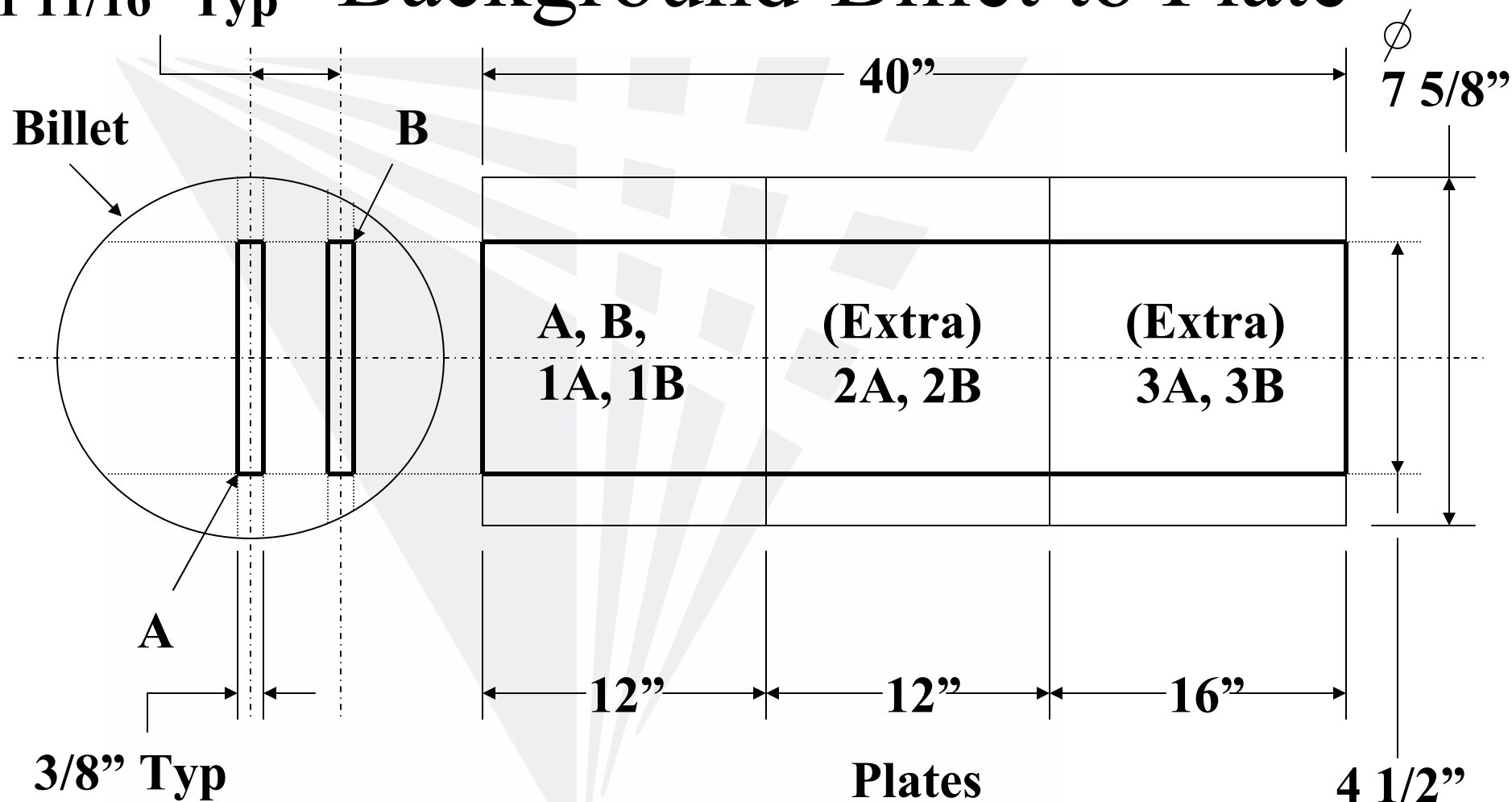
# Background-Nominal Chemistry

- Batch 1: Higher sulfur content: 1A, 2A, 3A & 1B, 2B, 3B

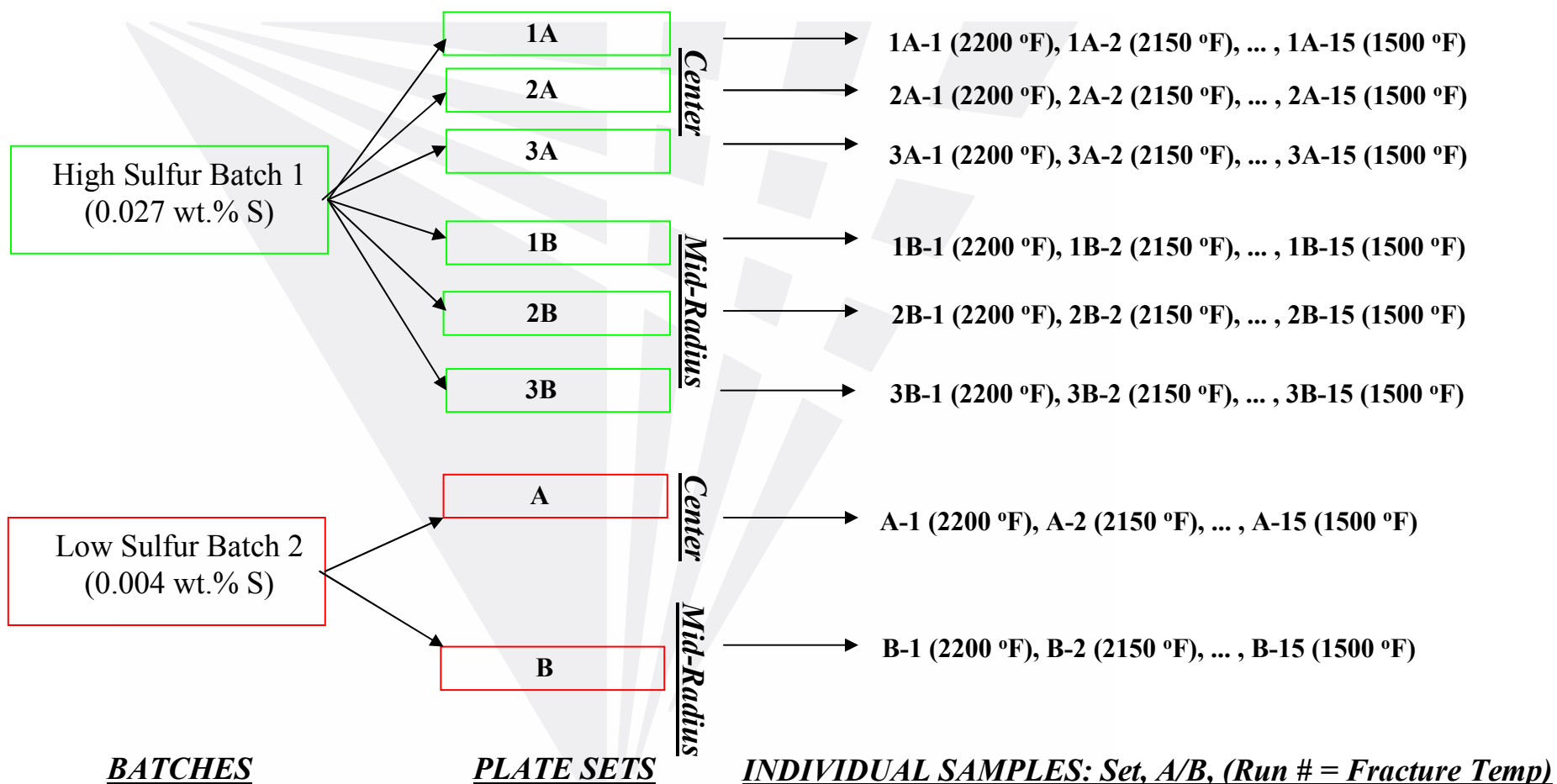
Batch	Plate Location	Heat #	Chemistry										
			C	Mn	P	S	SI	NI	CR	MO	CU	AL	V
			[%]	[%]	[%]	[%]	[%]	[%]	[%]	[%]	[%]	[%]	[%]
1	1A Center	Heat H6975	0.13	0.85	0.017	0.027	0.320	0.37	11.57	0.04	0.07	0.019	0.010
	2A Center												
	3A Center												
	1B Mid Radius												
	2B Mid Radius												
	3B Mid Radius												
2	A Center	Heat K1949	0.14	0.94	0.012	0.004	0.180	0.47	12.05	0.05	0.11	0.010	0.044
	B Mid Radius												

- Batch 2 : Lower sulfur content: A & B

# 1 11/16" Typ Background-Billet to Plate



# Background-Sample Numbering



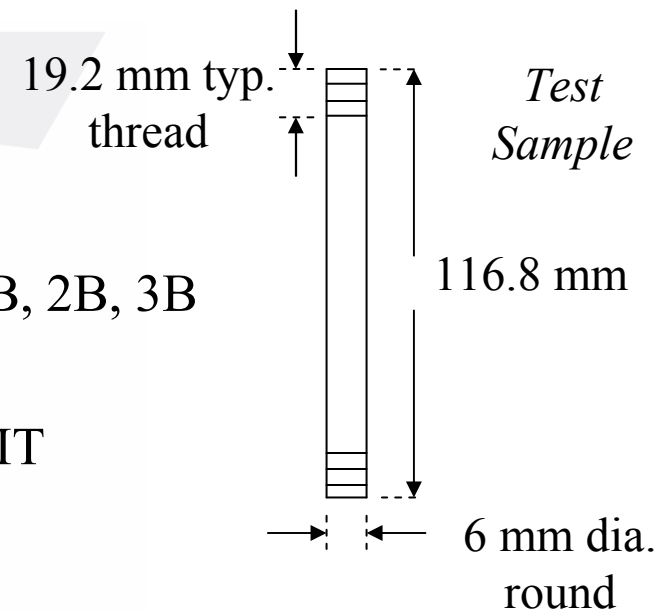
# Background-Sample Numbering

- **Batch 1:**

- The first batch of material to arrive at IIT
- Higher sulfur content: 0.027 wt.% Sulfur
- Each batch set labeled: 1A, 2A, 3A and 1B, 2B, 3B

- **Batch 2 :**

- The second batch of material to arrive at IIT
- Lower sulfur content: 0.004 wt.% Sulfur
- Each batch set labeled: A and B



- 1<sup>st</sup> digit: 1, 2, 3 = 1<sup>st</sup>, 2<sup>nd</sup> or 3<sup>rd</sup> set in a plate
- Nothing = only one set in a plate
- 2<sup>nd</sup> digit: A = Center
- B = Mid Radius
- 3<sup>rd</sup> digit: 1..15 = Run Number  
(1 = 2200 °F .. 15 = 1500 °F test temps.)

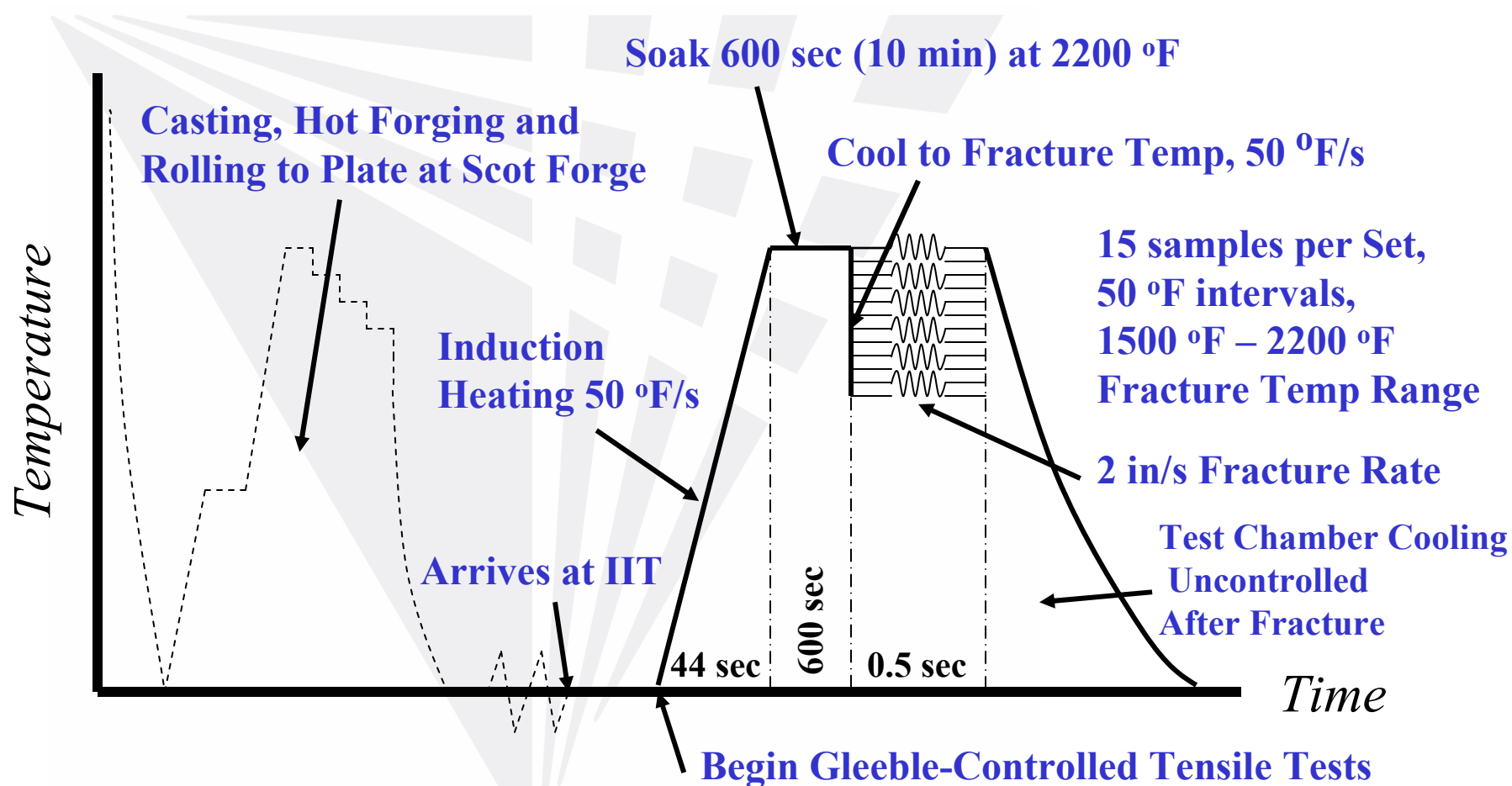
- **Examples:**

**2A-5** 2<sup>nd</sup> set, Center, Run 5, batch 1

**2B-1** 2<sup>nd</sup> set, Mid Rad, Run 1, batch 1

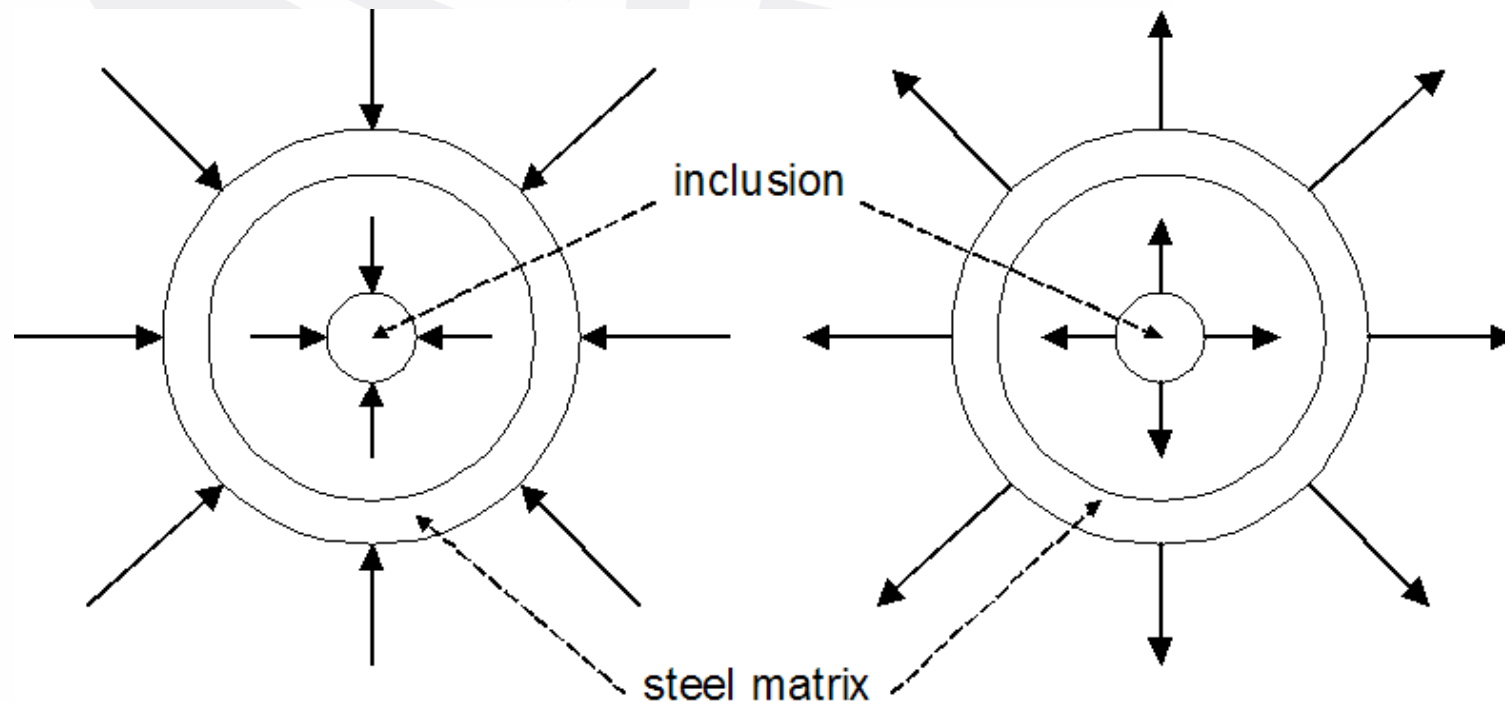
**B-4** only set, Mid Rad, Run 4, batch 2

# Background-Thermal History



# Inclusion Properties

- **Coefficient of Thermal Expansion (CTE) helps determine the effect of heating and cooling at the inclusion-matrix interface.**



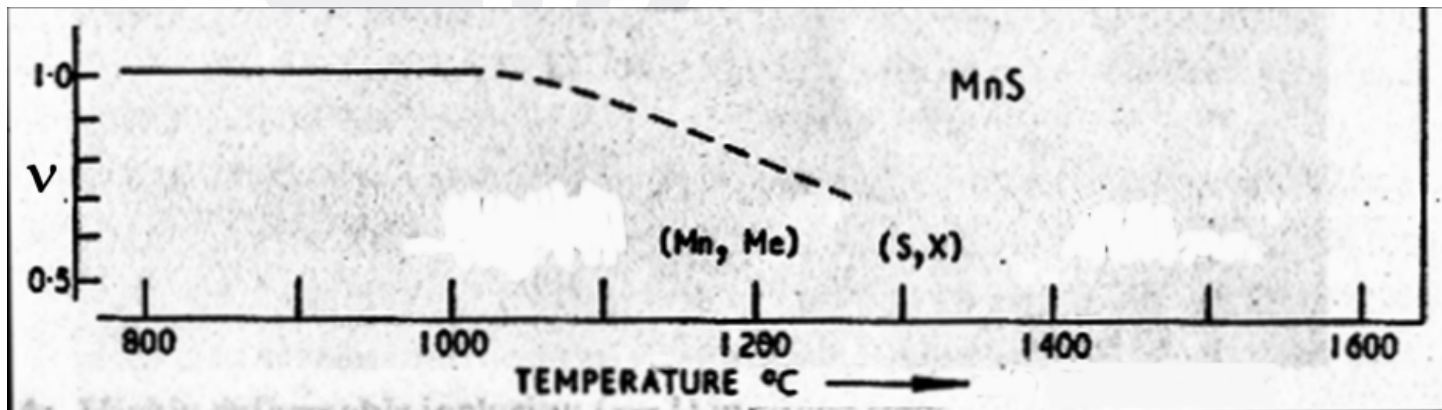
Cooling Direction (contraction)

Heating Direction (expansion)

# Inclusion Properties

- “ $v$ ” is the “index of deformation,” the relative plasticity between inclusion and matrix, or the ratio of inclusion strain to matrix strain.
  - For MnS, “ $v$ ” = 1 (inclusion deforms with matrix) for  $T < 1000\text{ }^{\circ}\text{C}$
  - For MnS, “ $v$ ” = 0 (inclusion rigid) for  $T > 1000\text{ }^{\circ}\text{C}$
  - Sulfide relative plasticity was said to increase with cooling rate of solidification and also with iron content. [12]
  - Cr and Fe solid solutioning may reduce sulfide plasticity. Also, both are said to increase MnS R.T. microhardness 2X. [12]

$$v = \frac{2}{3} \cdot \frac{\ln \varepsilon_i}{\ln \varepsilon_m}$$





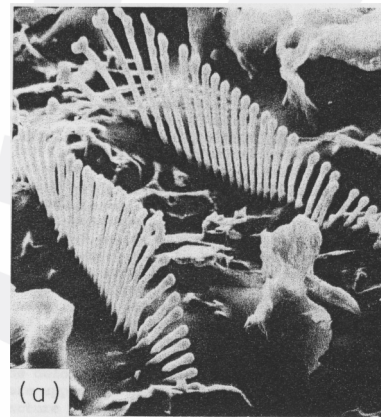
# Inclusion Properties

- **Sulfide Formation and Orientation.**
  - Sulfides and oxysulfides are formed only in the solute-enriched interdendritic liquid, during the solidification of the steel. [32]
  - A reaustenitizing heat treatment was said to cause transfer of sulfur in the interdendritic region into nearby grain boundaries. [32]
  - It is noted that there is a tendency for ingot segregation of inclusions and that following rolling processes, inclusion clusters form as more tightly or densely grouped particles. [15]

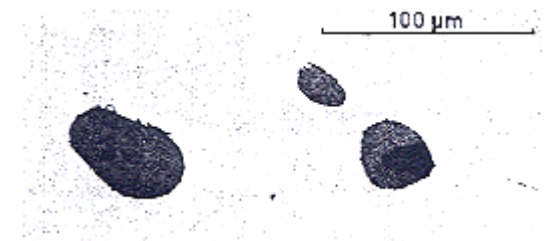
# Inclusion Properties

- **Sulfide Formation and Orientation.**

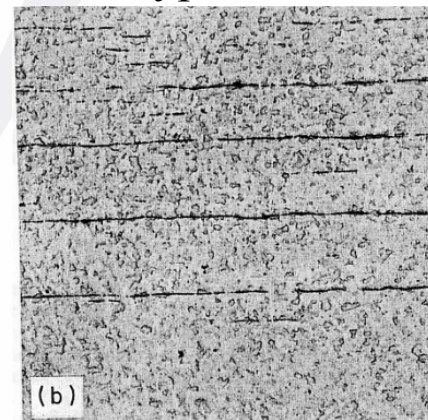
- Type I: Equiaxed (ie: globular or spherical) inclusions that form nearby or are surrounded by other oxide compounds (“Duplex”). It is also called “*intragranular sulfide*.” [37]
- Type II: “Parallel fences constrained to grow between parallel dendrites.” These are “*interdendritic sulfides*,” or “*grain boundary sulfides*.” Found in some fully killed steels where  $[O] < 0.1 \text{ wt.}\%$ .
- Type III: Fully killed steels with  $[O] < 0.1 \text{ wt.}\%$  O and Type II not present. Due to the addition of C, Al, Si and P elements. “*Perfect octahedral*.”



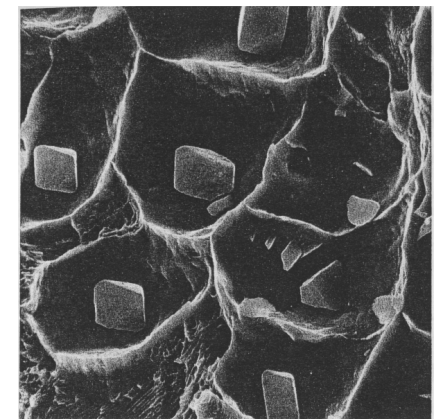
Type II



Type I



Type II



Type III



# Inclusion Properties

- **Sulfide Formation and Orientation.**

- It is said that subsequent hot working following casting further elongates interdendritic “fern-like” stringers, orienting them in the rolling direction into thin sheets of parallel arrays. [15]
- The reorientation of Type II rods to become aligned in a coincident direction with the deformation direction is said to reduce the volume of matrix involved in rupture, presumably when strain in the deformed matrix is transferred to the realigned inclusions (so long as contact between inclusions and matrix is maintained). [2]
- It was said that for deformations of steel below 1200 °F, there is a more rapid reorientation of both the overall network of interdendritic inclusions and of interconnecting inclusion arms than at temperatures above 1200 °F. [2]
- Deformation of steels following inclusion reorientation is said to hurt steel toughness more at deformations temperatures below 1200 °F than above 1200 °F. [2]

# Inclusion Properties

- **Inclusion Solid Solutioning.**

- MnS can have up to 37 wt.% Cr in solution, aiding fragmentation of inclusions into individual particles. [26]
- “During slow cooling, FeS present in the steel could decrease due to solid state diffusion of Mn from matrix to sulfide and Fe from sulfide to matrix.” However, “at high cooling rate solute entrapment during growth of the sulfide could raise [Fe] total.” [12]
- “Steel containing 0.1 wt.% Mn and 0.25 wt.% S, sulfides can form with as much as 35 wt.% FeS.” [12]
- For homogenization following hot rolling of AISI 4340 medium carbon steel plate, sulfides were seen to reject Fe but accepted Mn from the surrounding matrix.
- Additionally, it was said that in tests of Mn surface segregation in Fe-1%Mn at 590, 680 and 760 °C, segregation always occurred with no further dependence on temperature. [19]
- MnS inclusions are therefore expected for inclusions at G.B.s and elevated temperatures.

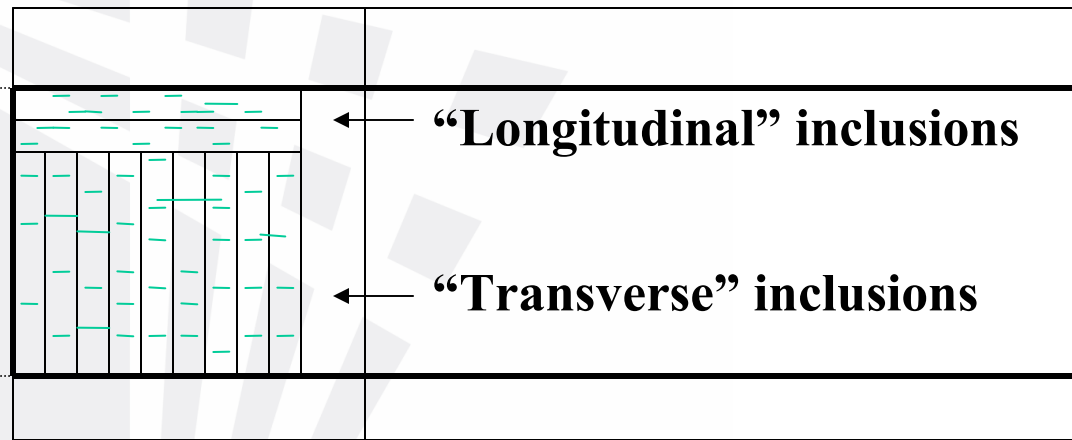
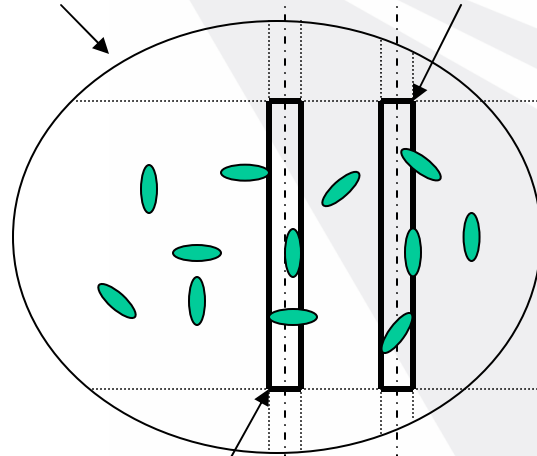
# As-Received Plate

1 11/16" Typ

**Billet**

**B**

- The directionality of inclusion morphology a parameter originally unaccounted for in test sample preparation.



**Rolling Direction (RD)**

- Rolling-to-plate elongated soft inclusions in the RD.
- Some samples were mostly Longitudinal Inclusions
- Remaining samples were mostly Transverse Inclusions

3/8" Typ



# Sample & Plate Orientations

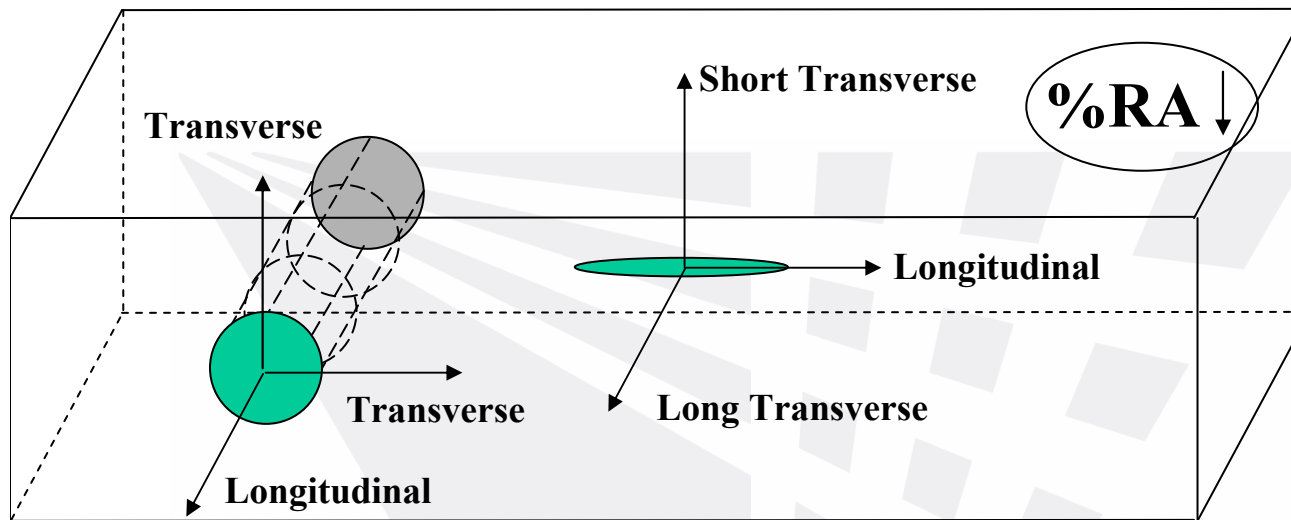
SCOT FORGE



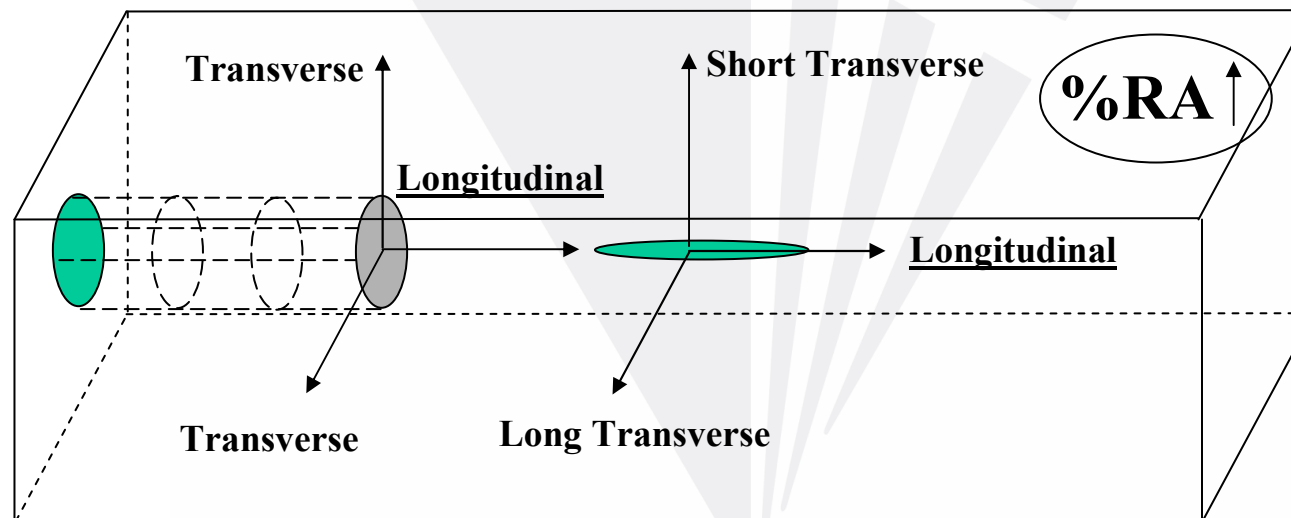
ILLINOIS INSTITUTE  
OF TECHNOLOGY



← **Rolling Direction (RD)** →

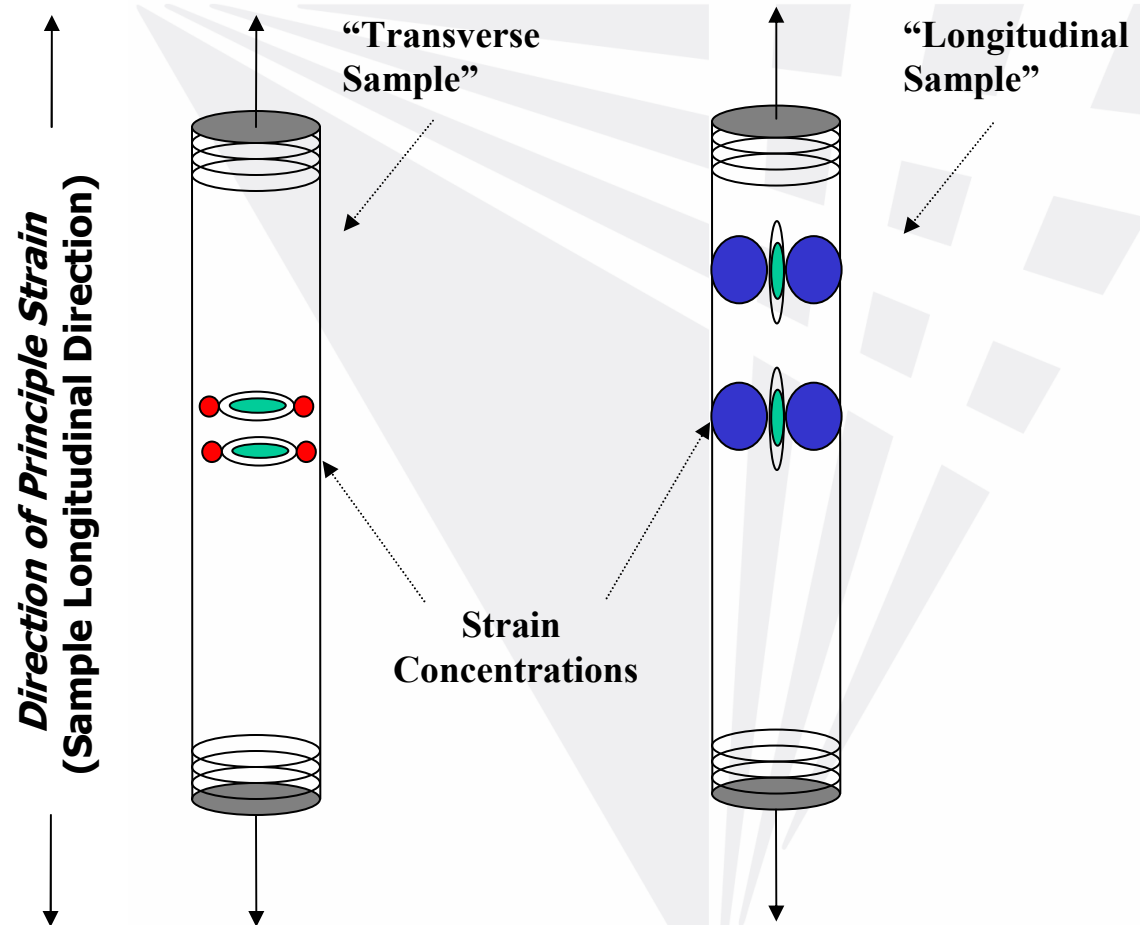


- TOP: Tensile sample and plate coordinate systems opposite.
- TOP: Tensile sample will be less ductile.
- “*Transverse Sample*”



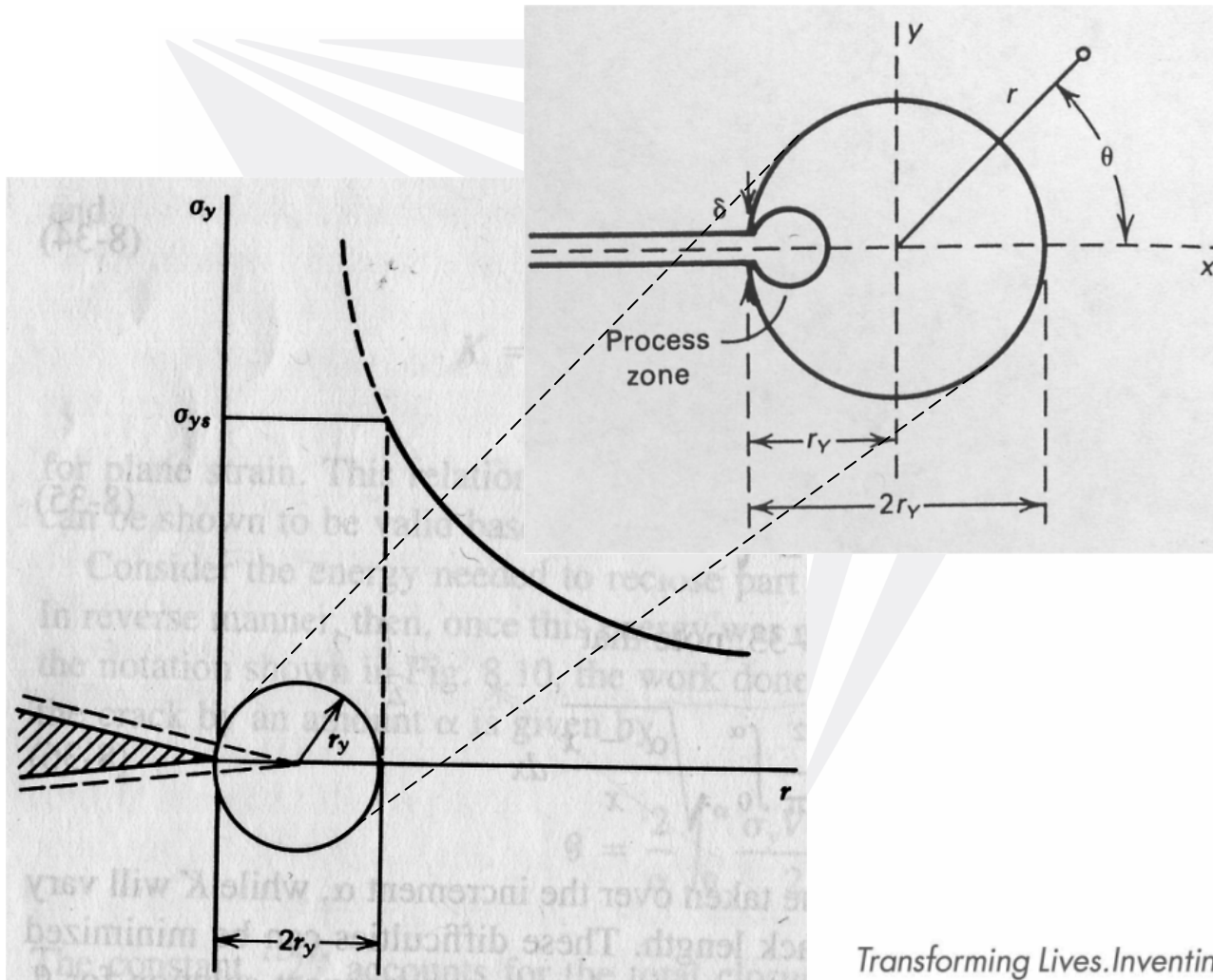
- BOTTOM: Sample and plate coordinate systems coincident.
- BOTTOM: Tensile sample will be more ductile.
- “*Longitudinal Sample*”

# Tensile Sample Void Formation



- Cohesion loss between inclusion and matrix at elevated temperature and strain nucleates voids at inclusions.
- Inclusion clustered-distribution may promote variation in %RA and  $e_f$  values.
- Strain concentrations (s.c.) at sharp cracks and inclusion tips aid sample plastic yielding.

# S.C. and Plastic Zone at Crack Tip



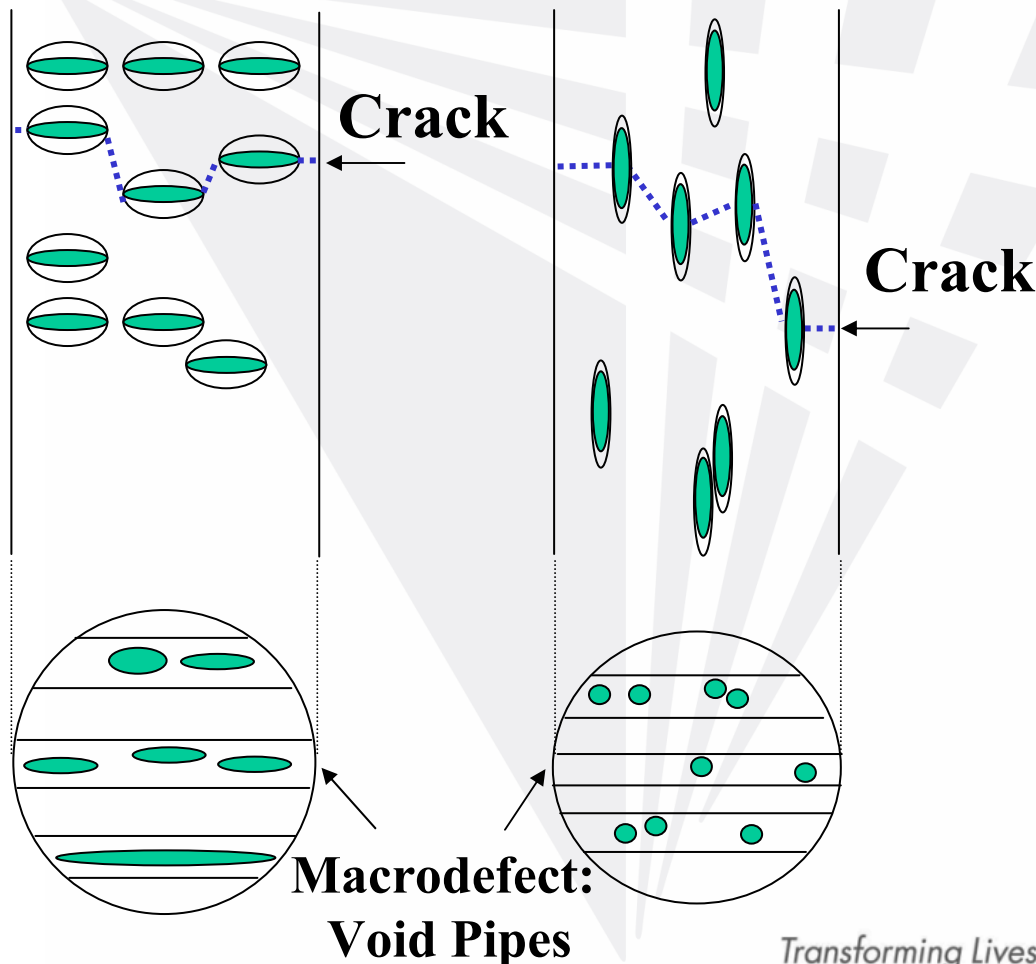
- Voids nucleated at elongated transverse inclusions aided by strain concentrations (s.c.) at crack tips.
- Crack **initiation** and crack **growth** require s.c. + triaxial stress condition at crack tip.
- Stress in process zone elevated to plastic regime.



# Microvoid Coalescence (MVC)

“TRANSVERSE” VOID PIPES

“LONGITUDINAL” VOID PIPES

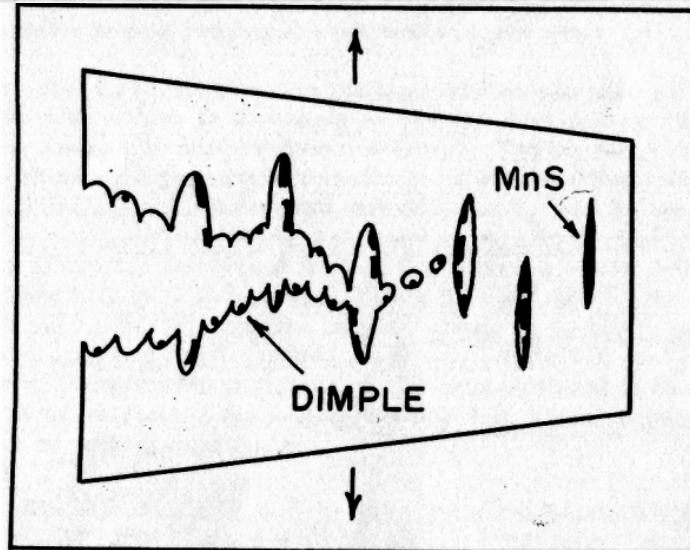
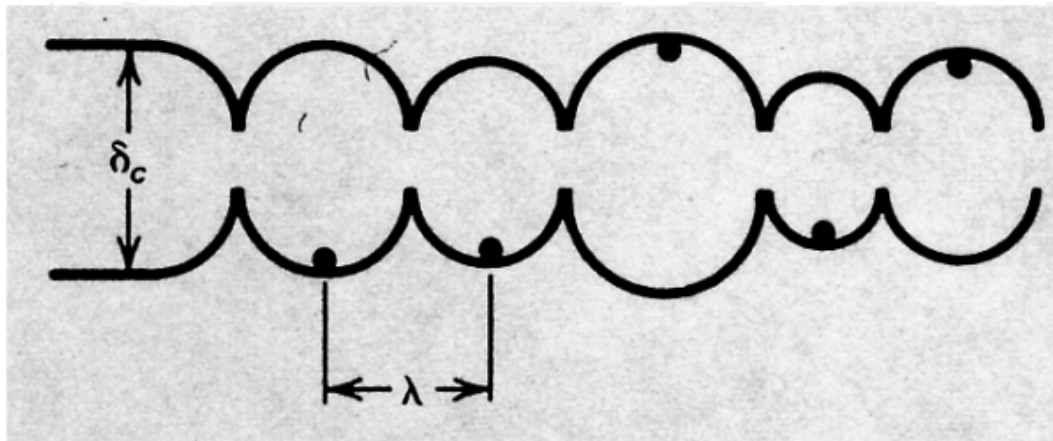


- Array of “Void Pipes” form along pre-existing array of inclusions if inclusion content high enough.

- Stages of MVC:

- Accommodation of plastic deformation around inclusions.
- **Initiation** of cavities.
- **Growth** of cavities.
- Localization of deformation by shearing.
- **Coalescence** of cavities.
- Creation of a macrodefect.
- Propagation of this macrodefect.
- Final fracture of the specimen.

# Microvoid Coalescence (MVC)



- Dimples on fracture surface of samples, formed by voids nucleated on inclusions.
- Longitudinal inclusions connected by propagating crack.
- Inclusions preceding crack are brittle fractured.
- Smaller inclusions between elongated one help propagate crack.

# Grain Boundary Embrittlement

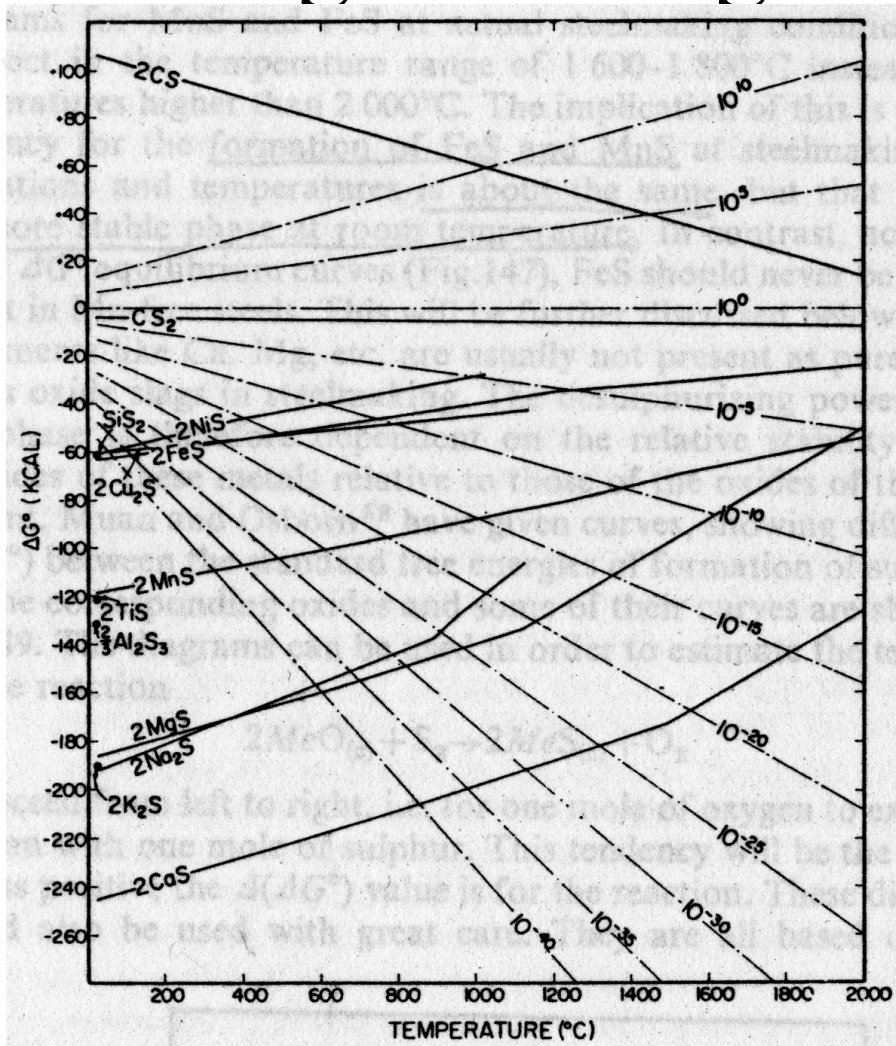
- **Sulfur tends to segregate to prior austenitic grain boundaries, promoted by elevated temperature diffusion.**
  - Sulfides form at grain boundaries (G.B.s) if sulfur content,  $[S]$ , is high.
  - Sulfides form intragranularly if nominal sulfur content,  $[S]$ , is low.
- **Elevated temperatures melt some sulfides at G.B.s, weakening the G.B. cohesive strength.**
- **Sulfur in solid solution pins grains, while both solid and liquid sulfides promote “grain boundary sliding” by weakening the G.B.**
- **Combination of pinning and sliding of the grain is the basis for “Grain Boundary Embrittlement” or “Hot Shortness” of samples.**

# Free Energy of Formation

- Energy required to form a compound depends on the partial pressures of either the solid or the liquid sulfides present.
  - $\Delta G^\circ = RT \ln p_s$
- Tendency of sulfide formation increases with decreasing Free Energy (increasing negative value).
- In order of increasing tendency of sulfide formation:
  - Ni, Fe, V, Nb, Ta, Cu, Mn, Ti, Al, Mg, Na, K, Ca
- When Mn present, MnS forms in preference to FeS.



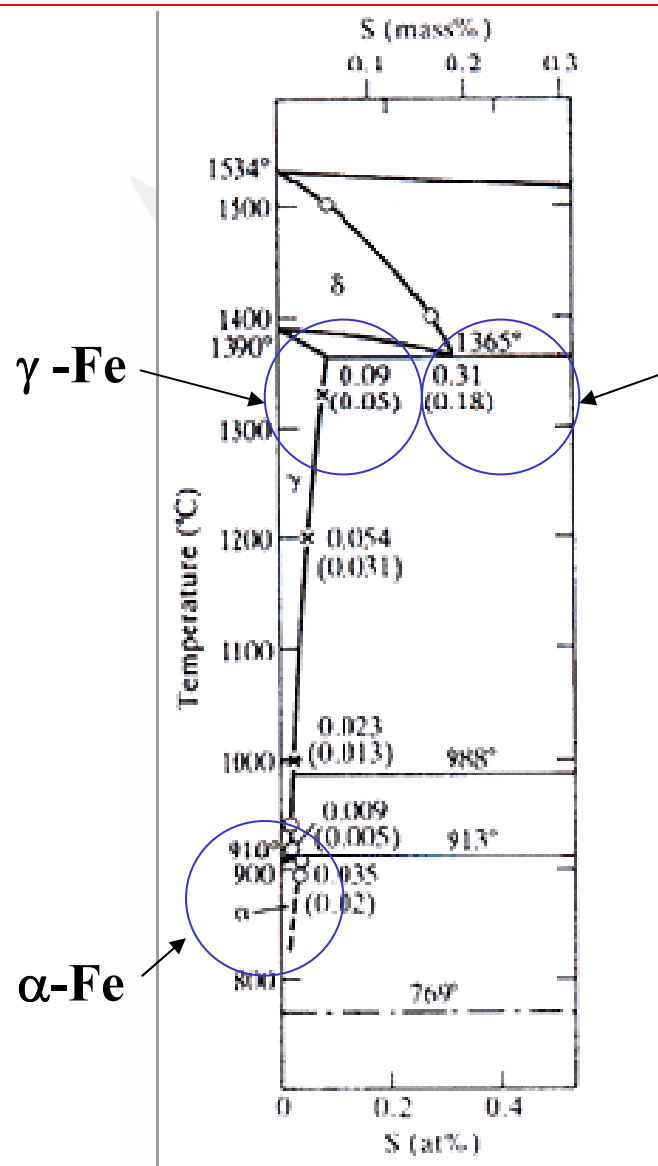
# Ellingham Diagram for Sulfides



- Sulfide stability increases with negative magnitude of  $\Delta G^\circ$ .
- $2CS$ ,  $CS_2$ ,  $2NiS$ ,  $SiS_2$ ,  $2FeS$ ,  $2Cu_2S$ ,  $2MnS$ ,  $2TiS$ ,  $\frac{2}{3}Al_2S_3$ ,  $2MgS$ ,  $2Na_2S$ ,  $2K_2S$ ,  $2CaS$ .
- $2MnS$  more stable than  $2FeS$ .
- $2CaS$  more stable than  $MnS$ , used to globularize elongated  $MnS$ .
- Non-metallic Inclusions in Steel, 1968, vol. II, sec. J, p.98

# Melting Temperatures

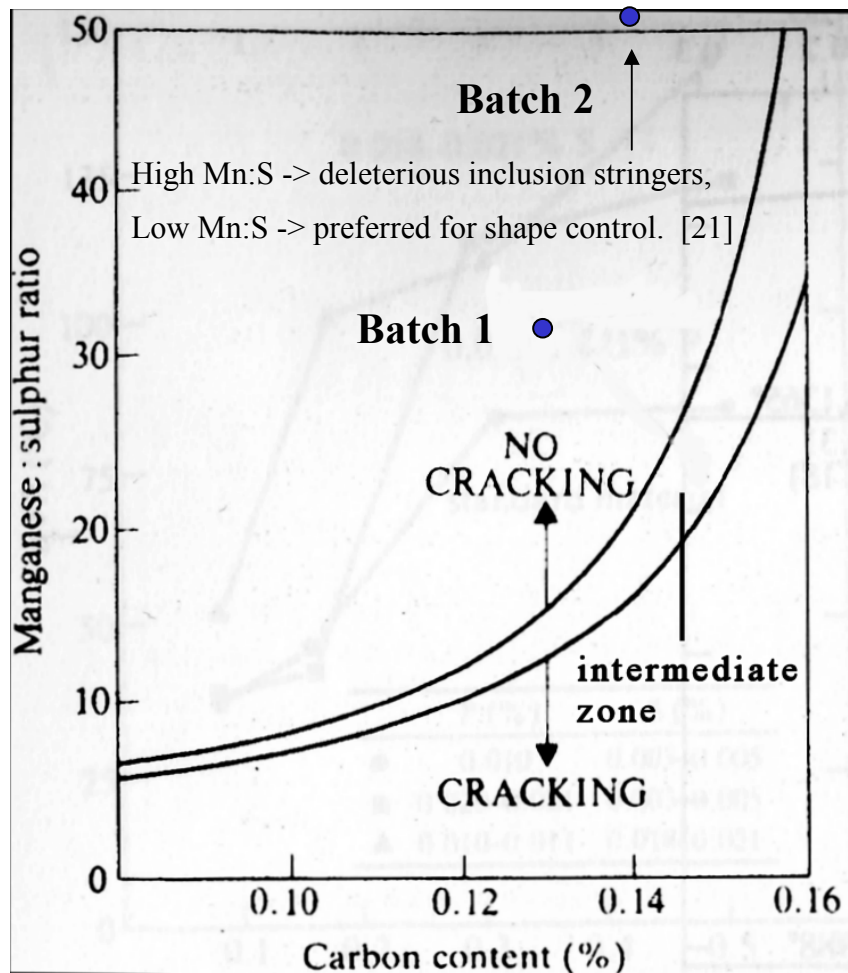
- Pure Fe melts at about 1534 °C.
- FeS melting point is lower than both pure Fe and MnS, down to minimum at the 32 wt.% S eutectic melting temperature of 988 °C.
- MnS melting point higher than pure Fe, at 1610 °C.
- At elevated temperatures, FeS inclusions are expected to melt and embrittle steel, while MnS inclusions remain solid.
- This is the primary reason for designing steel with MnS rather than FeS inclusions.



# Sulfur Solubility

- Maximum solubility of sulfur in  $\alpha$ -Fe (**Ferrite**): 0.035 wt.% Sulfur
- Maximum solubility of sulfur in  $\gamma$ -Fe (**Austenite**): 0.090 wt.% Sulfur
- Maximum solubility of sulfur in  $\delta$ -Fe (**Delta Ferrite**): 0.310 wt.% Sulfur
- Hot Workability testing is in  $\gamma$ -Fe range.
- 0.027 wt.% S should be in solution for  $\gamma$ -Fe, but higher C in steel would aid sulfide embrittlement (see next slide).
- Metallurgy of Welding, 1999, p. 224

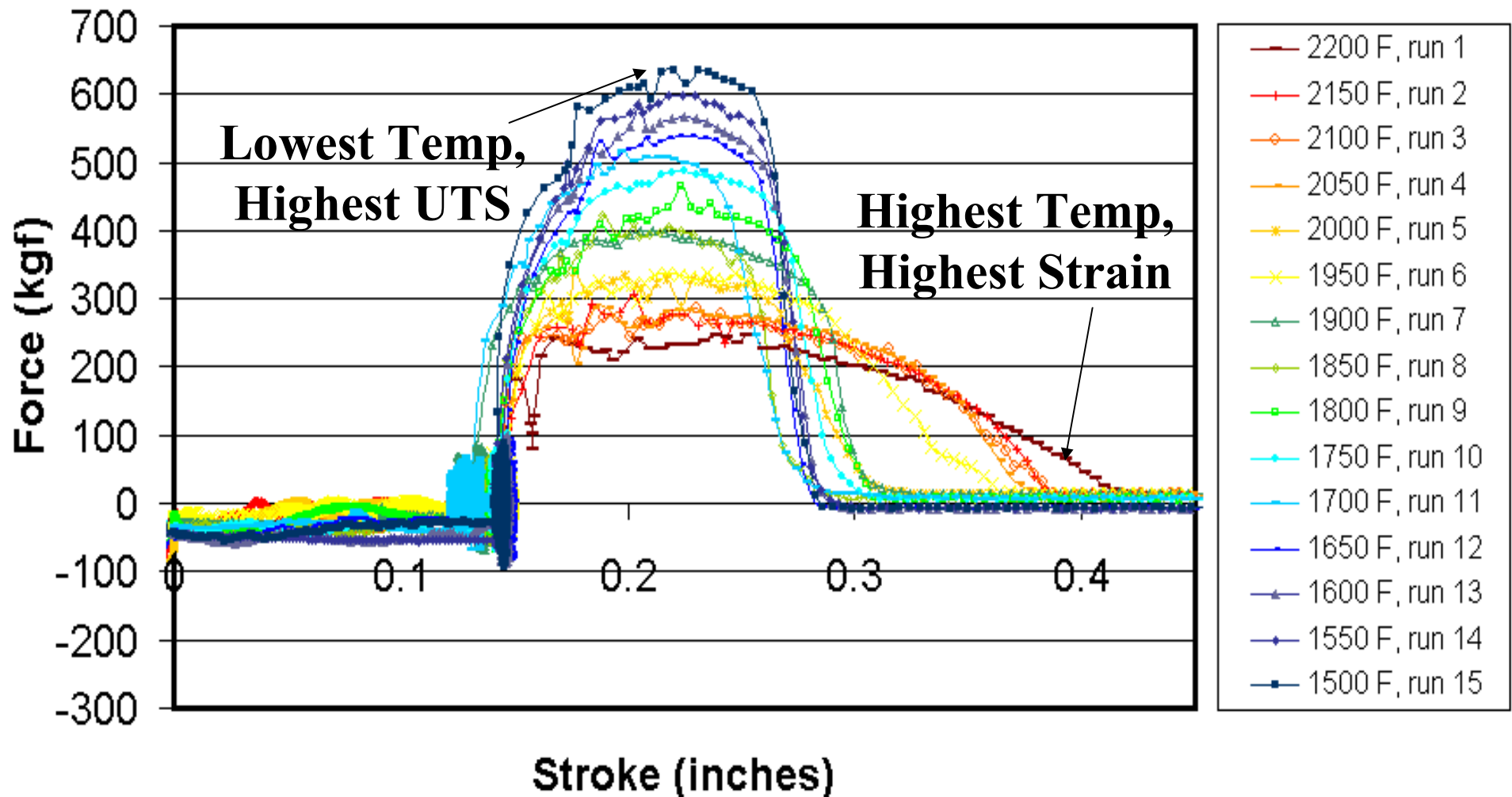
# Mn Concentration & Mn:S Ratio



- Mn Concentration required to prevent FeS embrittlement:
  - $(\%Mn) = 1.25(\%S) + 0.03$
- Batch 1: 1A, 2A, 1B, 2B
  - Nominal:  $[\%Mn] = 0.89$ , Needed to prevent embrittlement:  $[\%Mn] = 0.064$
  - Mn:S = 31.5,  $[\%C] = 0.13$  wt. %
- Batch 2: A, B
  - Nominal:  $[\%Mn] = 0.94$ , Needed to prevent embrittlement:  $[\%Mn] = 0.035$
  - Mn:S = 235,  $[\%C] = 0.14$  wt. %
- Both batches are in “no cracking” zone.
- Metallurgy of Welding, 1999, p. 223



## Force vs Stroke, Heat 2A Center, Batch 1



- 1900 °F, highest temp with  $\Delta$  stroke  $\sim 0.3$  max.
- 1950 °F, transition to higher  $\Delta$  stroke max.
- This transition is the beginning of the contribution of grain boundary sliding to elevated temperature assisted plasticity.

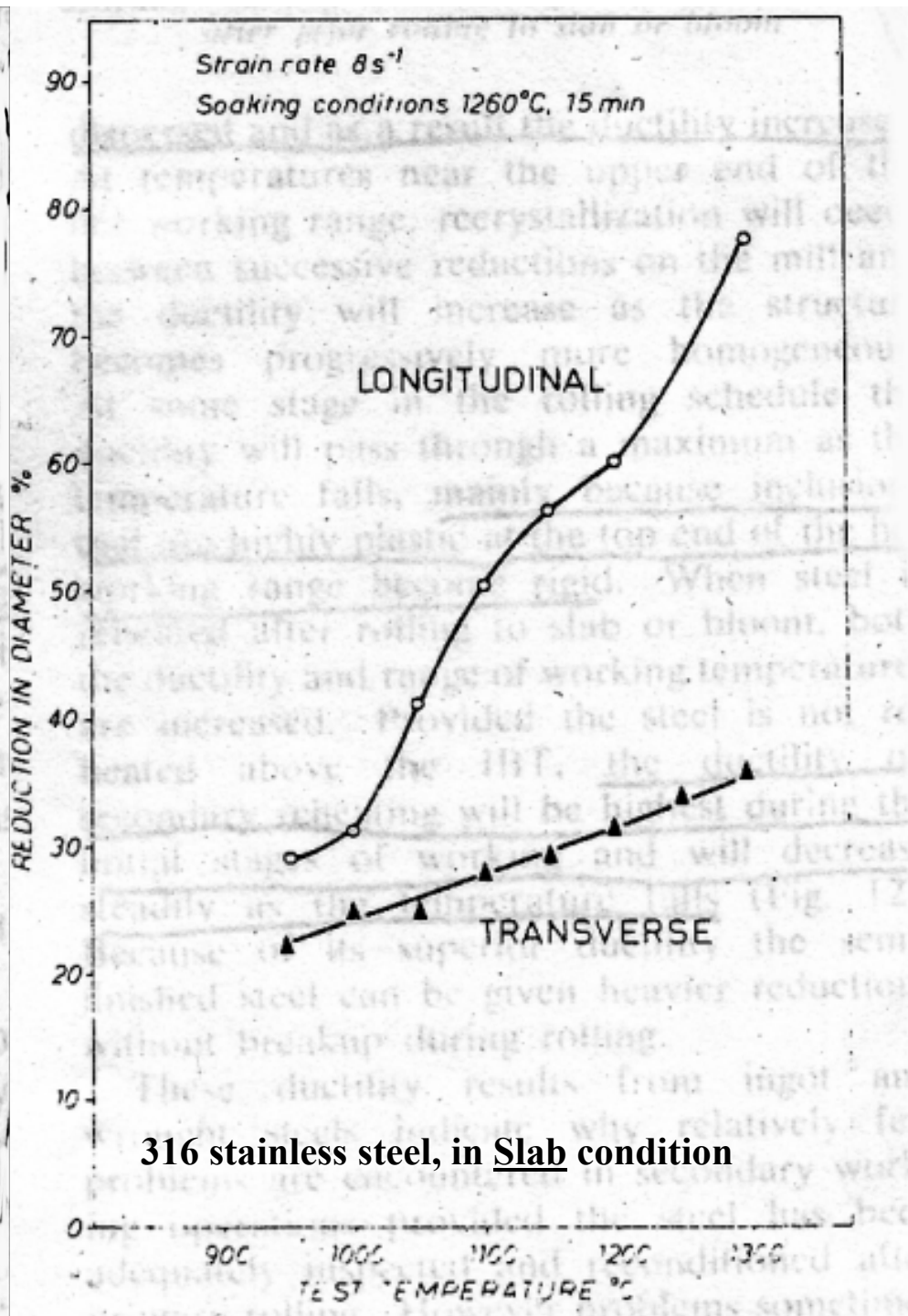
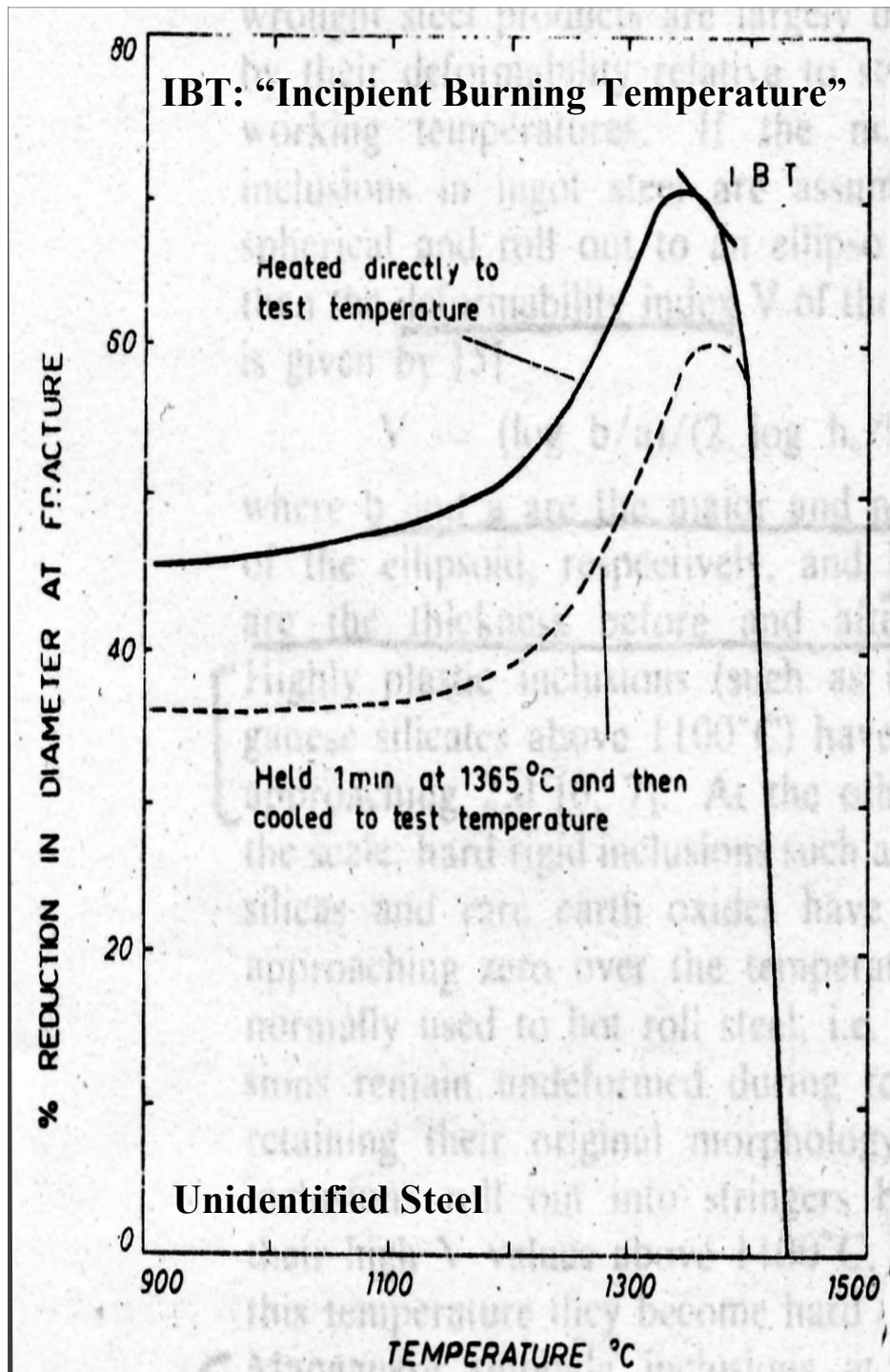
## %RA and $\epsilon_f$

- Examination in trends of:

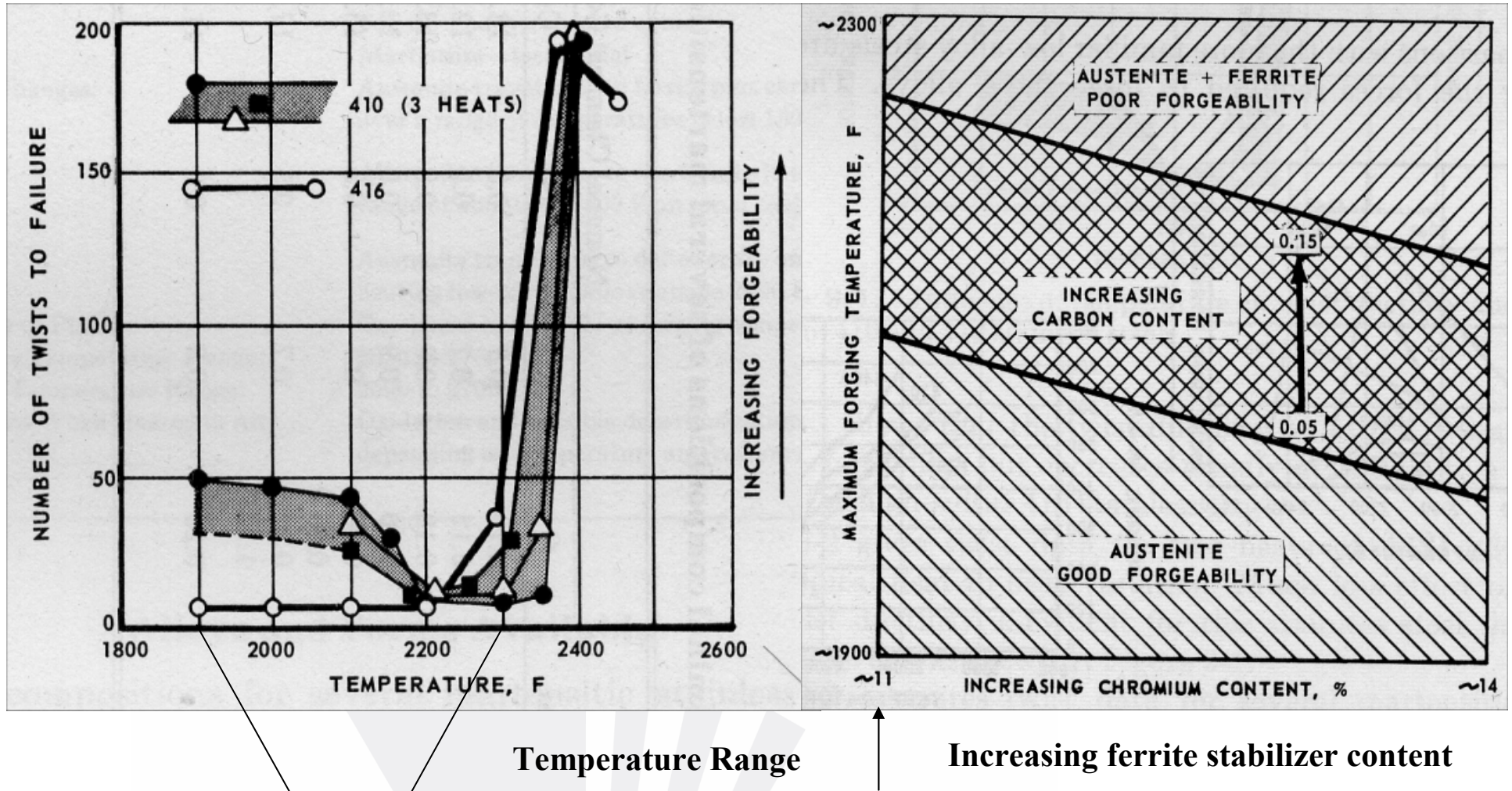
**% Reduction in Area (%RA) and True Strain at Fracture ( $\epsilon_f$ )  
vs. Fracture Temperature (°F)**

$$\%R.A. = \left( \frac{A_o - A_f}{A_o} \right) \bullet 100\% \quad \epsilon_f = \ln \left( \frac{l}{l_0} \right) = \ln \left( \frac{A_o}{A_f} \right)$$

- Sulfur content influence (Batch 1 vs Batch 2).
- Concentration gradient influence (Center vs Mid Radius).
- Inclusion morphology influence (Longitudinal vs Transverse).

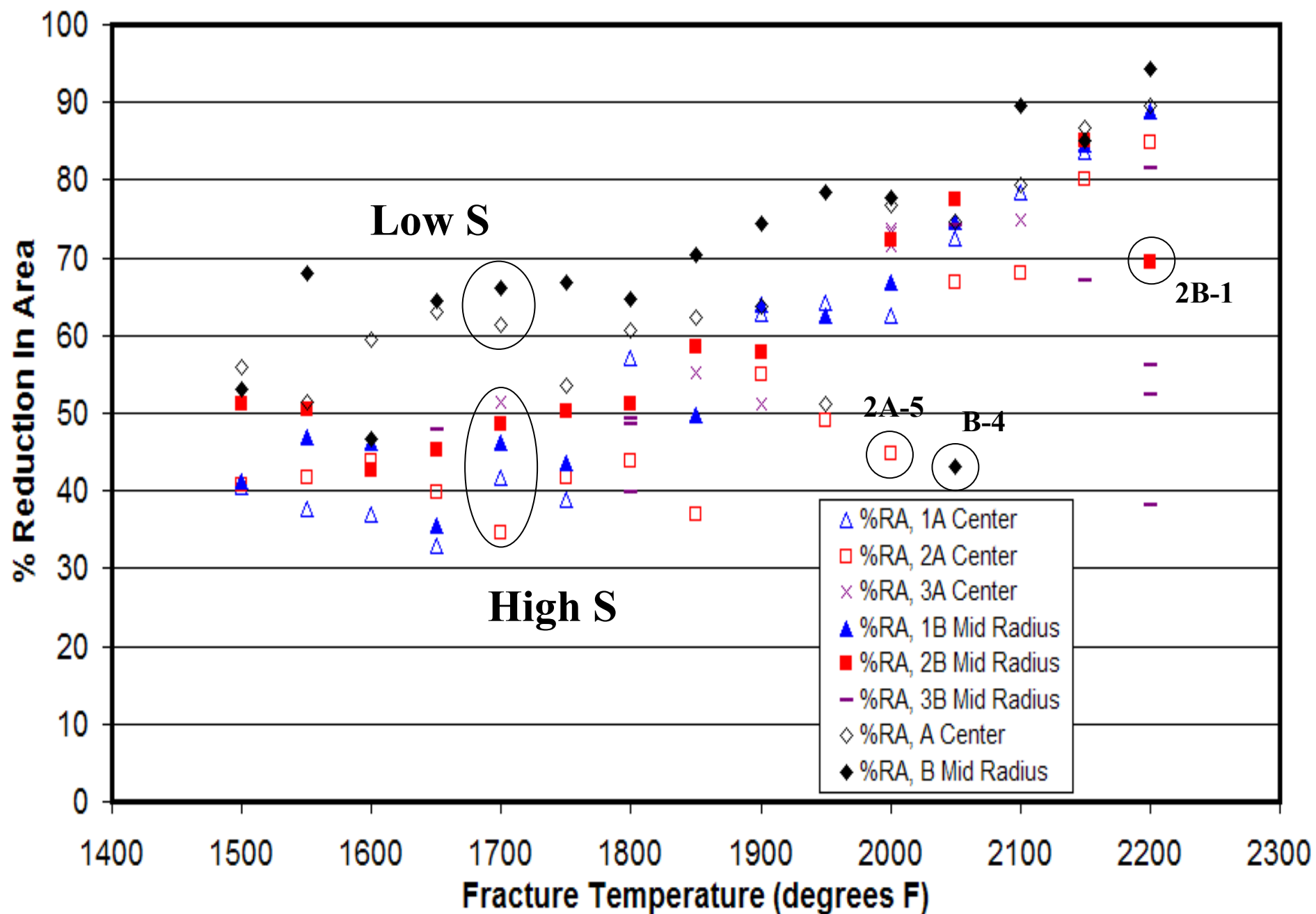




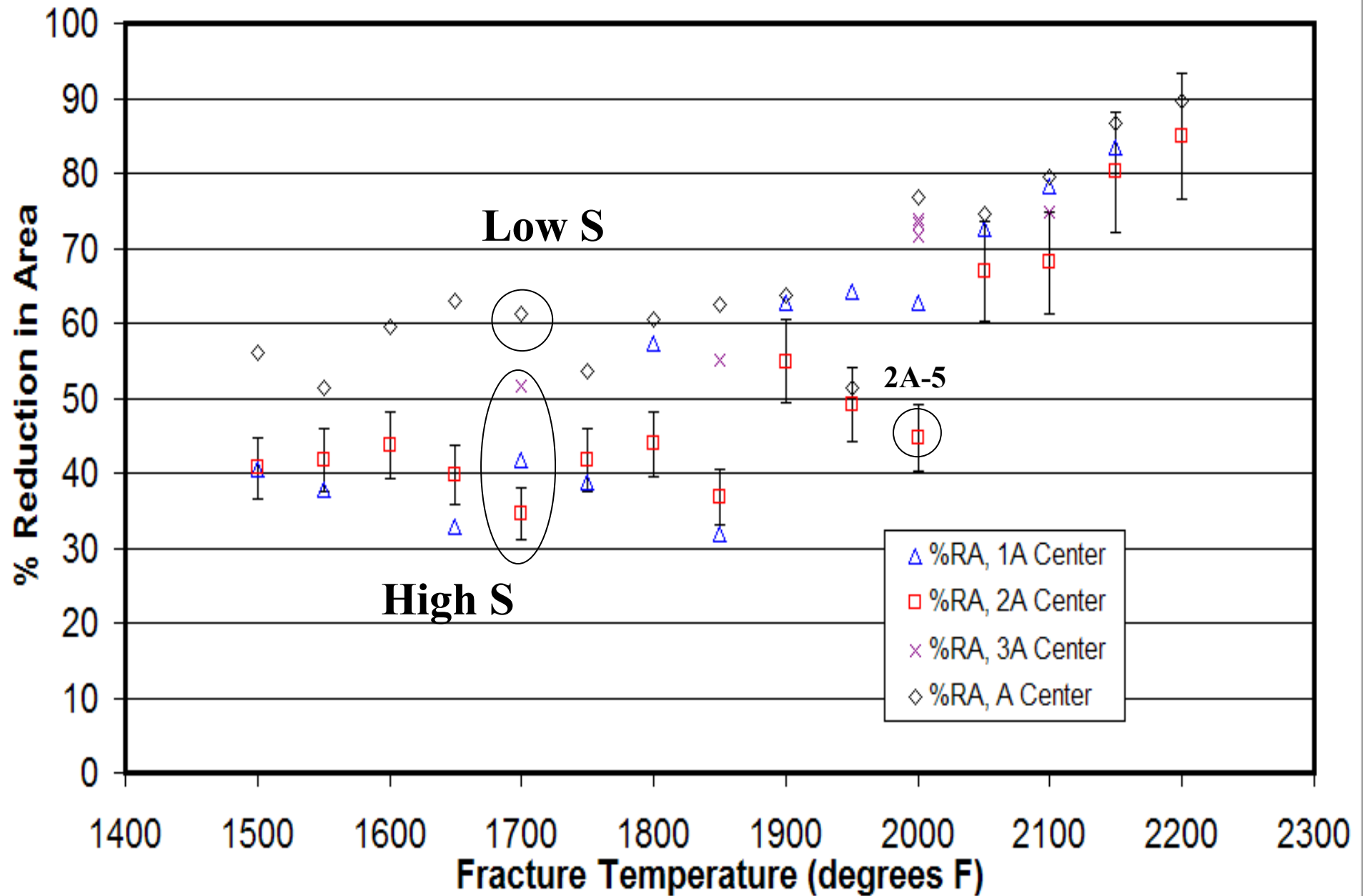


- Austenite ( $\gamma$ -Fe) to Delta Ferrite ( $\delta$ -Fe) transition said to be partially responsible for loss of billet forgeability and subsequent plate rolling processes at hot working temperatures.
- 410 ductility loss said to result in ductility comparable to high sulfur 416 steel.
- Boulger, F.W., Henning, H.J., Sabroff, A.M., Forging Materials and Practices, pp. 206-209, Reinhold Book Corporation, New York, 1968.

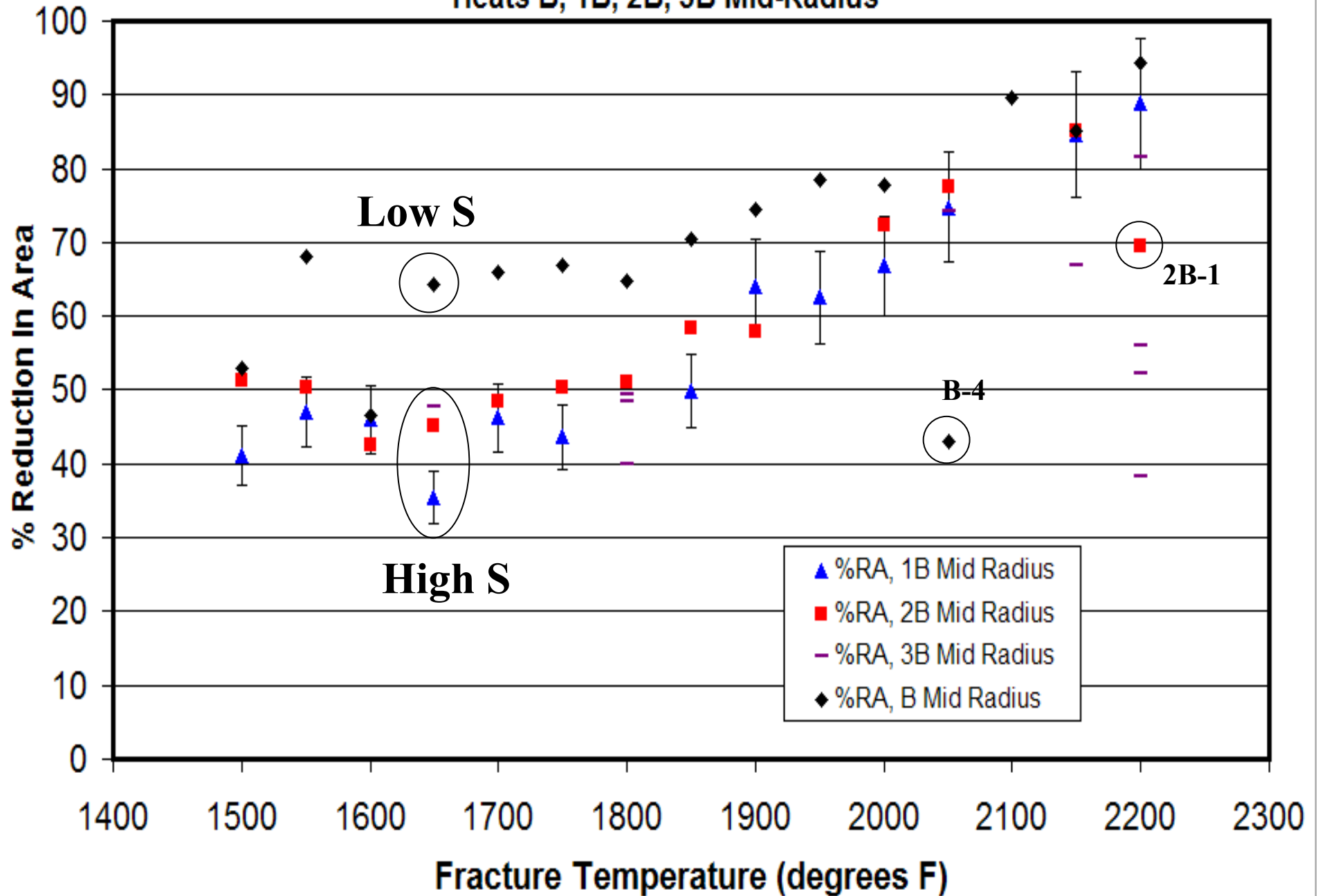
**% Reduction in Area vs. Fracture Temperature**



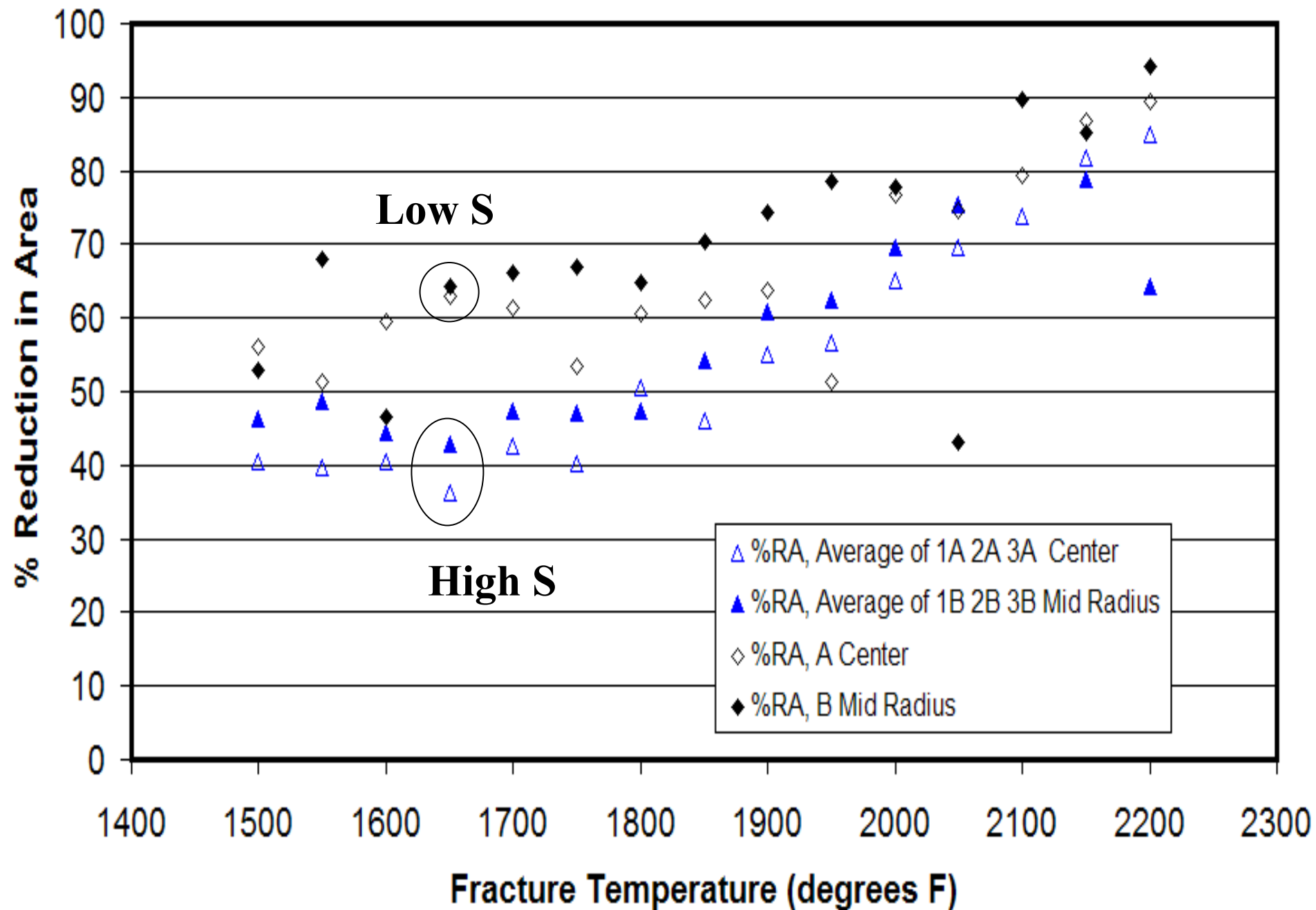
**% Reduction in Area vs. Fracture Temperature,  
Heats A, 1A, 2A, 3A Center**



**% Reduction in Area vs. Fracture Temperature,  
Heats B, 1B, 2B, 3B Mid-Radius**

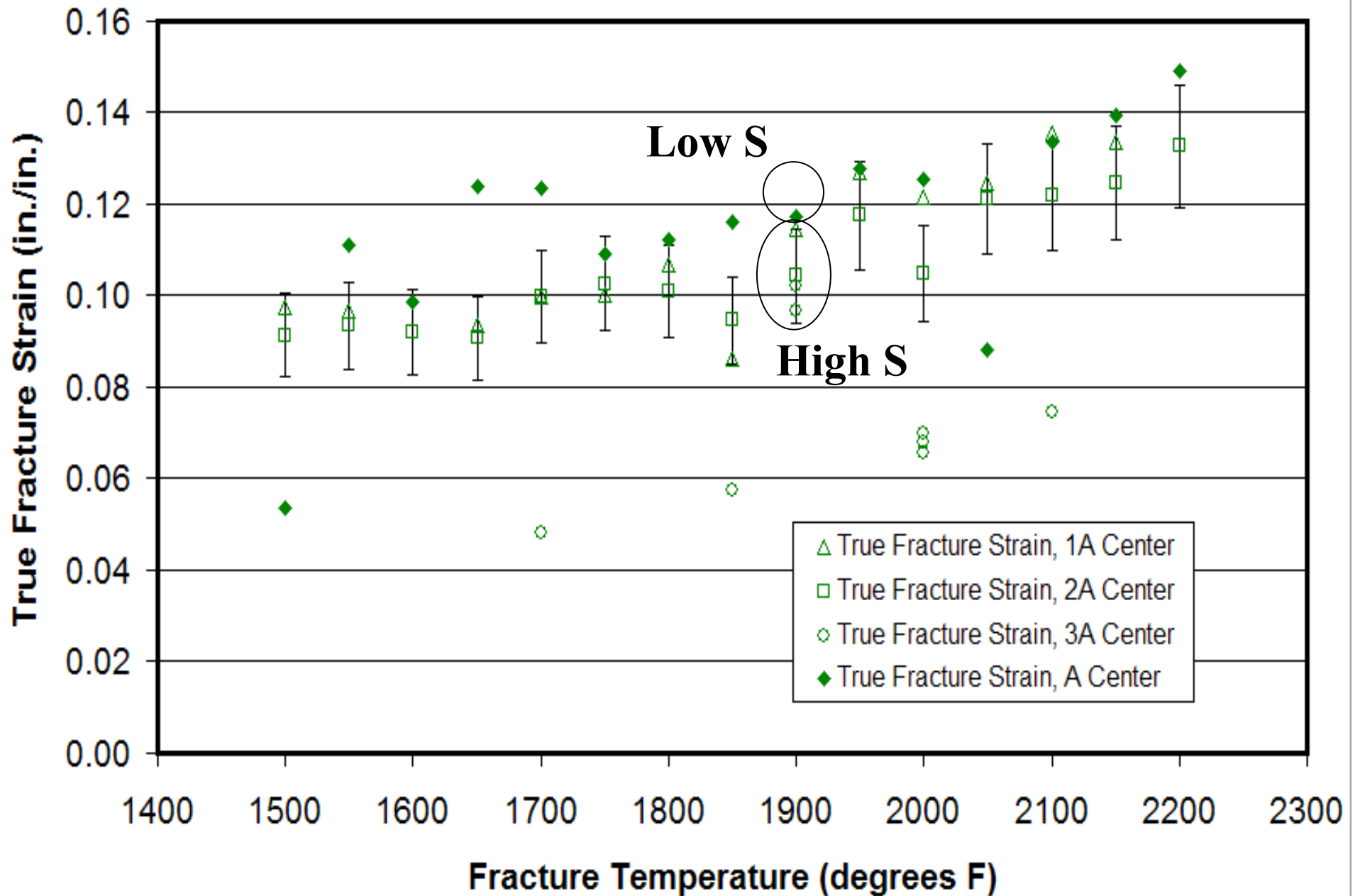


**% Reduction in Area vs Fracture Temperature**

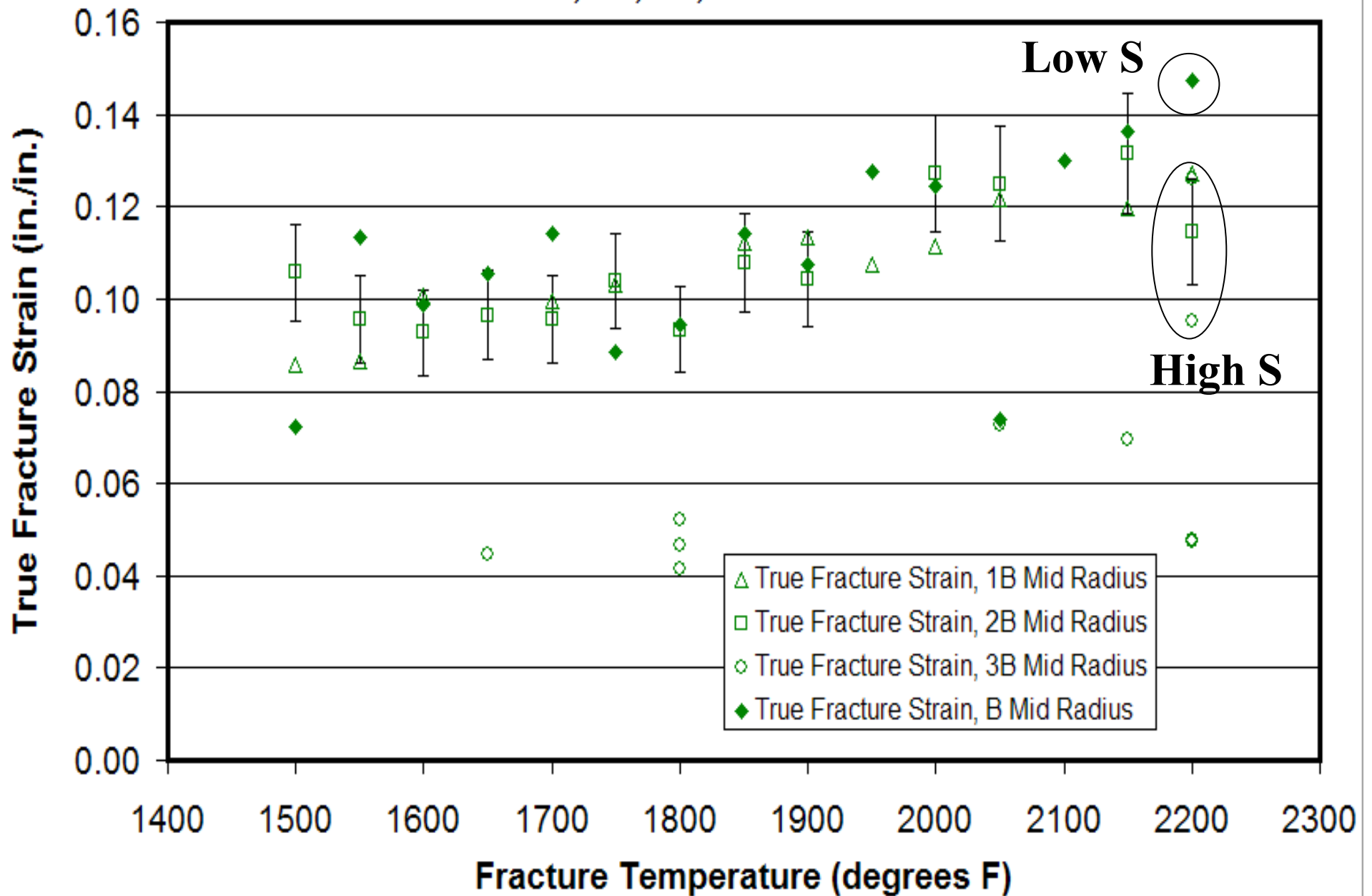




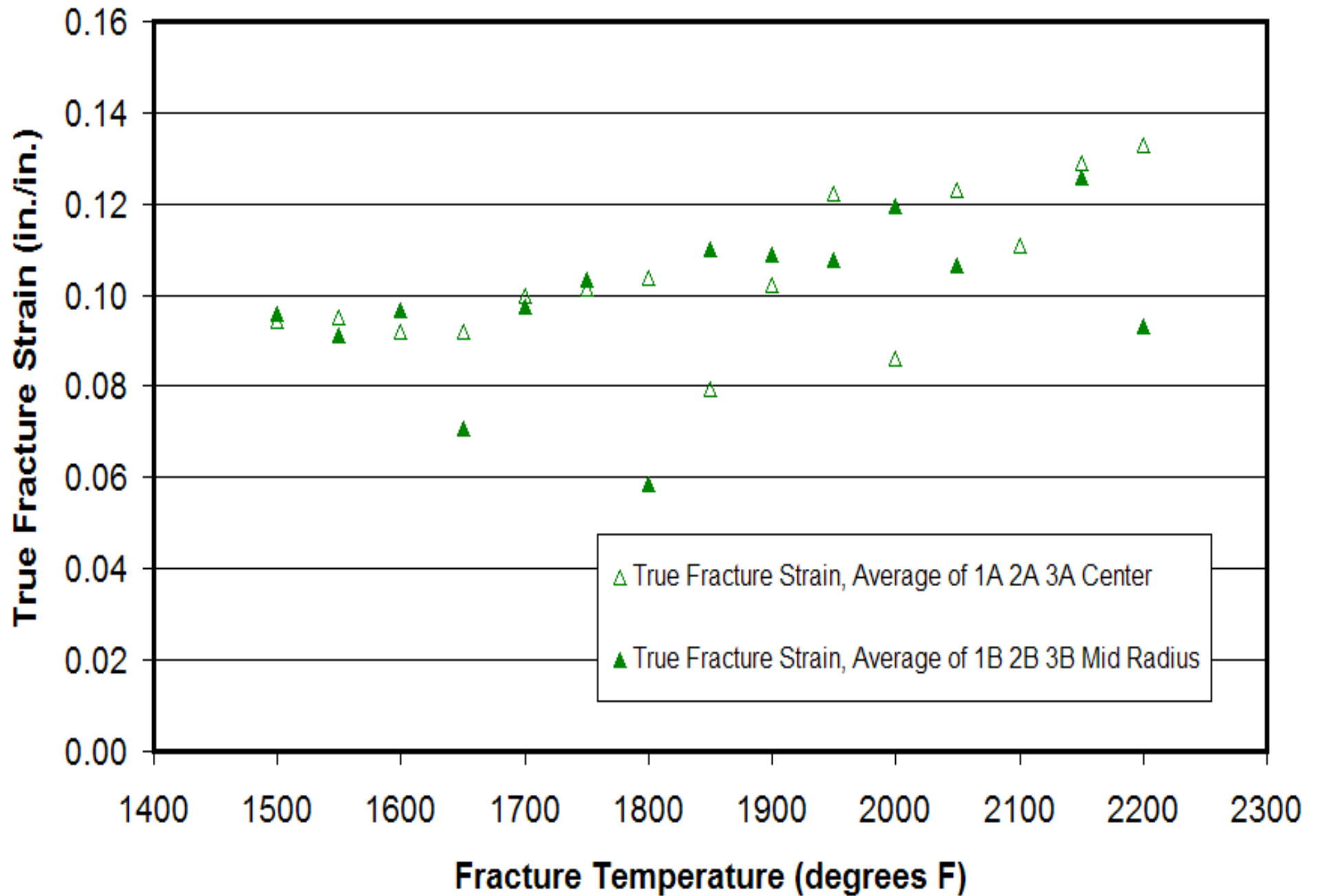
# True Fracture Strain vs Fracture Temperature Heats A, 1A, 2A, 3A Center



**True Fracture Strain vs Fracture Temperature**  
**Heats B, 1B, 2B, 3B Mid-Radius**




**Average True Fracture Strain vs Fracture Temperature**

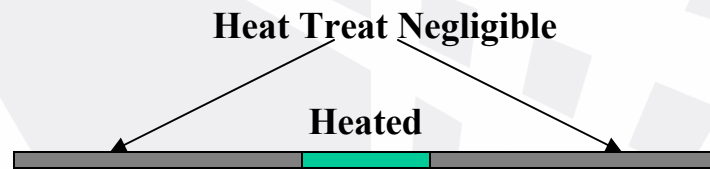


# L.O.M., S.E.M. and E.D.S. Results

- **Identify chemistry of inclusions and surrounding matrix.**
  - Sulfides:  $\text{MnS}$ ,  $\text{FeS}$ ,  $\text{Cr}_x\text{S}_y$ ,  $\text{Fe}_{1-x}\text{S}$ , etc.
  - Sulfide solid solutions:  $(\text{Mn}, \text{Me}) (\text{S})$  with  $\text{Me} = \text{Fe}, \text{Cr}$ .
  - Matrix: nominal steel chemistry.
- **Confirm MVC fracture mechanism and inclusion orientations.**
  - Dimpled fracture and ductile fracture surfaces.
  - “Longitudinal” and “transverse” inclusions.
  - “Longitudinal” and “transverse” inclusion arrays or pipes.

# As-Received Material

- **#1**  **Plate**
  - Used remaining material for examination of as-received condition.
  - Examined polished and etched microstructure with L.O.M.

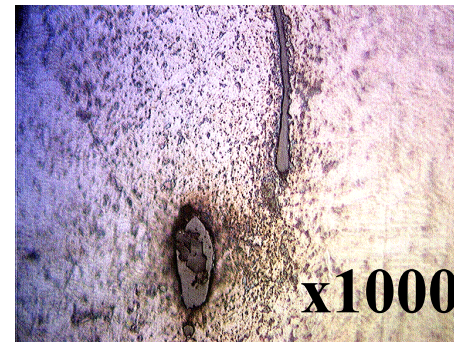
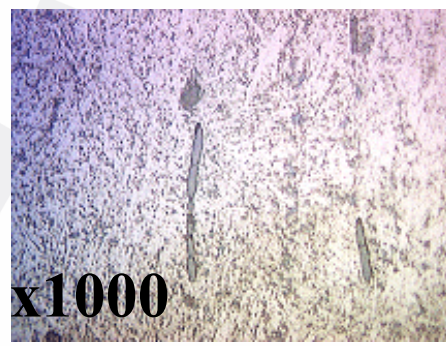
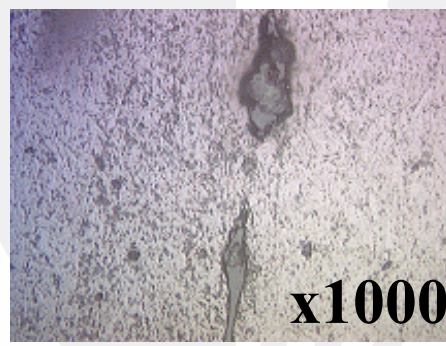
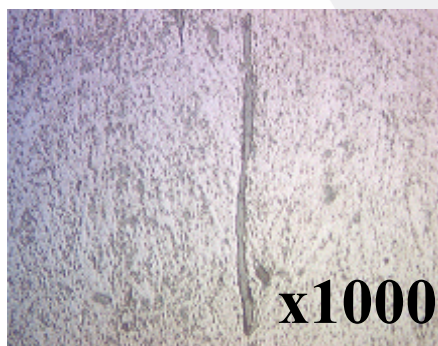
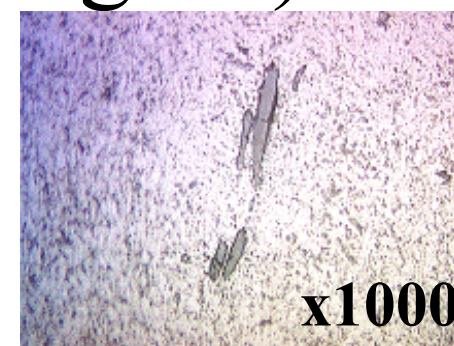
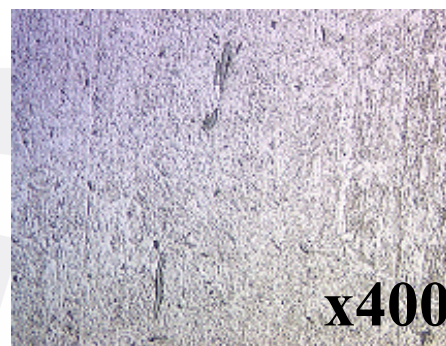
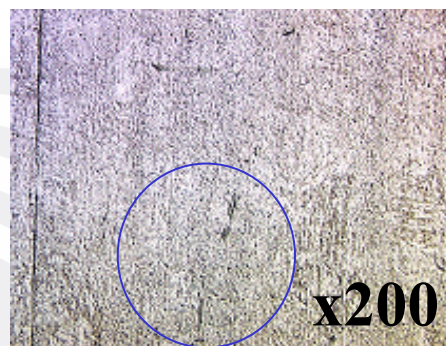
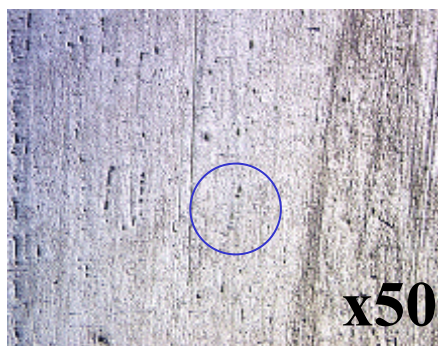


- **#2** **Test Sample**
  - Used SiC cutting wheel to obtain non-heat-treated portion of tensile samples.
  - Assumed far enough from heat input to retain unaffected microstructure (about 2 inches from center, adjacent to thread).
  - Used to examine as-received condition when remaining material not available.
  - Examined etched (Vigella's) microstructure w/ L.O.M. and S.E.M.





# #1 As-Received 1A Center (high S)

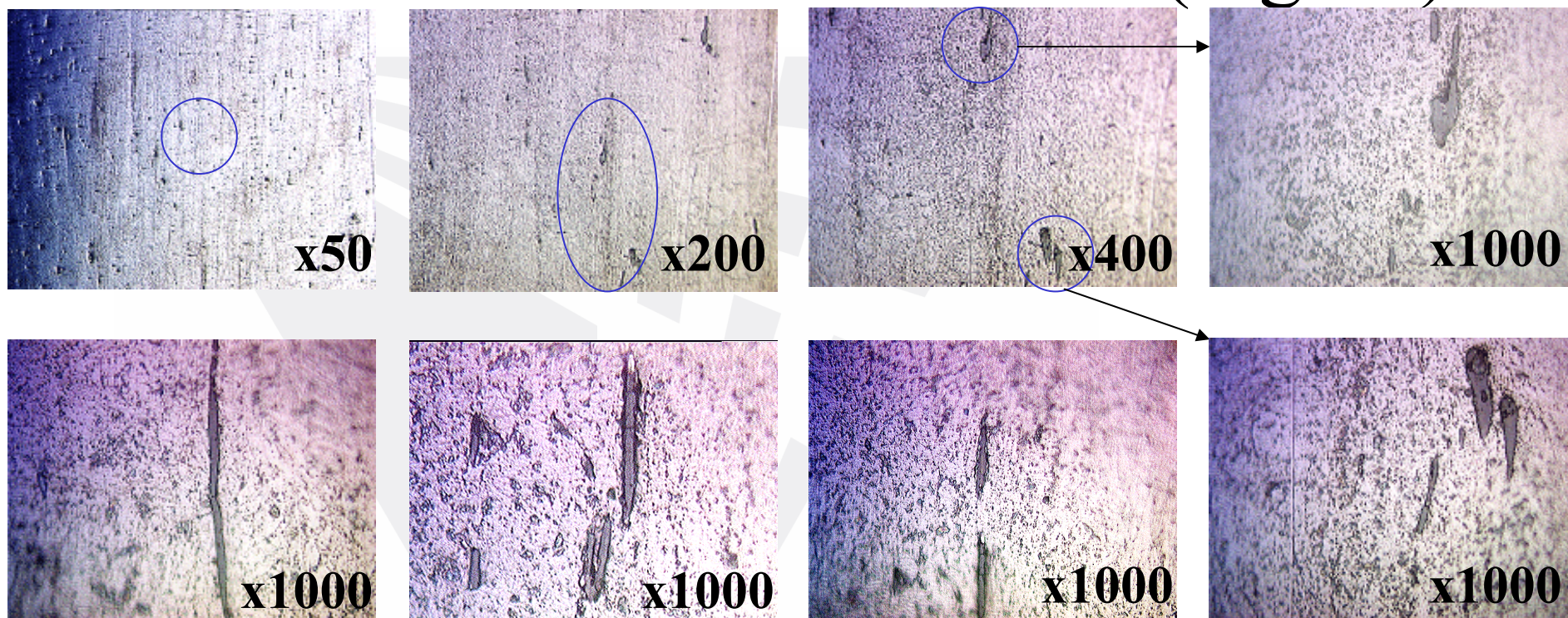


- Inclusions elongated in expected grain flow direction of as-received plates.





# #1 As-Received 2A Center (high S)

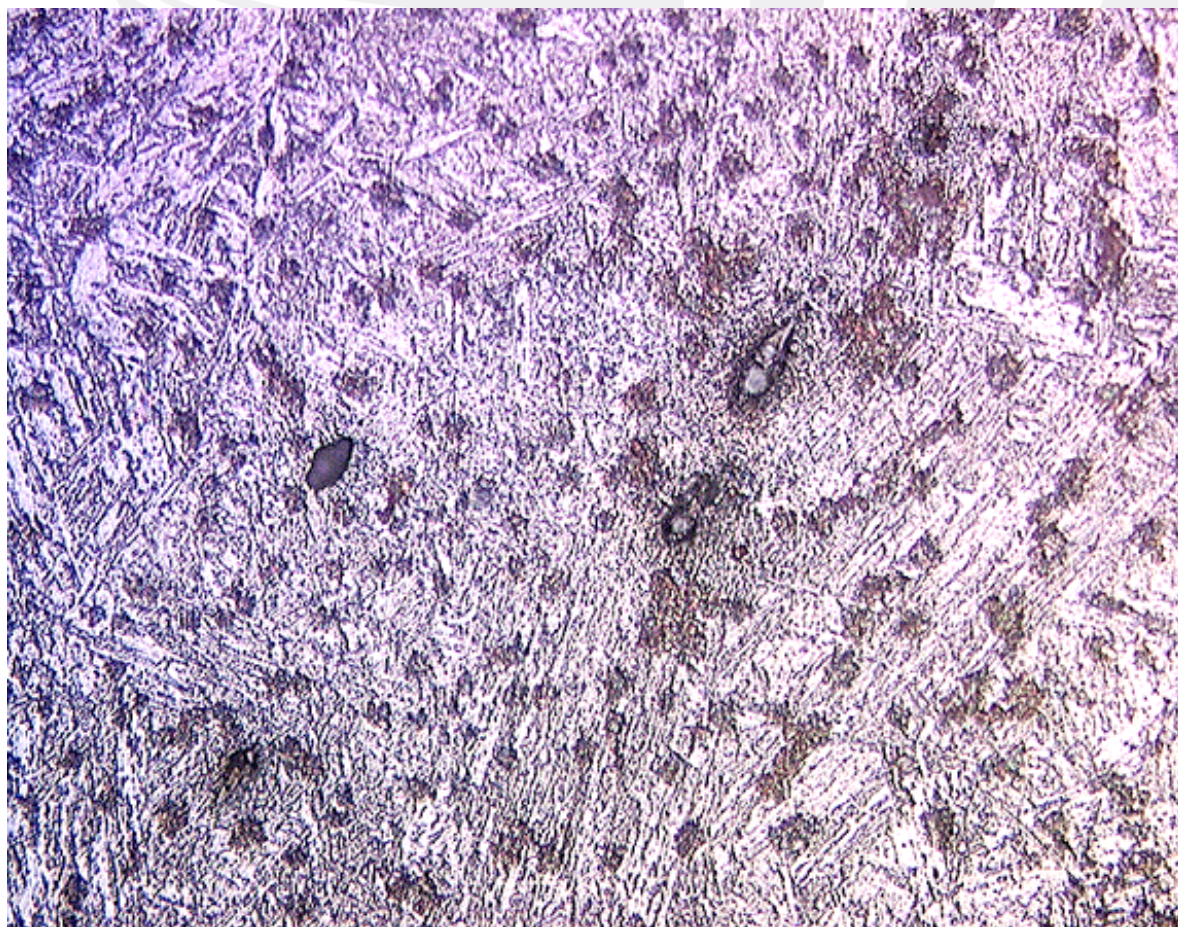


- Inclusions elongated in expected grain flow direction of as-received plates.
- Dove Grey color of stringers indicative of MnS inclusions.





## #2 As-Received Sample 2A-5

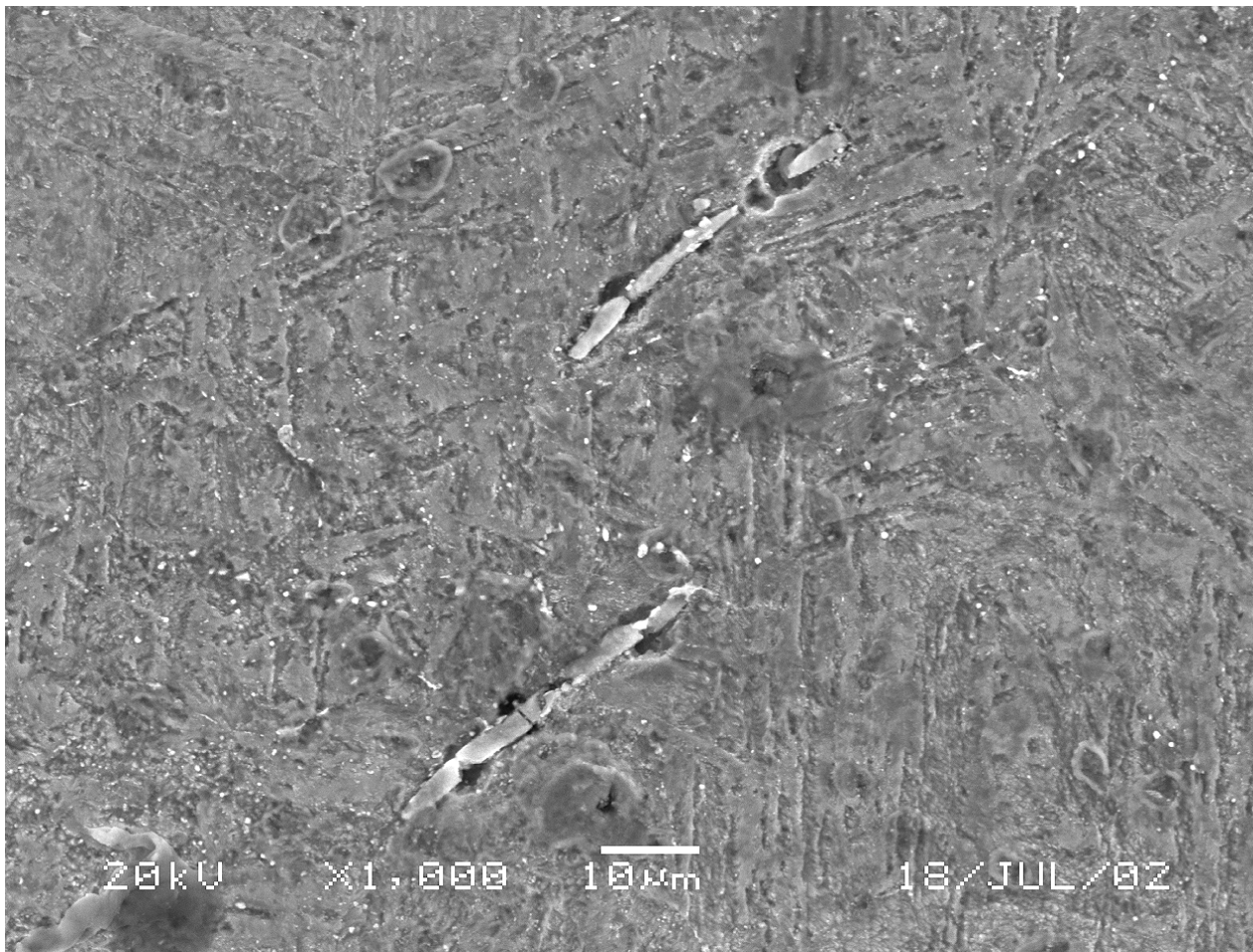


- **Magnification 40X.**
- **Inclusions elongated in identical direction.**
- **Etchant produces spotty appearance.**
- **Cut from 2A-5 test sample.**





## As Received 2A-5

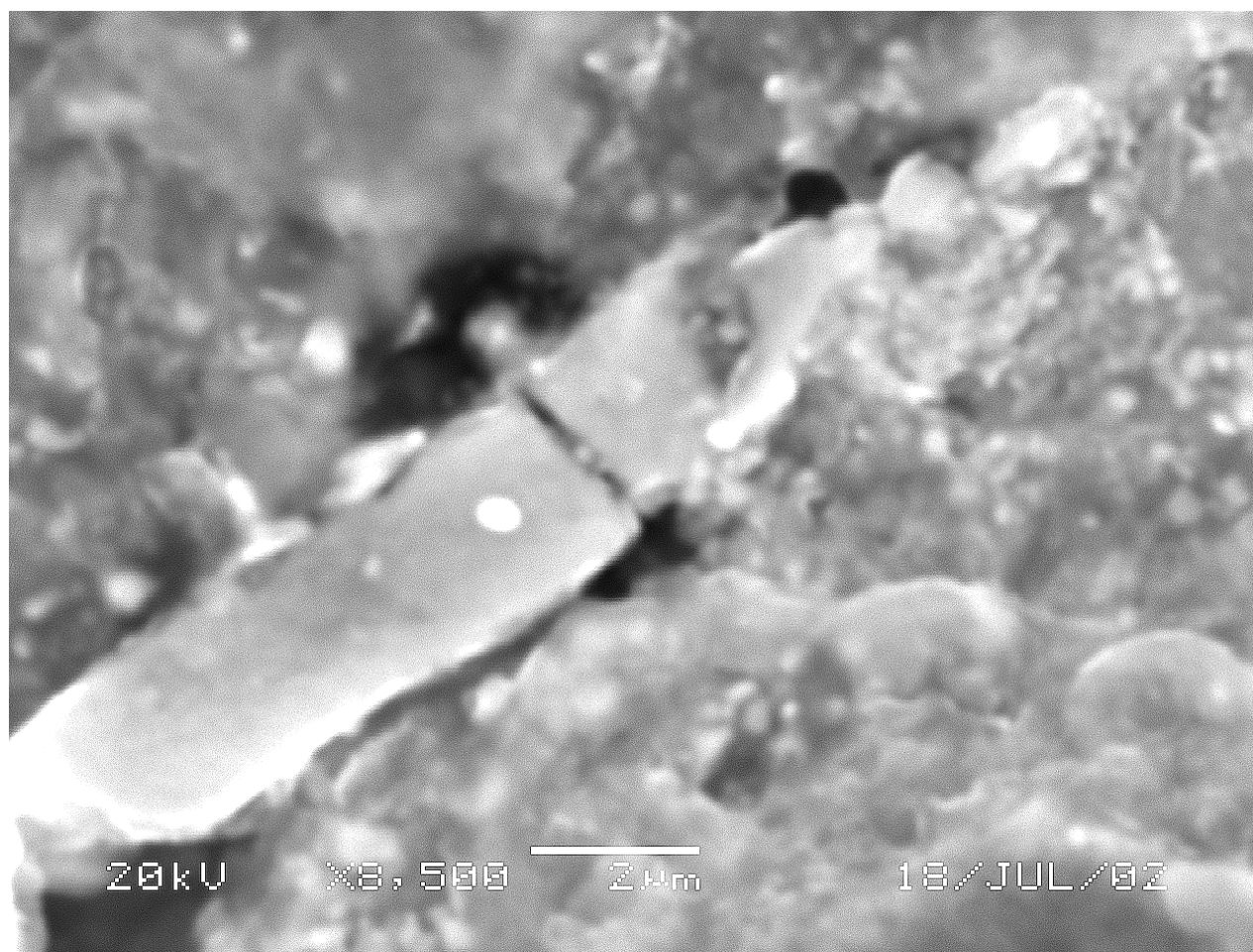


- **Magnification, 1000X.**
- **Elongated, parallel inclusions.**
- **Multiple brittle hair-line fractures inclusion width.**
- **Strain concentrations at inclusion tips and at cracks.**





## As Received 2A-5



- **Magnification, 8500X.**
- **Cubic  $\alpha$ -Fe MnS inclusion with perfectly brittle fracture.**
- **Voids formed (matrix yielding and brittle inclusion crack) serve as crack initiation sites for the sample.**





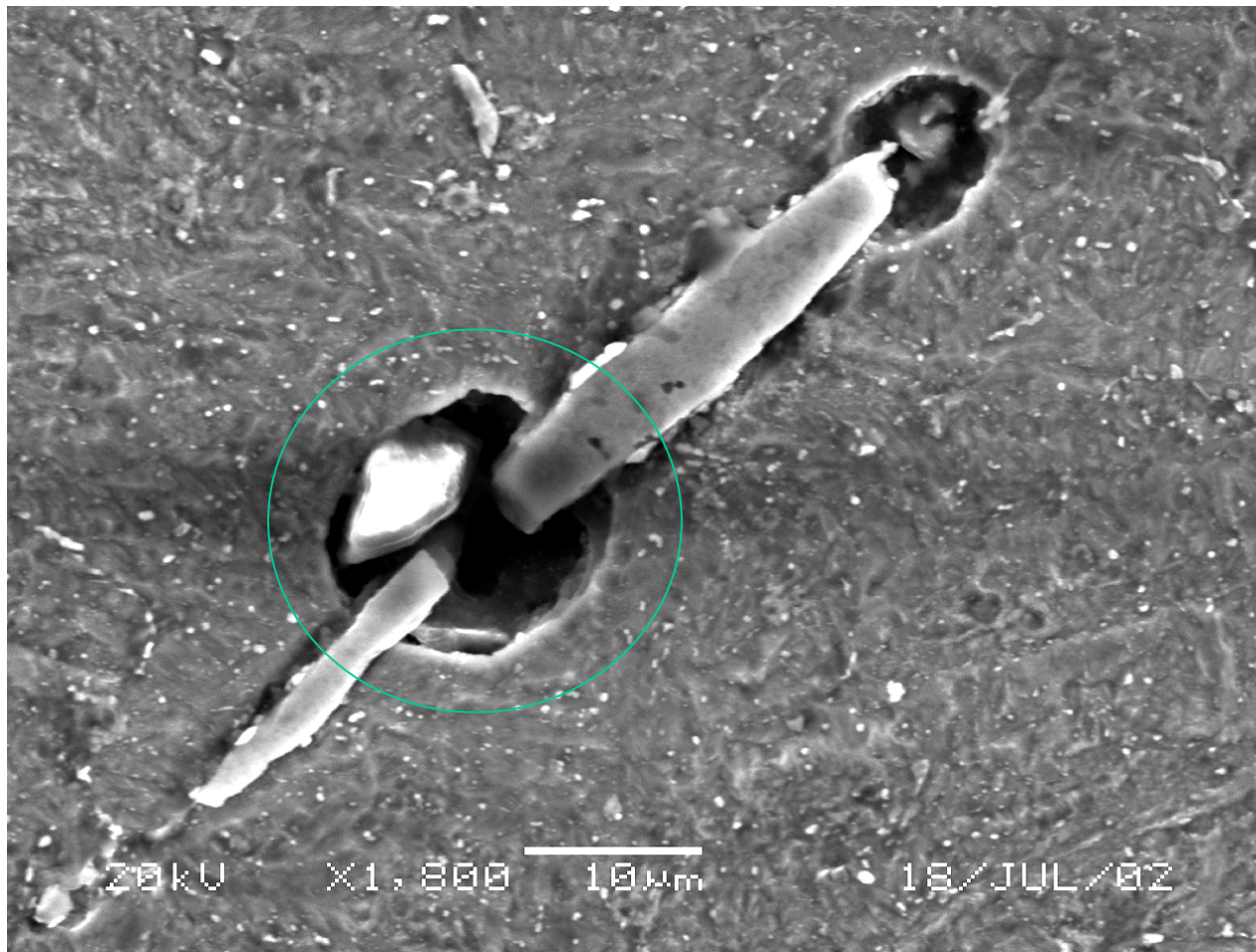
## As Received 2A-5



- **Magnification, 1800X.**
- **Parallel array of multiple inclusions.**
- **Multiple brittle inclusion fractures, closely spaced for a single inclusion.**



## As Received 2A-5

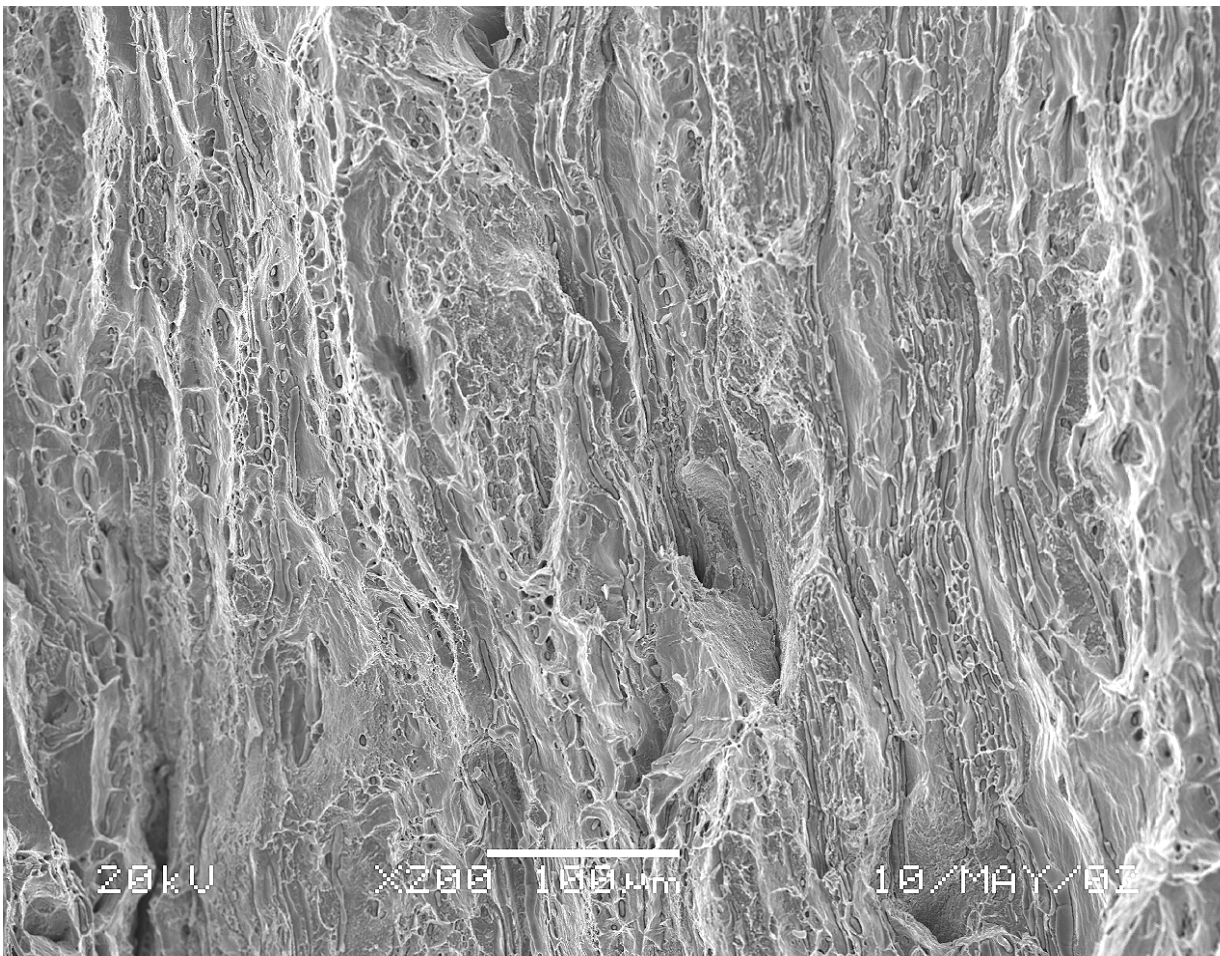


- Magnification, 1800X.
- Larger brittle fracture S.C.
- Bottom inclusion either pulled apart after fracture or piece missing & fracture spacing small.





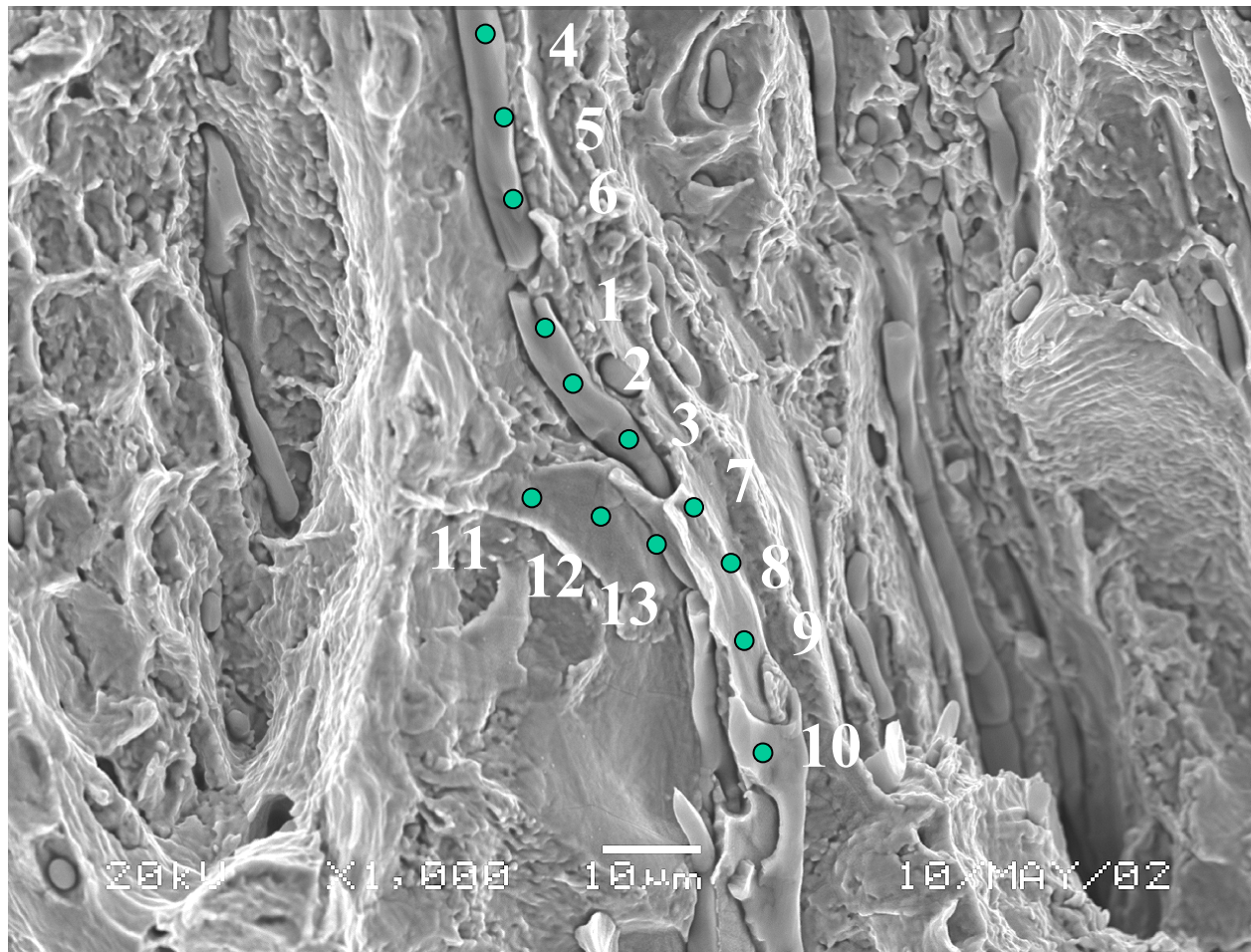
## Fracture Surface 2A-5



- **Magnification, 200X.**
- **Ductile fracture surface.**
- **Voids appear elongated, corresponding roughly with “void pipes”.**



## Fracture Surface 2A-5

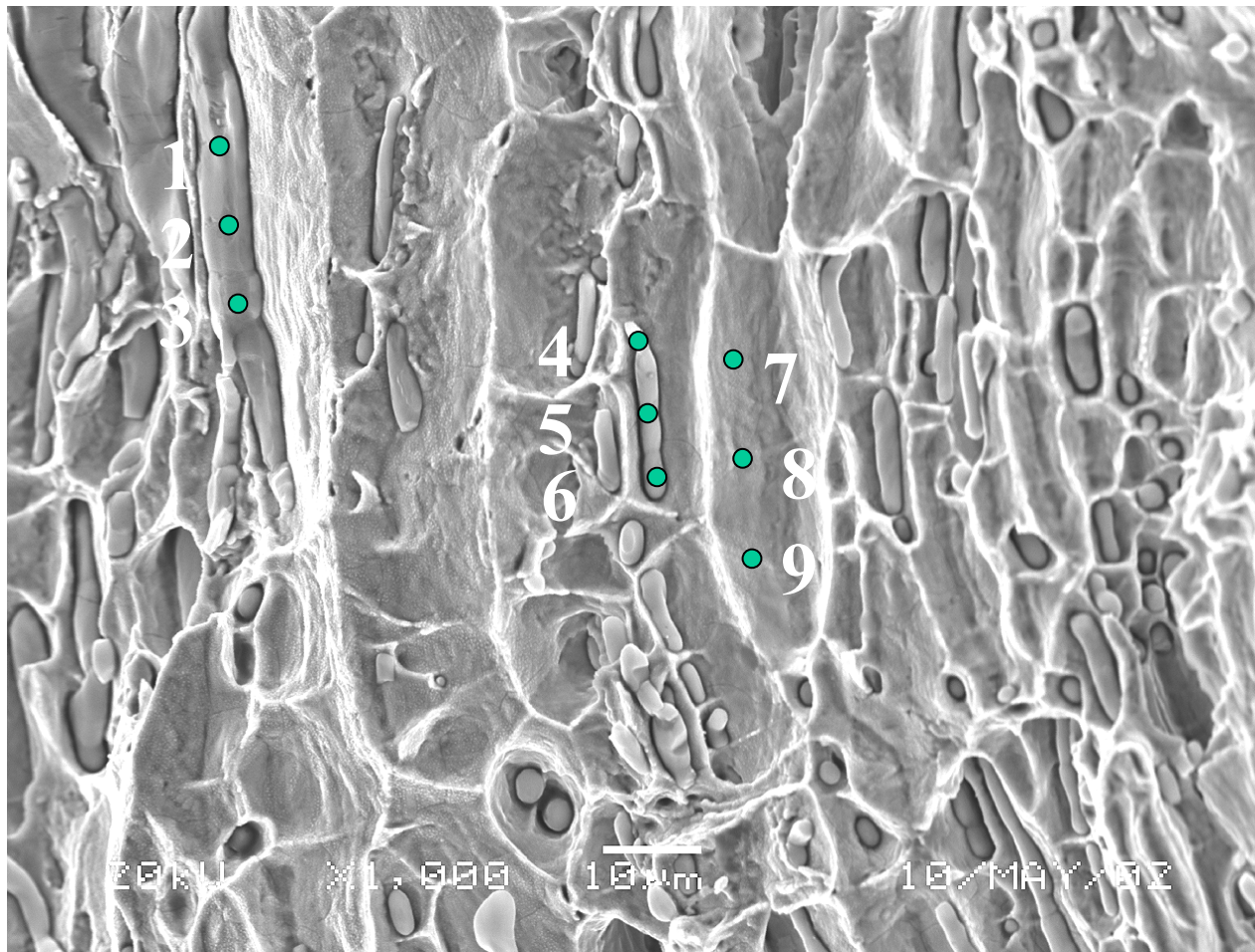


- **Magnification, 1000X.**
- **Elongated Stringers perpendicular to principle strain direction (out of page).**
- **High density of “transverse inclusions”.**





# Fracture Surface 2A-5

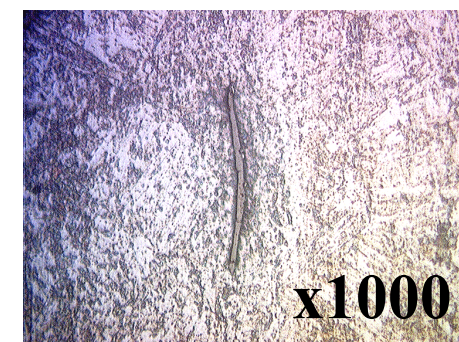
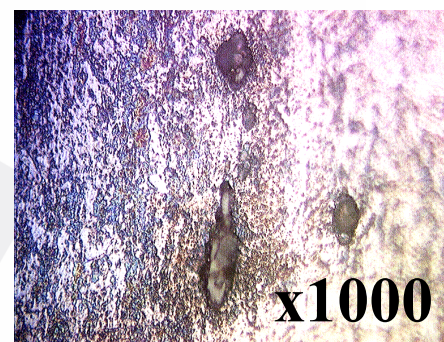
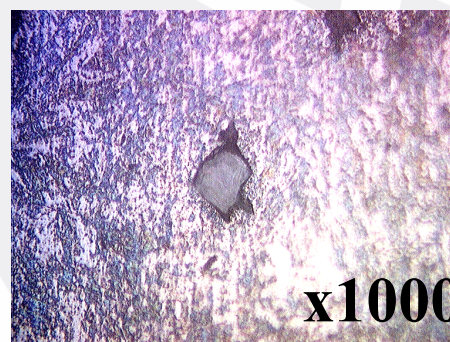
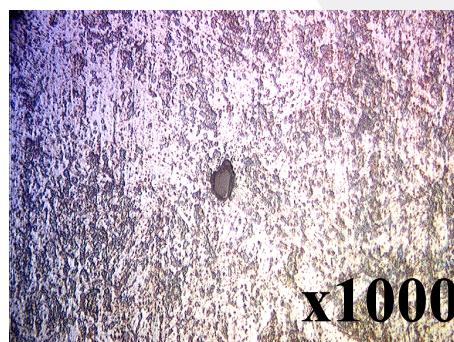
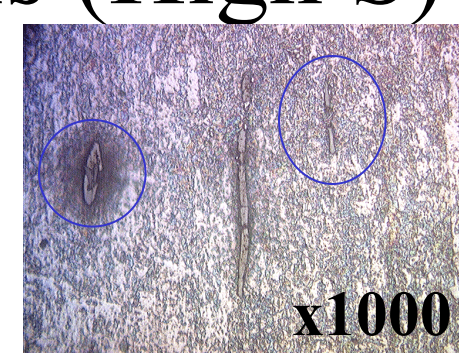
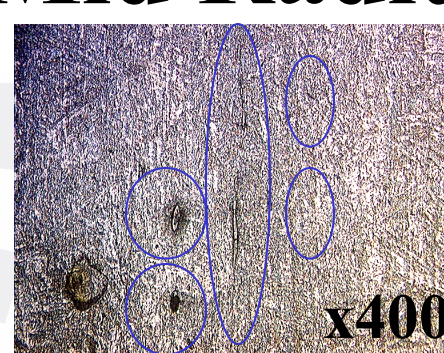
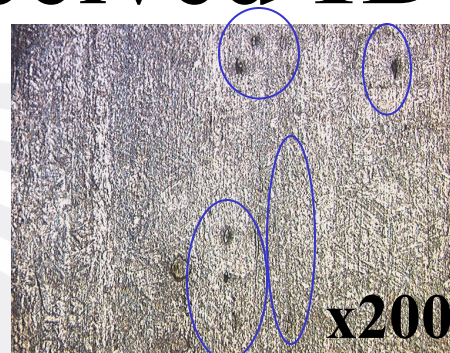
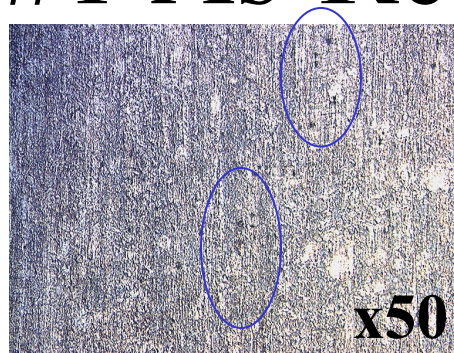


- Magnification, 1000X.
- Both “transverse” (elongated) and “longitudinal” (equiaxed) inclusions present.





# #1 As-Received 1B Mid Radius (High S)

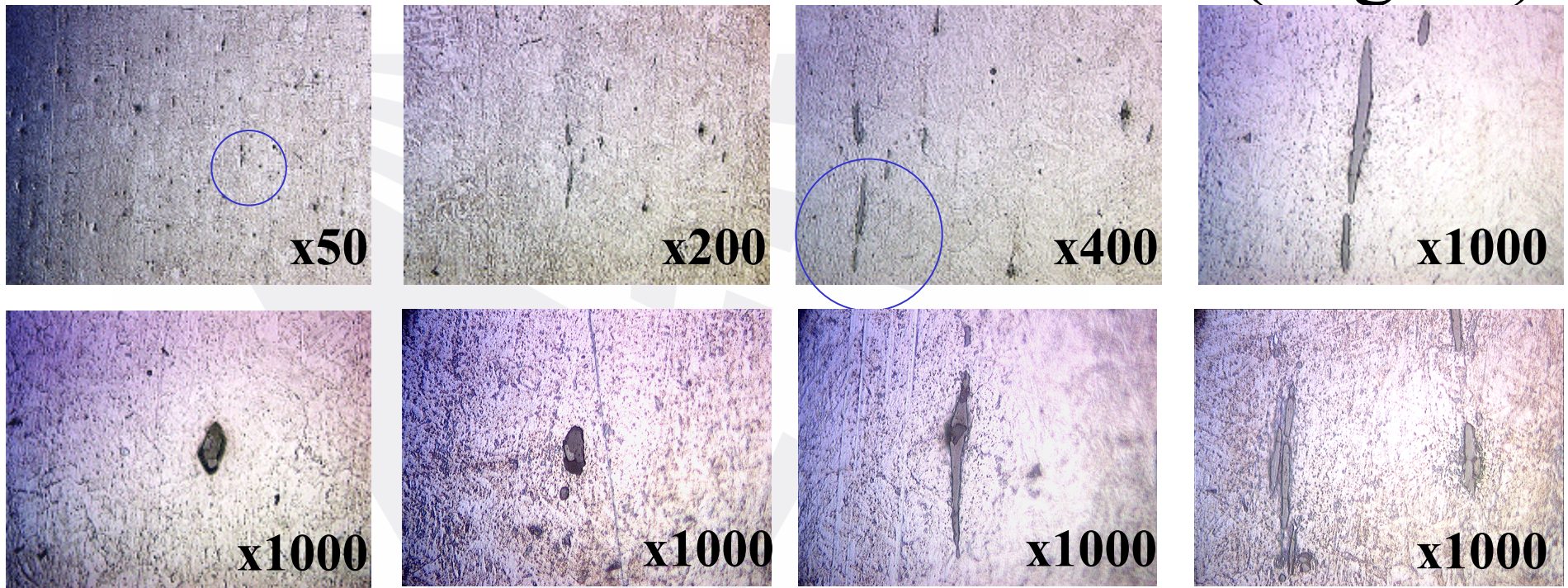


- Inclusions elongated in expected grain flow direction of as-received plates.
- Anisotropy of inclusions in as-received material reduces both subsequent cold and hot workability.





# #1 As-Received 2B Mid Radius (High S)

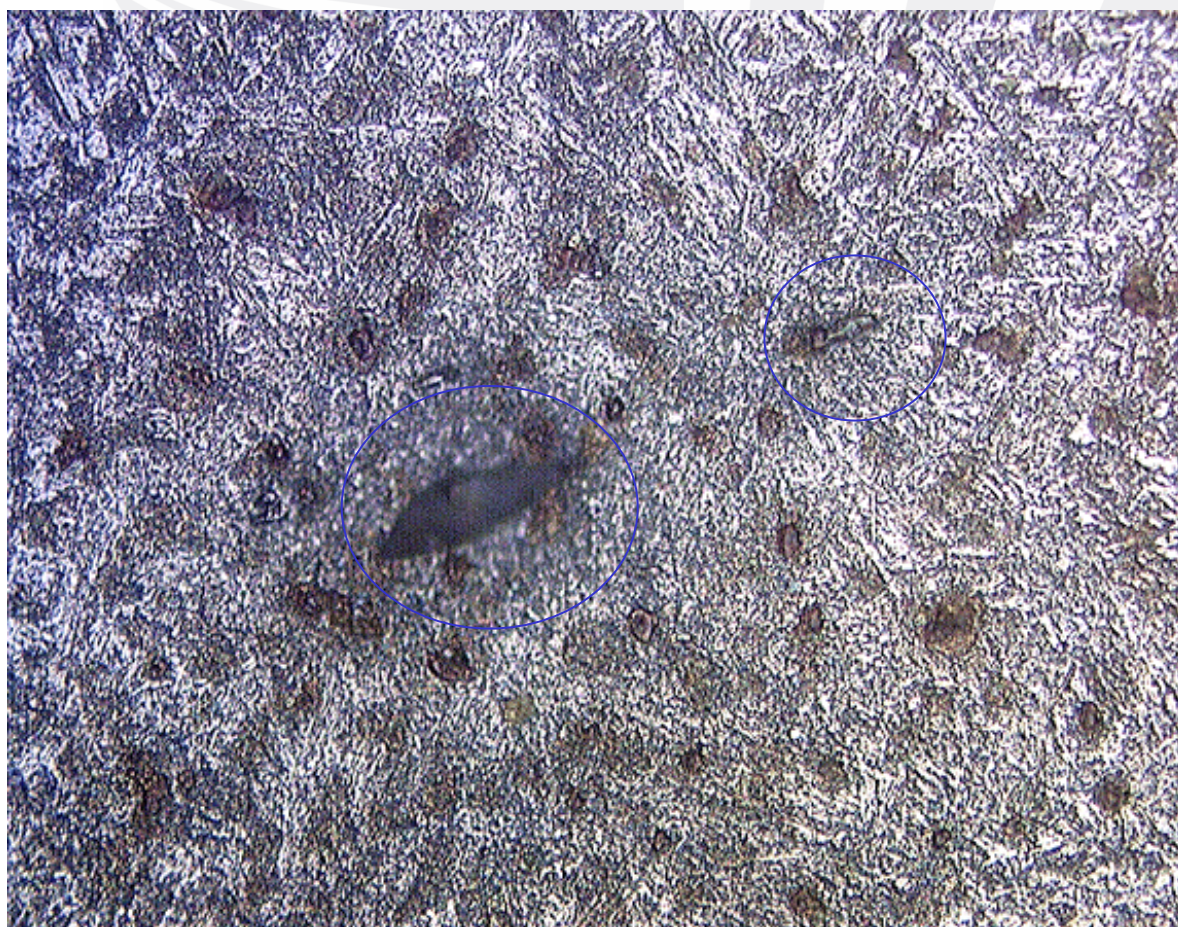


- Inclusions elongated in expected grain flow direction of as-received plates.
- Anisotropy of inclusions in as-received material reduces both subsequent cold and hot workability.





## #2 As-Received Sample 2B-1

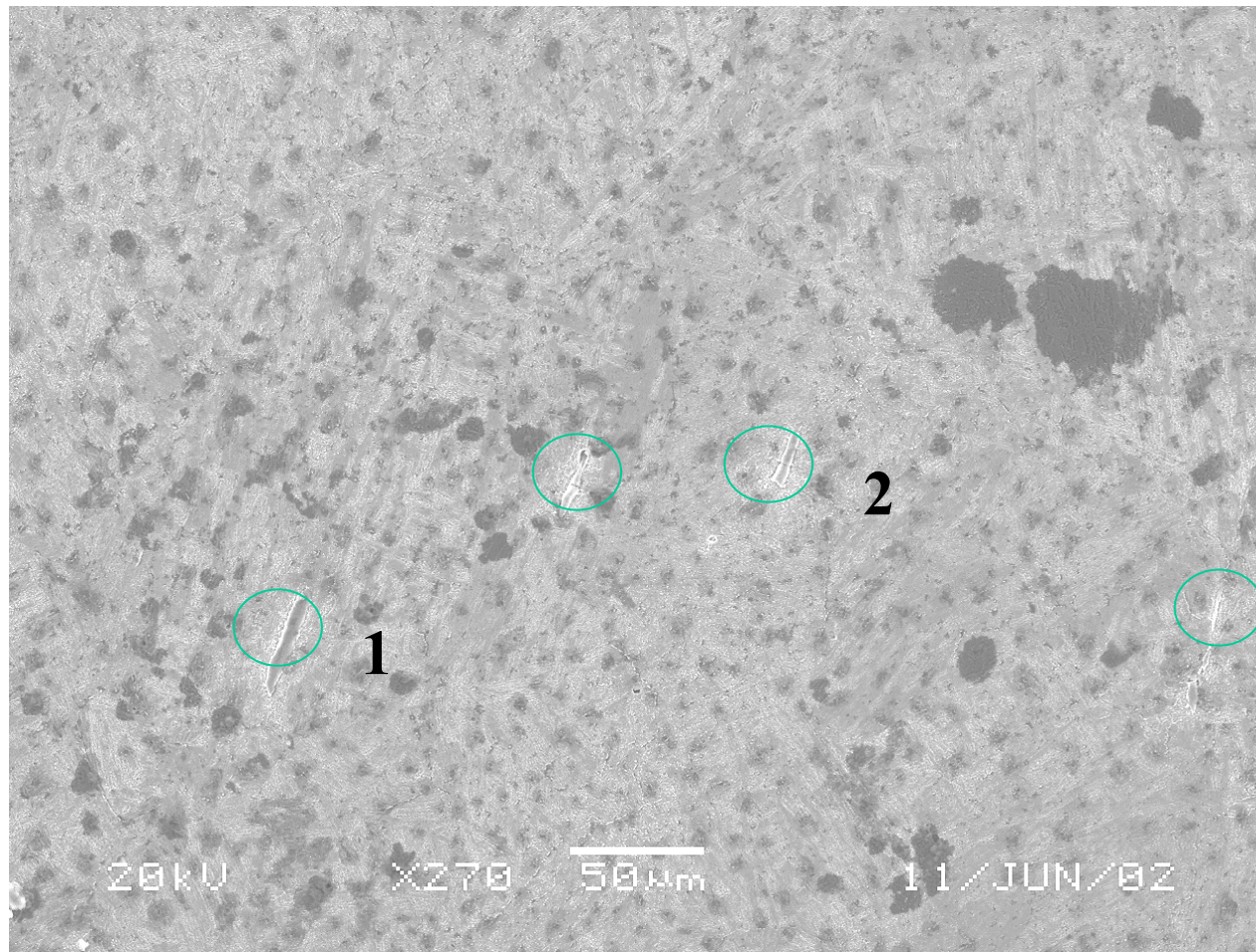


- Magnification, 400X.
- Inclusions elongated in identical direction.
- Etchant produces spotty appearance.
- Cut from 2B-1 test sample.





## As Received 2B-1



- **Magnification, 270X.**
- **Inclusions parallel, arranged in arrays.**

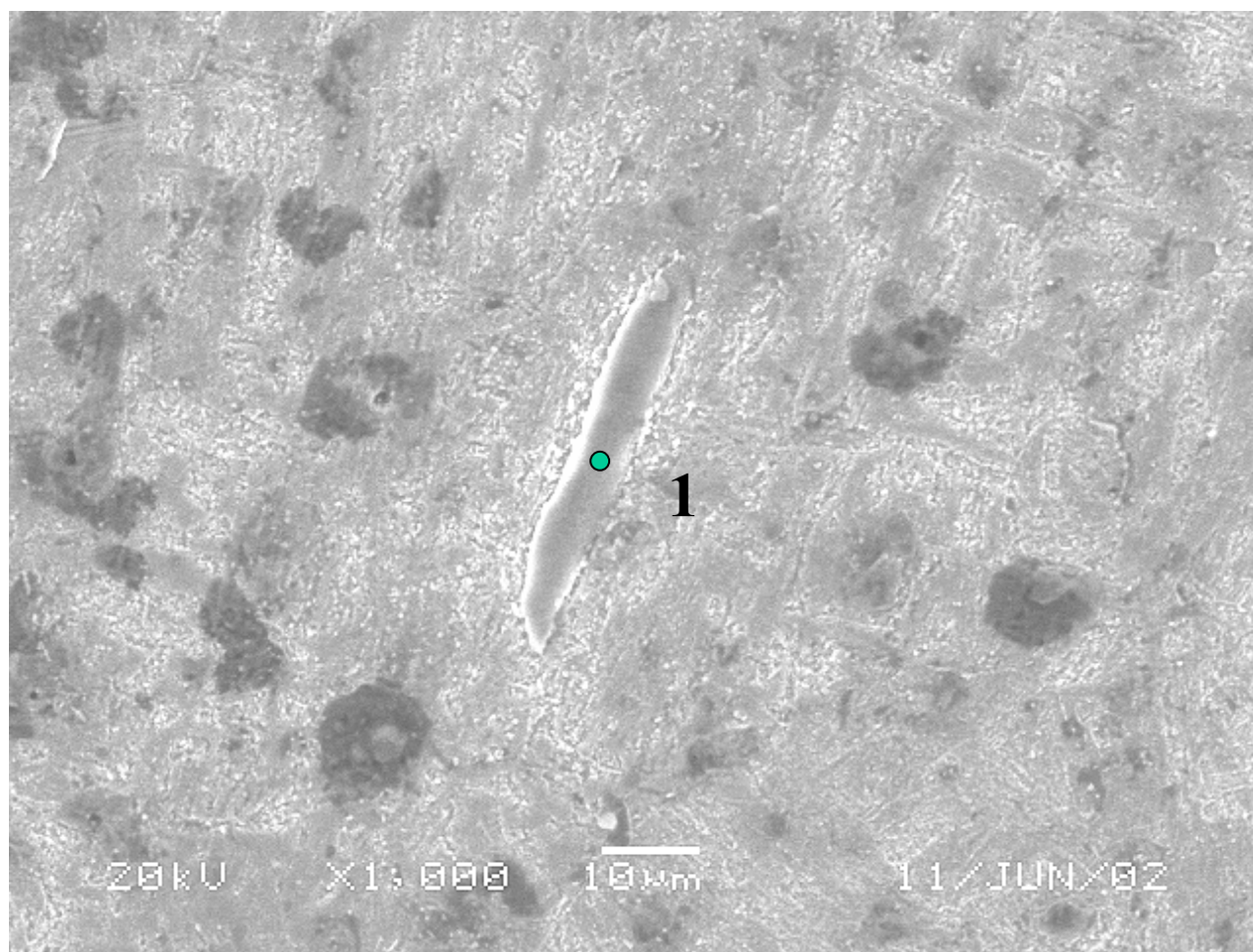


S.E.M.

ILLINOIS INSTITUTE  
OF TECHNOLOGY



## As Received 2B-1

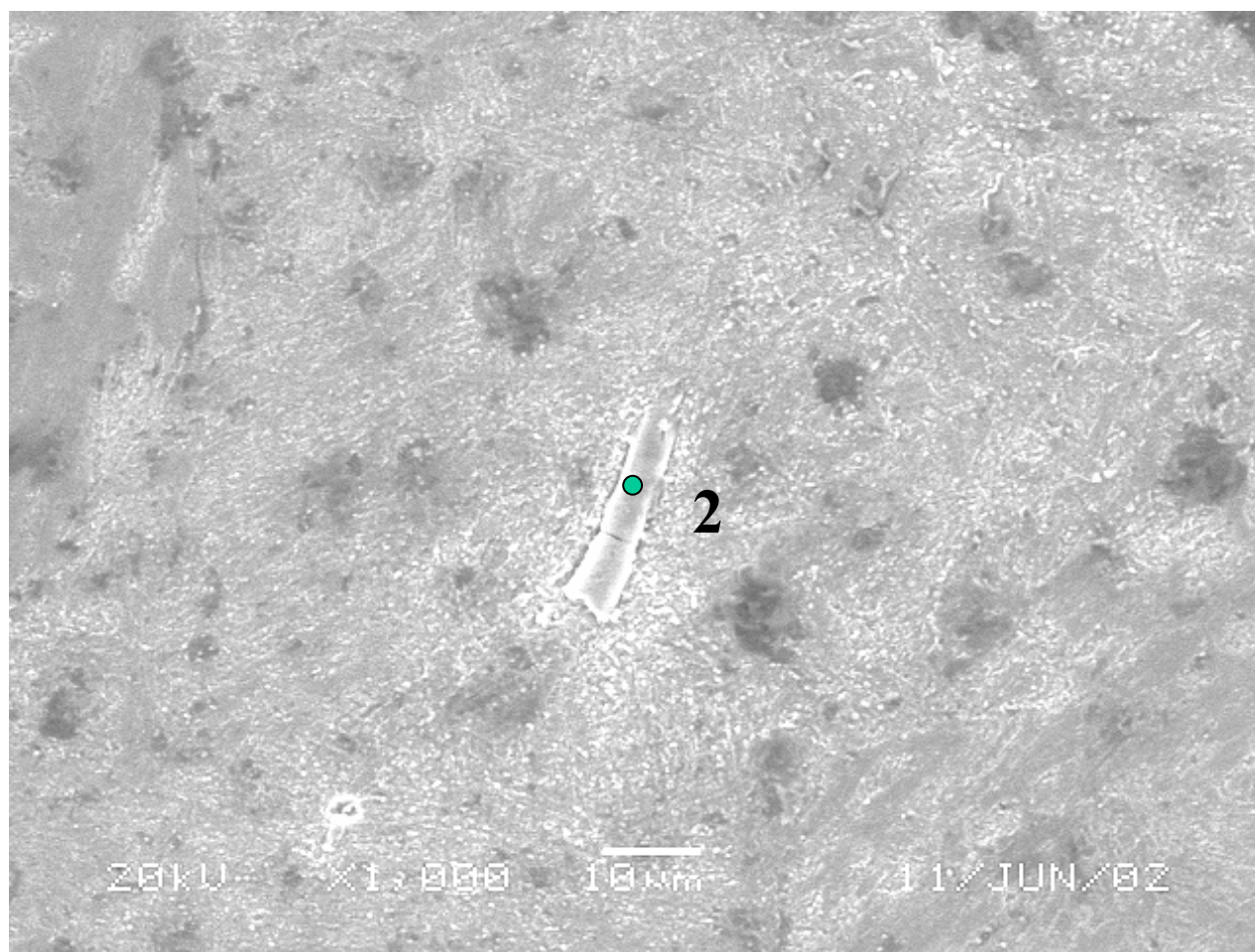


- **Magnification, Point 1, 1000X.**
- **No S.C. effects observed.**
- **Element (wt%/at%):**
  - Fe 3.16 / 2.48
  - S 34.82 / 47.56
  - P 0.59 / 0.84
  - Mn 56.15 / 44.76
  - Si 0.0 / 0.0
  - Ni 0.11 / 0.08
  - Cr 3.38 / 2.85
  - Mo 0.0 / 0.0
  - Cu 1.53 / 1.06
  - Al 0.22 / 0.36
  - V 0.04 / 0.03





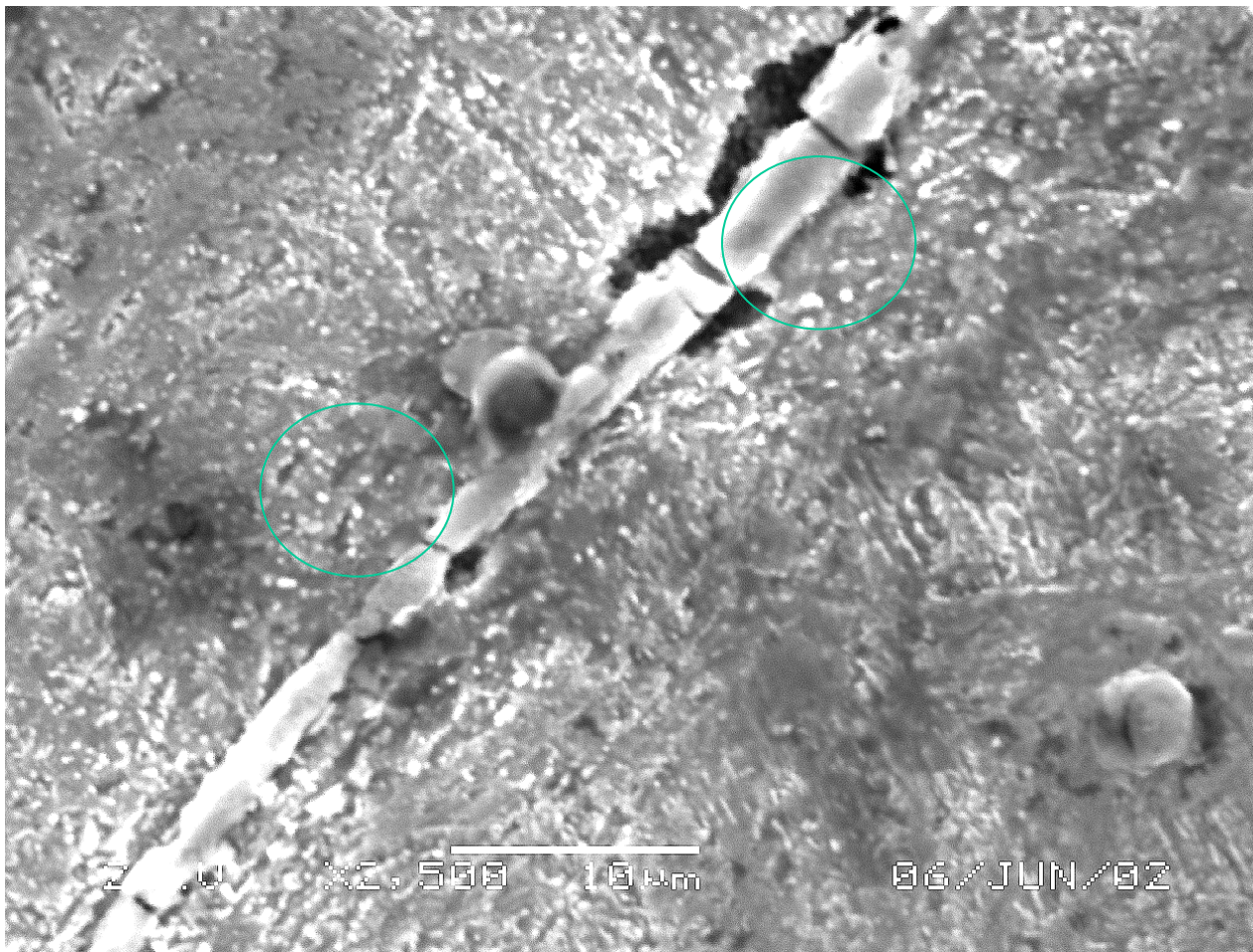
# As Received 2B-1



- **Magnification,  
Point 2, 1000X.**
- **Element  
(wt%/at%):**
  - Fe 1.70 / 1.31
  - S 37.54 / 50.38
  - P 0.49 / 0.68
  - Mn 56.96 / 44.61
  - Si 0.0 / 0.0
  - Ni 0.12 / 0.08
  - Cr 2.32 / 1.92
  - Mo 0.0 / 0.0
  - Cu 0.36 / 0.25
  - Al 0.43 / 0.68
  - V 0.08 / 0.07



## As Received 2B-1

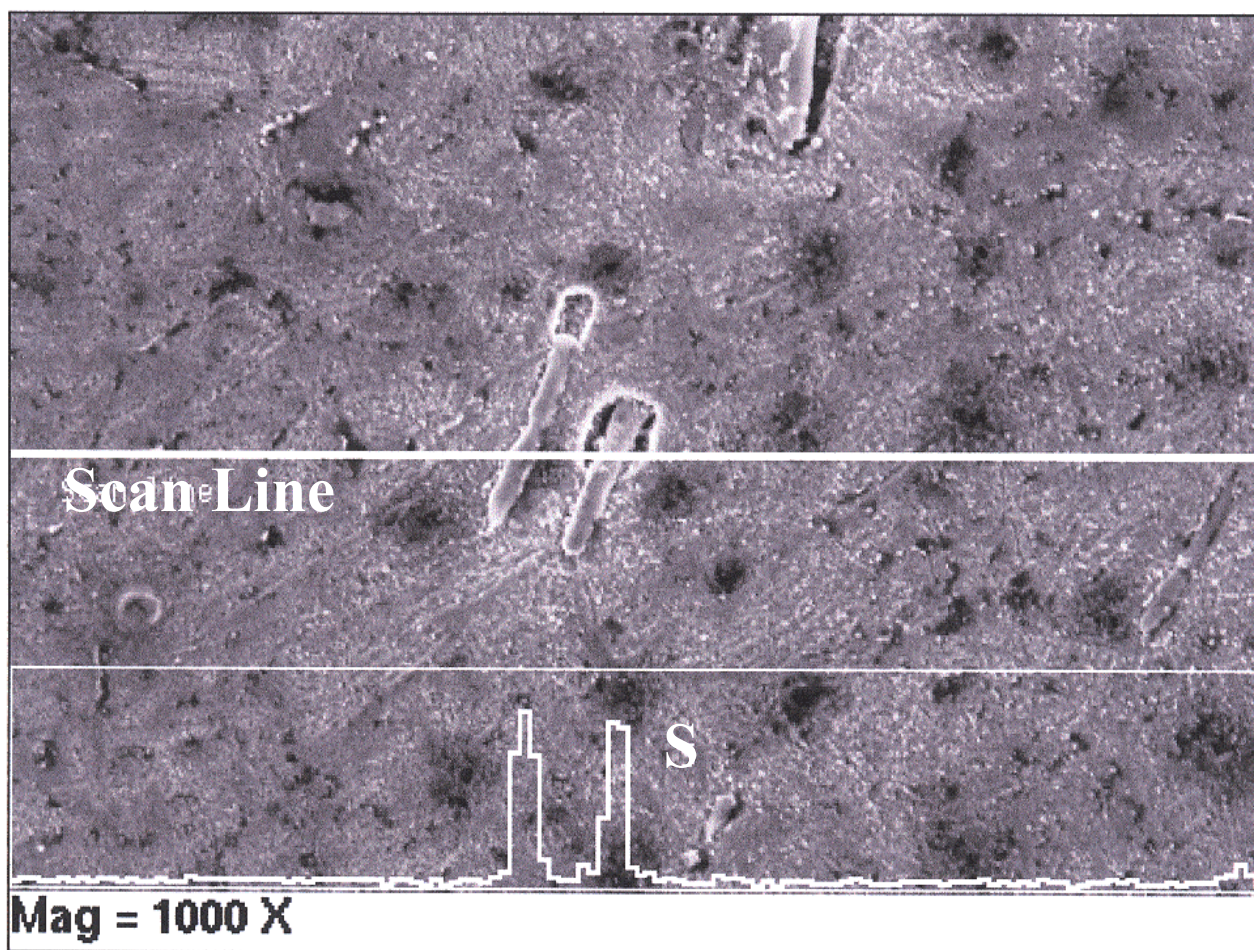


- **Magnification, 2500X.**
- **Multiple inclusion fractures, closely spaced.**
- **Matrix plastic zone near inclusion brittle cracks**
- **Matrix / inclusion interface circled.**





## As Received 2B-1

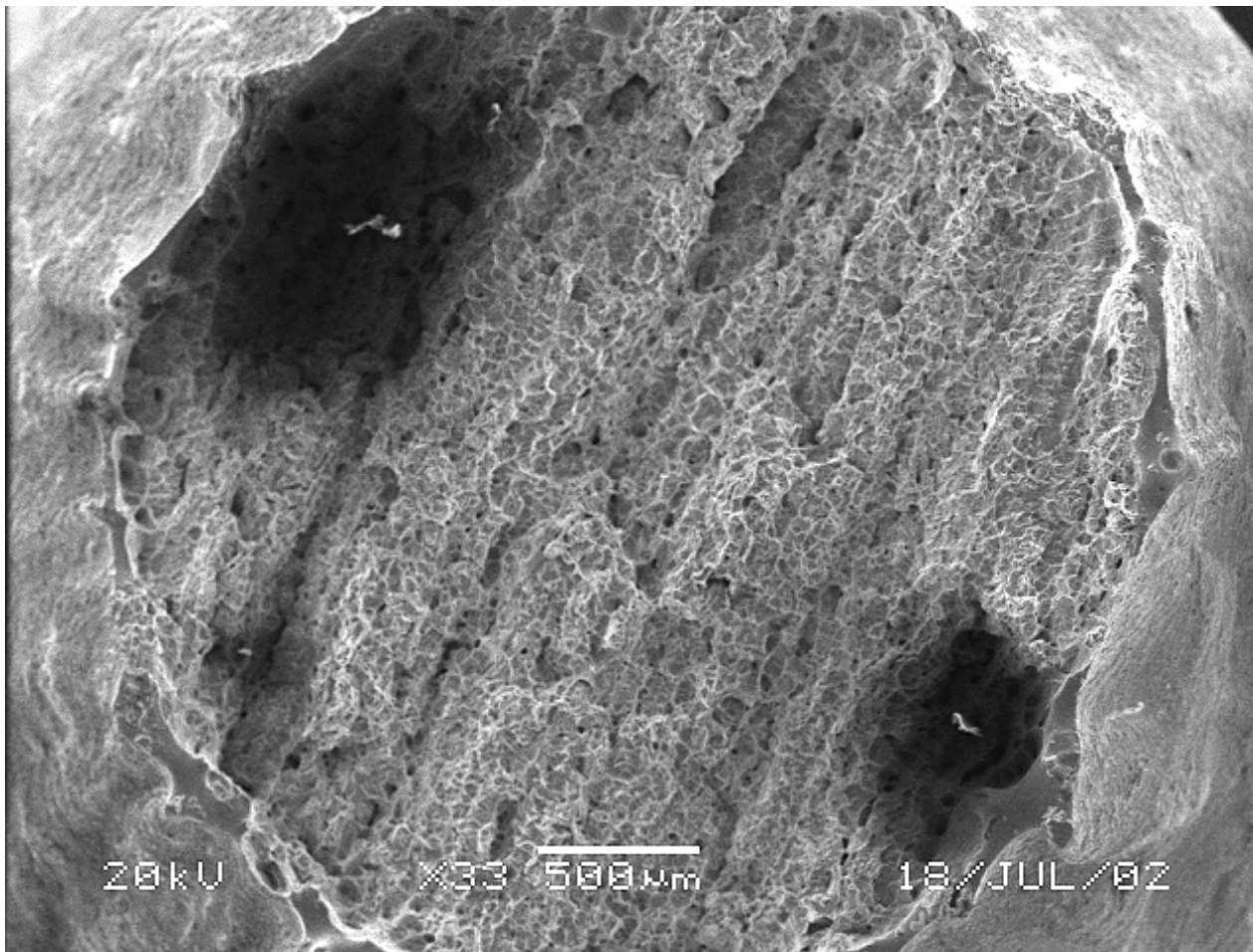


- **Magnification, 1000X.**
- **EDS Line Analysis shows sulfur concentrated in the inclusions.**
- **Sulfur concentration negligible in the matrix locally.**





## Fracture Surface 2B-1

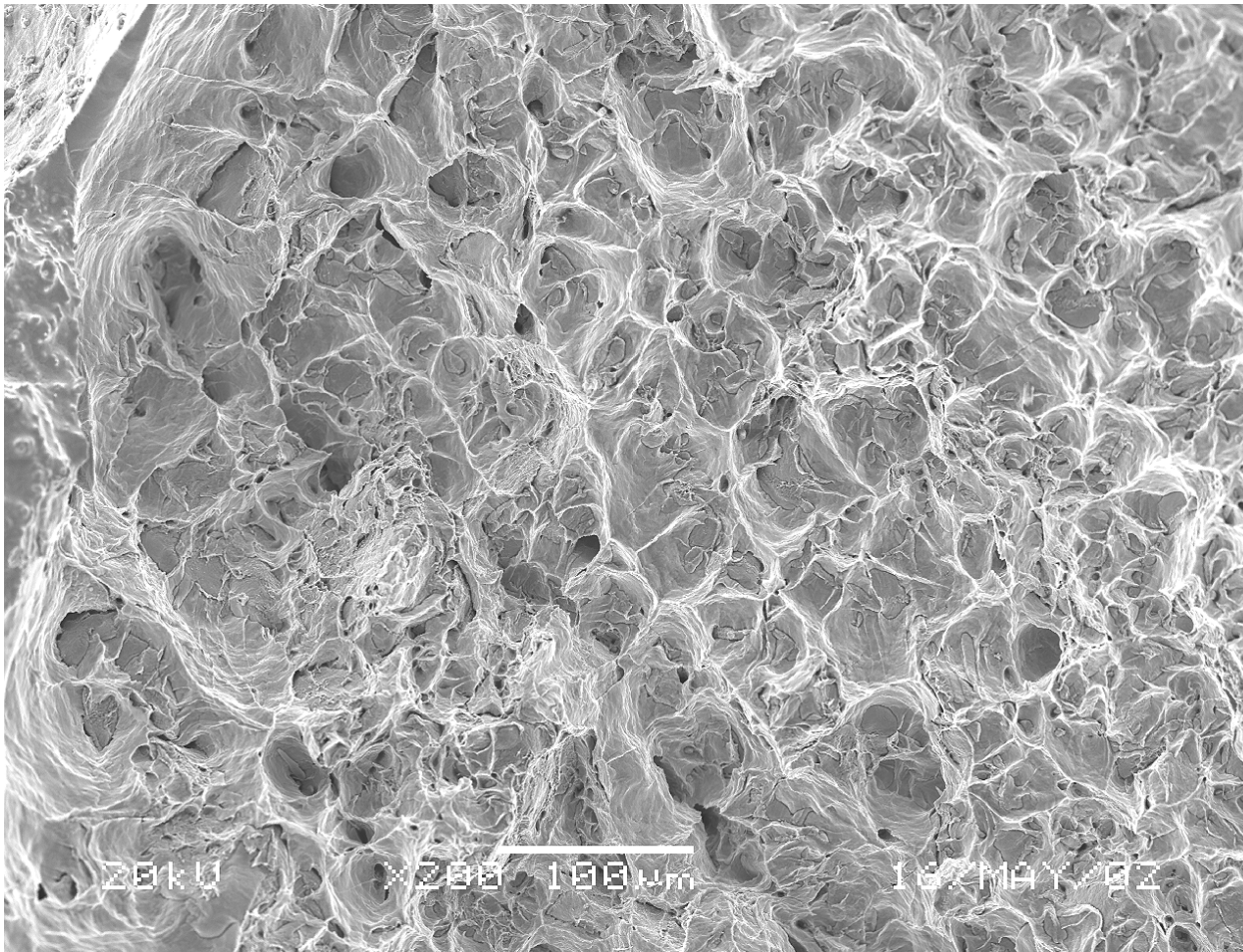


- **Magnification, 33X.**
- **Fracture face stepped similar to lamellar tearing.**
- **Dark patches where crack jumped to nearest level of inclusions.**
- **Evidence for “void piping”.**





## Fracture Surface 2B-1

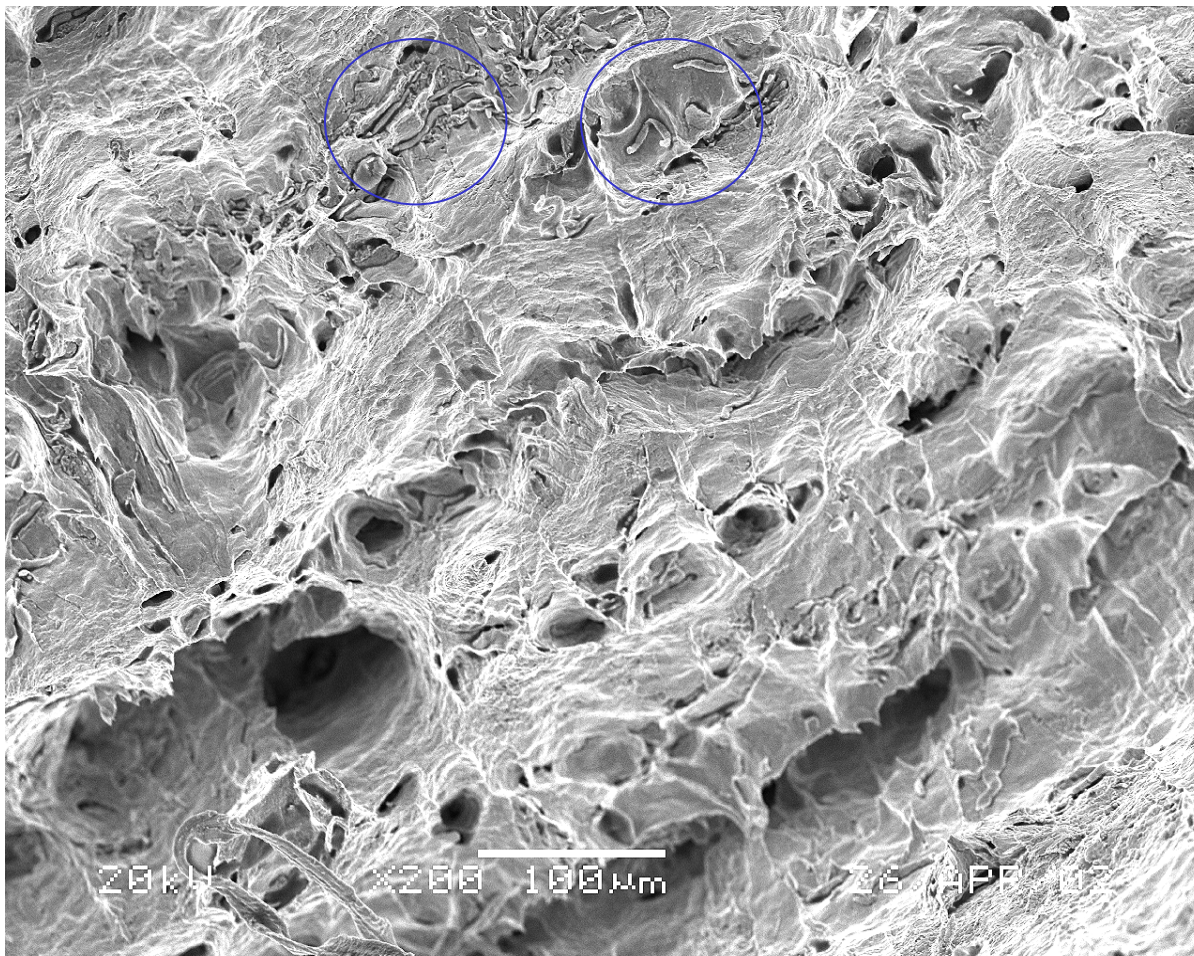


- **Magnification, 200X.**
- **Closer examination of dimpled fracture face.**
- **Expect fractured inclusions at bottoms of dimples.**





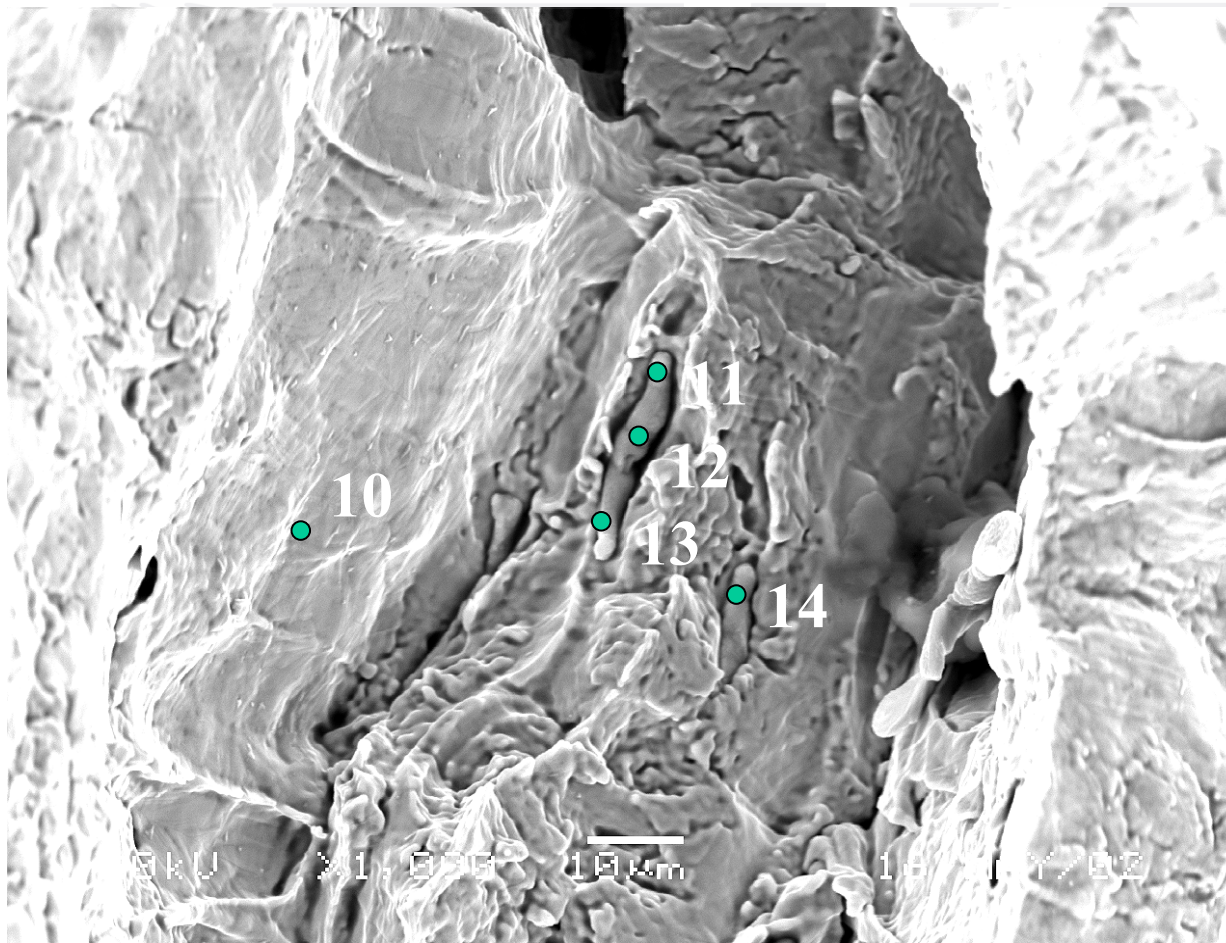
## Fracture Surface 2B-1



- **Magnification, 200X.**
- **Large void chains visible, with ductile fracture interconnecting shear walls.**
- **Elongated inclusions circled.**



## Fracture Surface 2B-1

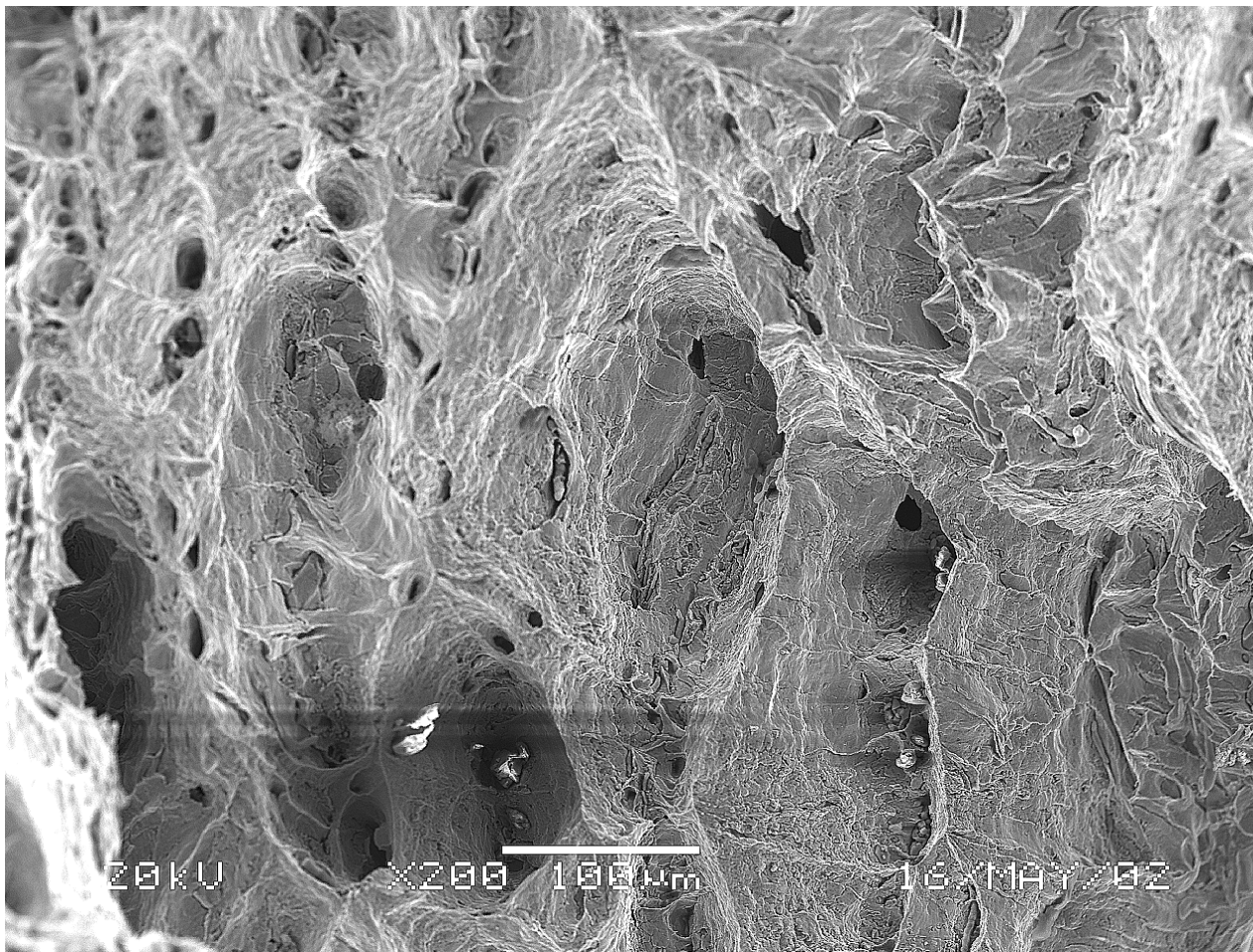


- **Magnification, 1000X (pts 1-9 not shown).**
- **Highly ductile surface; MVC mechanism.**
- **“Transverse inclusions” populated in arrays throughout.**





## Fracture Surface 2B-1

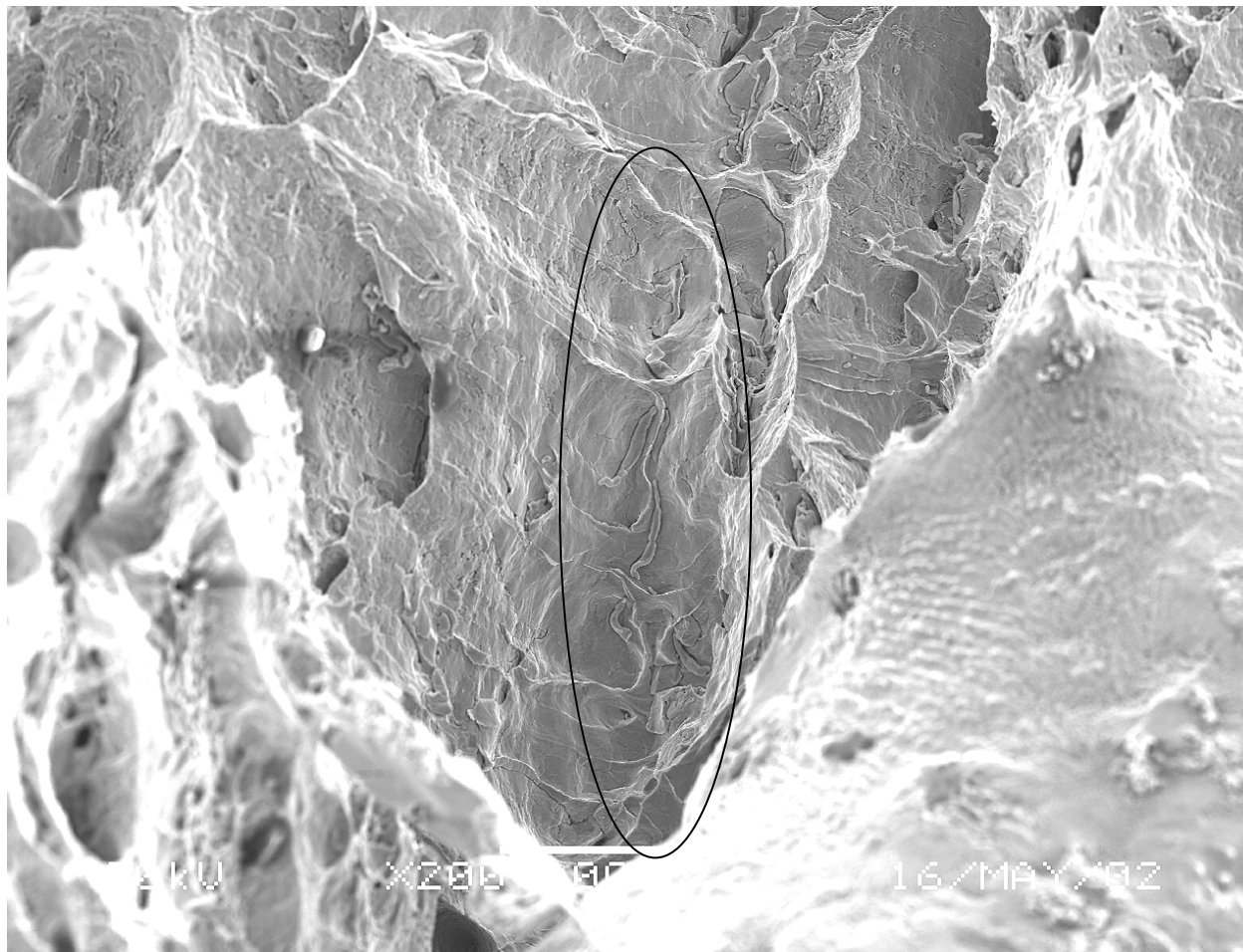


- **Magnification, 200X.**
- **Smaller spheroidal voids connect larger voids.**
- **In other materials higher in [C] and alloying elements, smaller voids caused by carbides.**





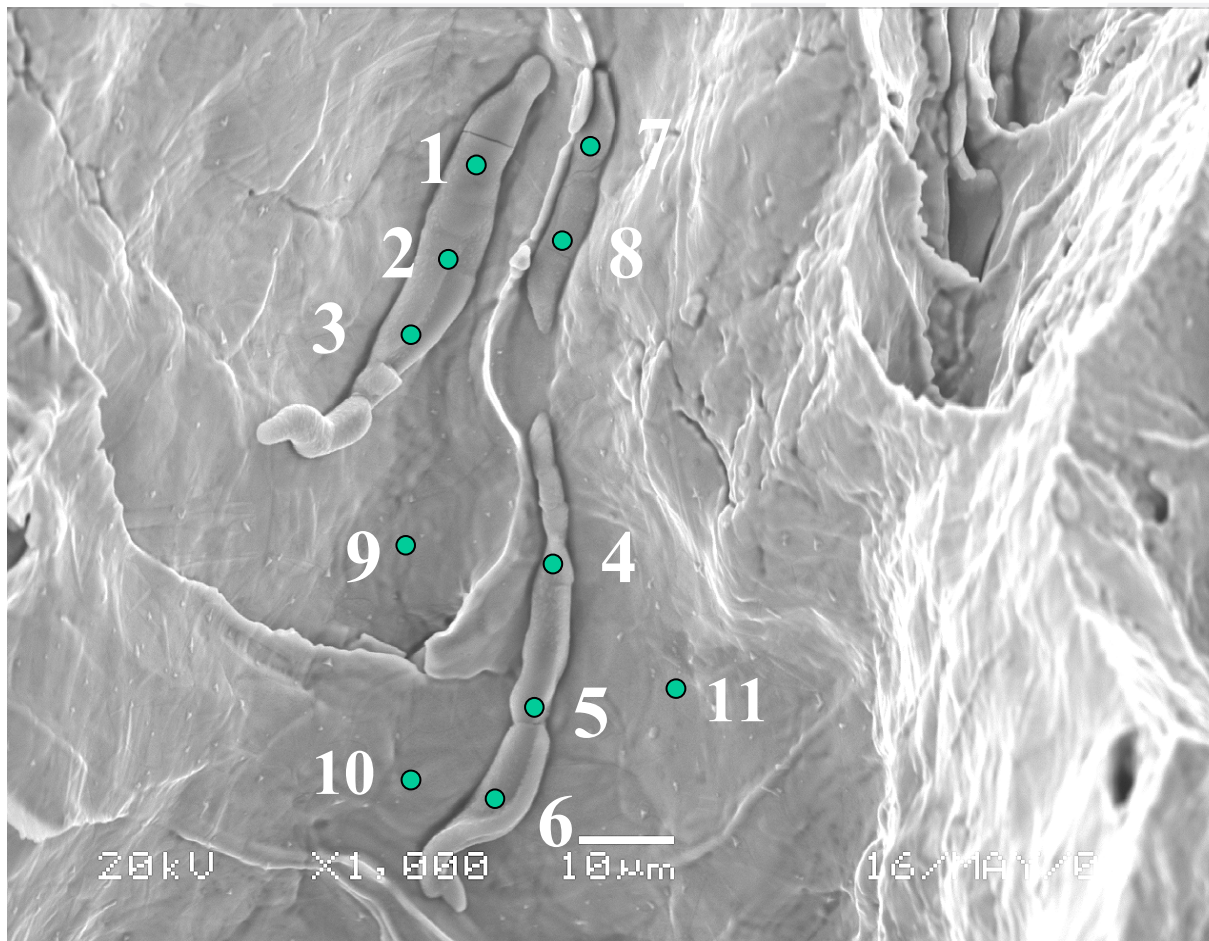
## Fracture Surface 2B-1



- **Magnification, 200X.**
- **Elongated array of inclusions identified.**



## Fracture Surface 2B-1

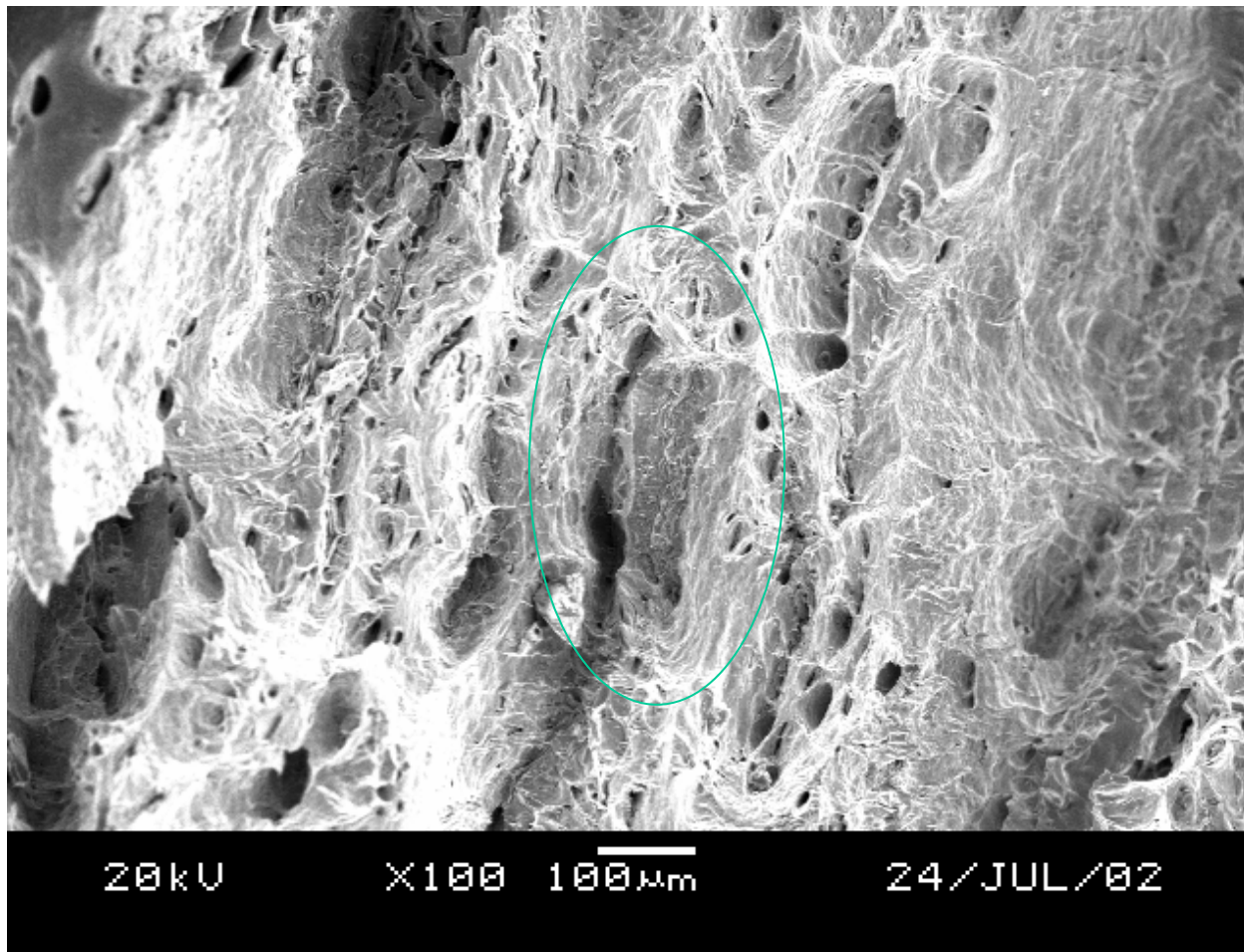


- **Magnification, 1000X.**
- **Elongated array of parallel inclusions seen, with inclusion necking and brittle fracture.**
- **Inclusion/Matrix cohesion caused some inclusion bending at fracture.**





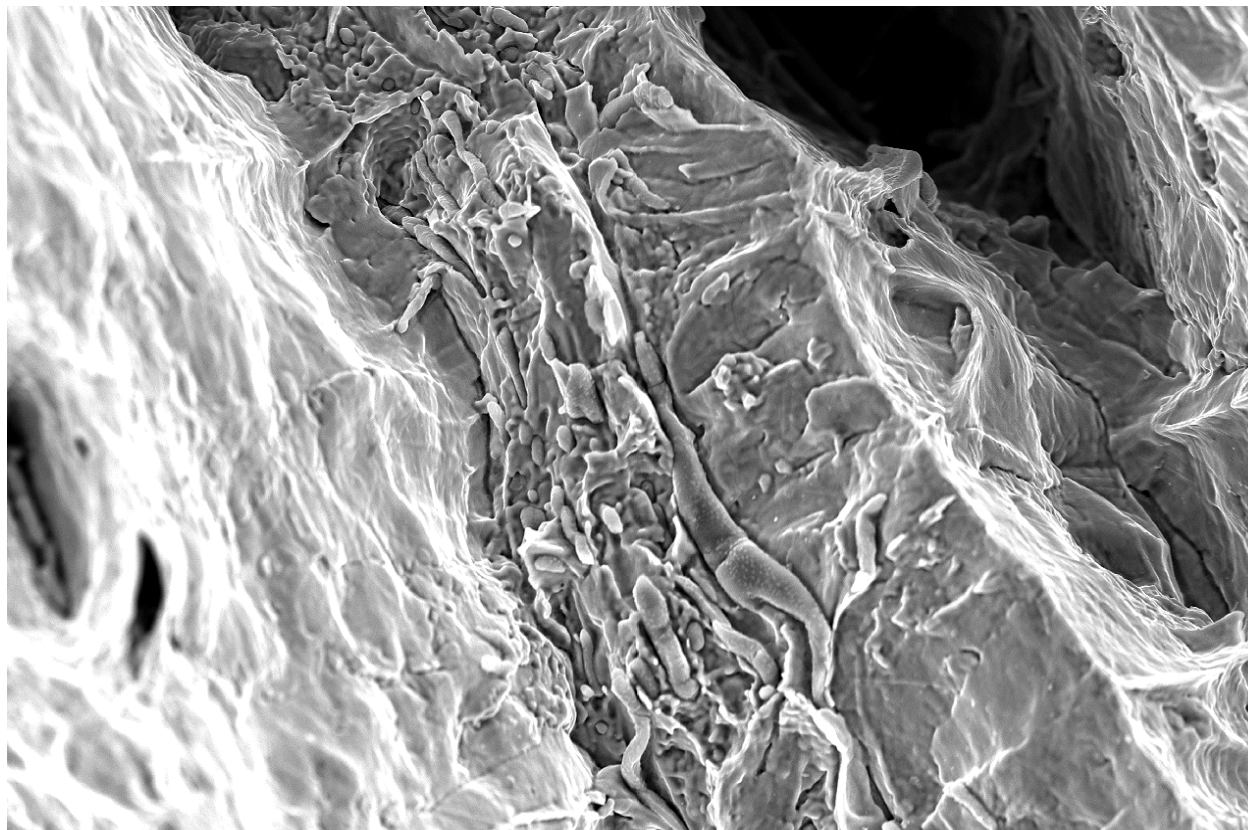
## Fracture Surface 2B-1



- Magnification, 100X.
- Large cluster of elongated inclusions noticed near a fairly long, deep crack.
- Nearby, equiaxed voids populate the matrix.



## Fracture Surface 2B-1



20kV

X750

20µm

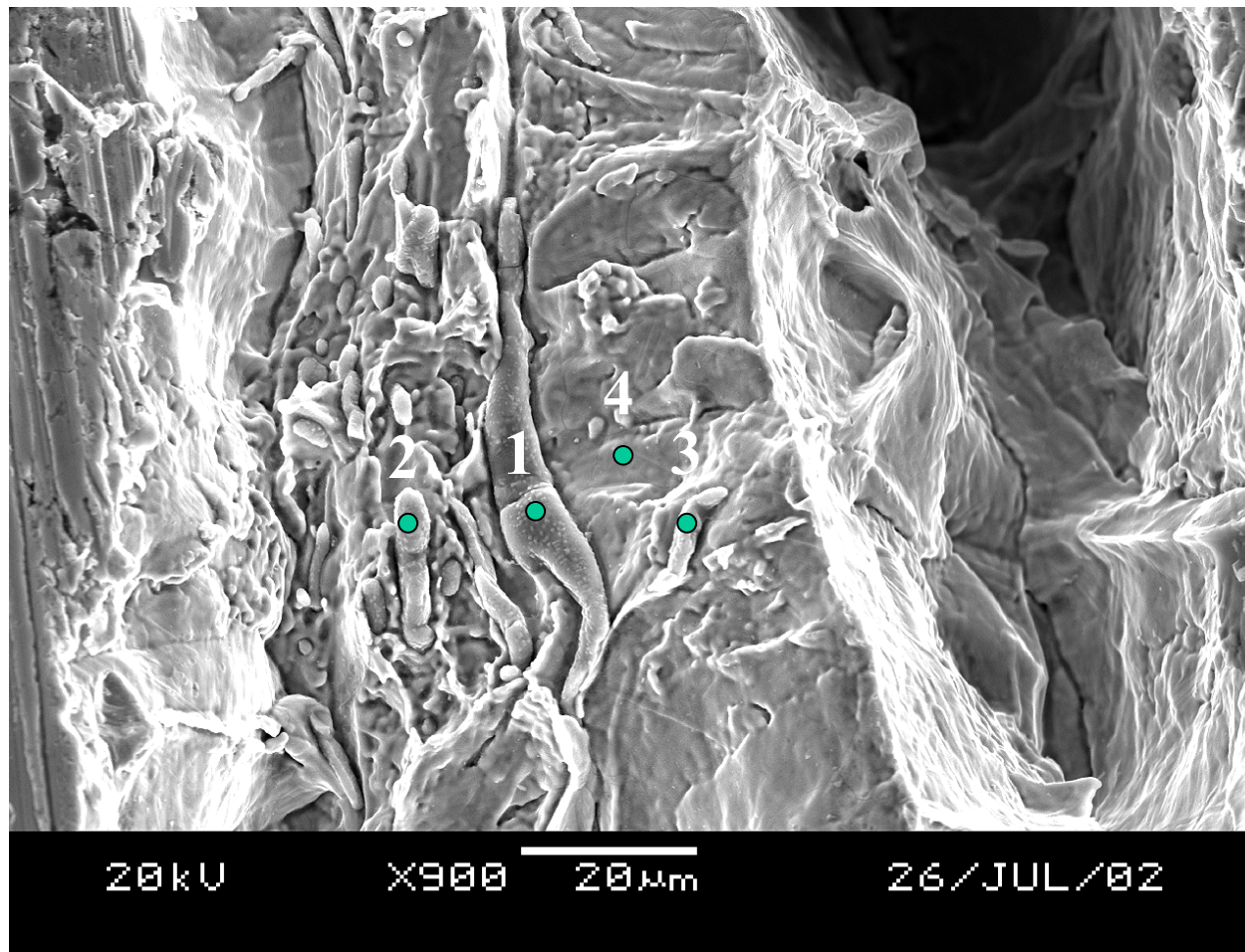
25/JUL/02

- Magnification, 650X.
- Successive steps of grinding the fracture surface to remove surrounding matrix obstructing EDS analysis yielded successively better results.





## Fracture Surface 2B-1



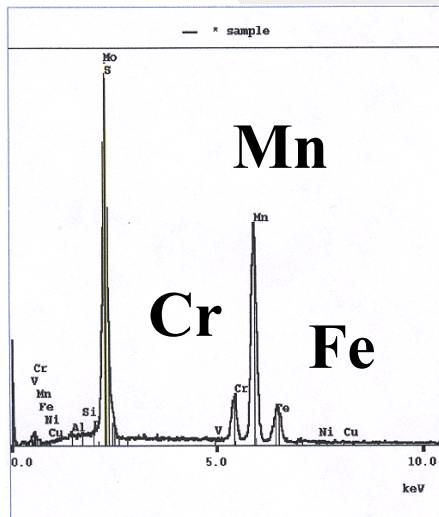
- Magnification, 900X.
- At this step in grinding the surface, EDS analysis was possible.
- Points 1, 2& 3 appear to be MnS inclusions, point 4 appears to be matrix material.





# Fracture Surface 2B-1

**S**

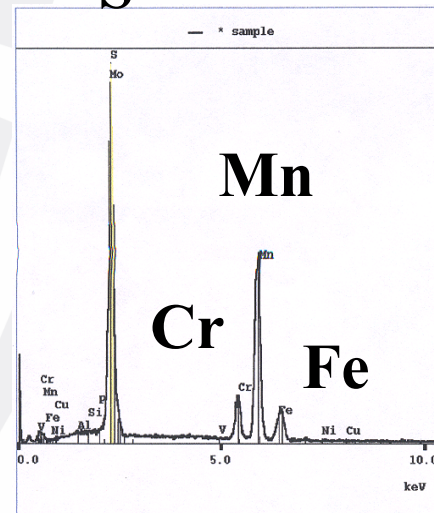


- Magnification, Point 2, 900X.

- Element (wt%/at%):

• Fe	4.95	/	4.04
• S	27.31	/	38.87
• P	0.13	/	0.19
• Mn	57.53	/	47.78
• Si	0.07	/	0.11
• Ni	0.0	/	0.0
• Cr	9.52	/	8.35
• Mo	0.0	/	0.0
• Cu	0.06	/	0.04
• Al	0.29	/	0.49
• V	0.14	/	0.12

**S**

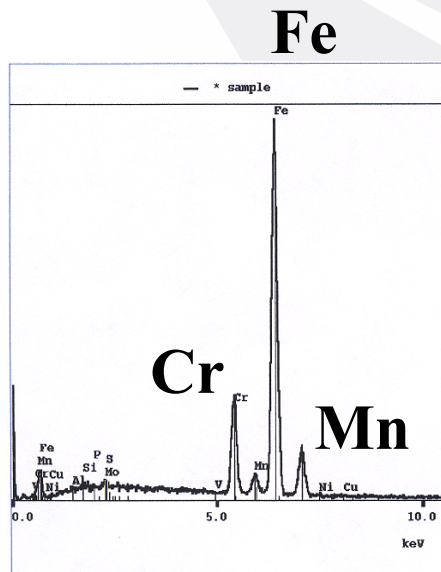


- Magnification, Point 1, 900X.

- Element (wt%/at%):

• Fe	4.49	/	3.59
• S	31.18	/	43.40
• P	0.25	/	0.35
• Mn	53.66	/	43.57
• Si	0.07	/	0.11
• Ni	0.0	/	0.0
• Cr	10.24	/	8.79
• Mo	0.0	/	0.0
• Cu	0.0	/	0.0
• Al	0.11	/	0.19
• V	0.0	/	0.0

## Fracture Surface 2B-1



- Magnification,  
Point 4, 900X.

- Element  
(wt%/at%):

- Fe 84.77 / 83.32
- S 0.23 / 0.39
- P 0.21 / 0.37
- Mn 2.55 / 2.55
- Si 0.19 / 0.39
- Ni 0.59 / 0.55
- Cr 10.92 / 11.52
- Mo 0.09 / 0.05
- Cu 0.0 / 0.0
- Al 0.40 / 0.82
- V 0.05 / 0.05

Similar to  
Point 1 and  
Point 2

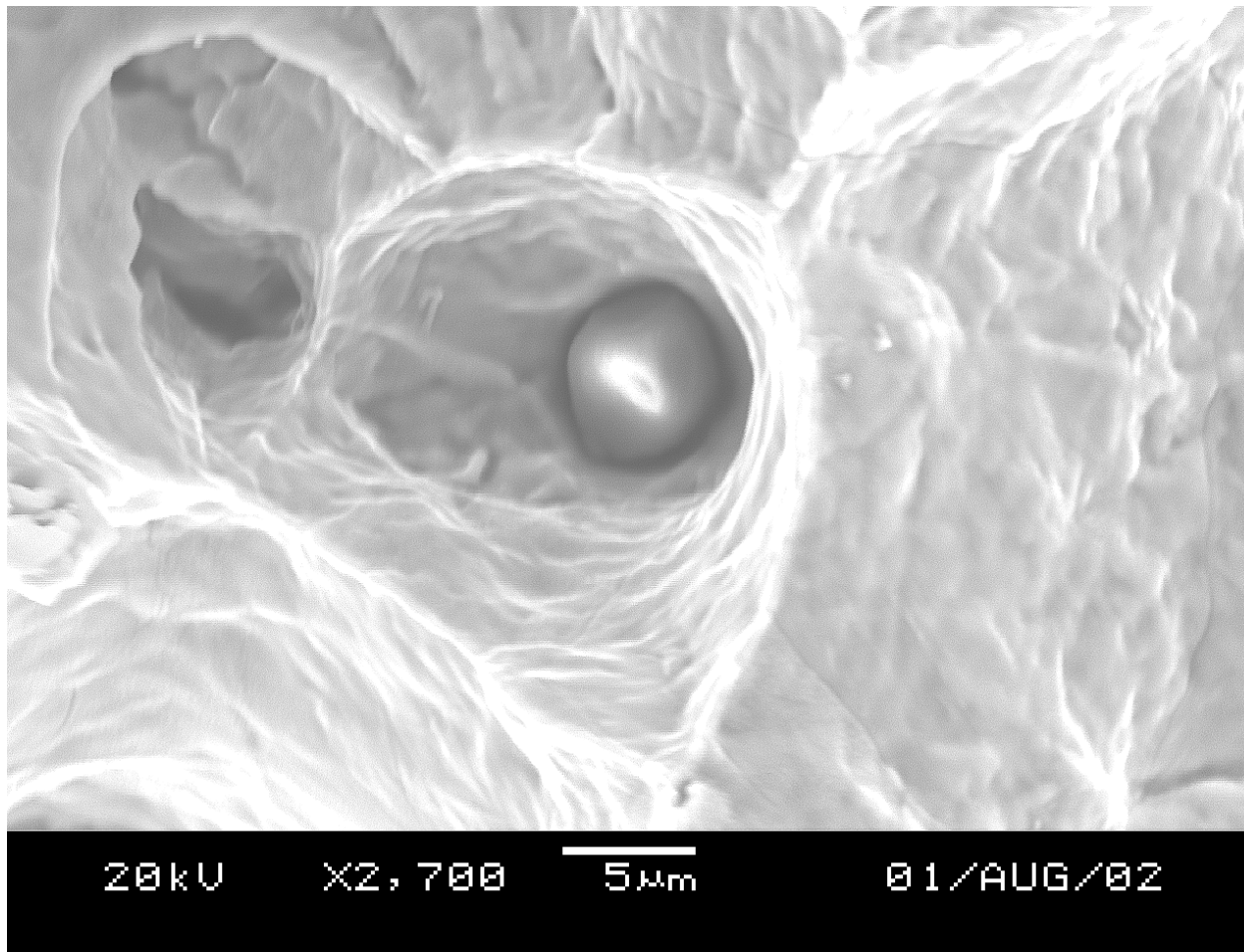
- Magnification,  
Point 3, 900X.

- Element  
(wt%/at%):

- Fe 8.64 / 7.09
- S 26.95 / 38.48
- P 0.19 / 0.29
- Mn 53.49 / 44.59
- Si 0.10 / 0.15
- Ni 0.36 / 0.28
- Cr 10.19 / 8.97
- Mo 0.0 / 0.0
- Cu 0.0 / 0.0
- Al 0.08 / 0.14
- V 0.0 / 0.0



## Fracture Surface 2B-1

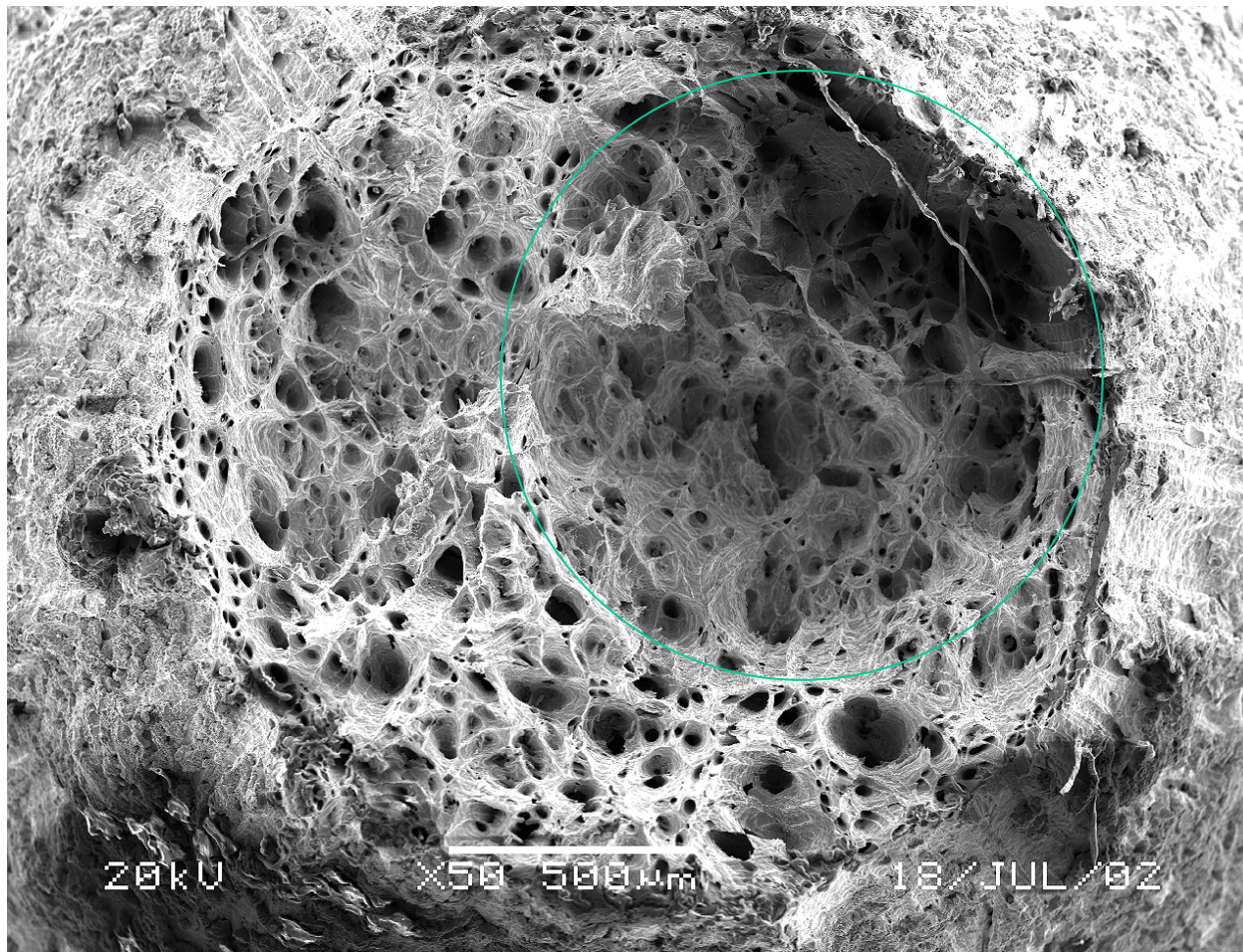


- **Magnification, 2700X.**
- **Likely inclusion particle found, but still too deep to analyze accurately.**
- **Likely the head of a necked “longitudinal inclusion” oriented along the strain axis.**





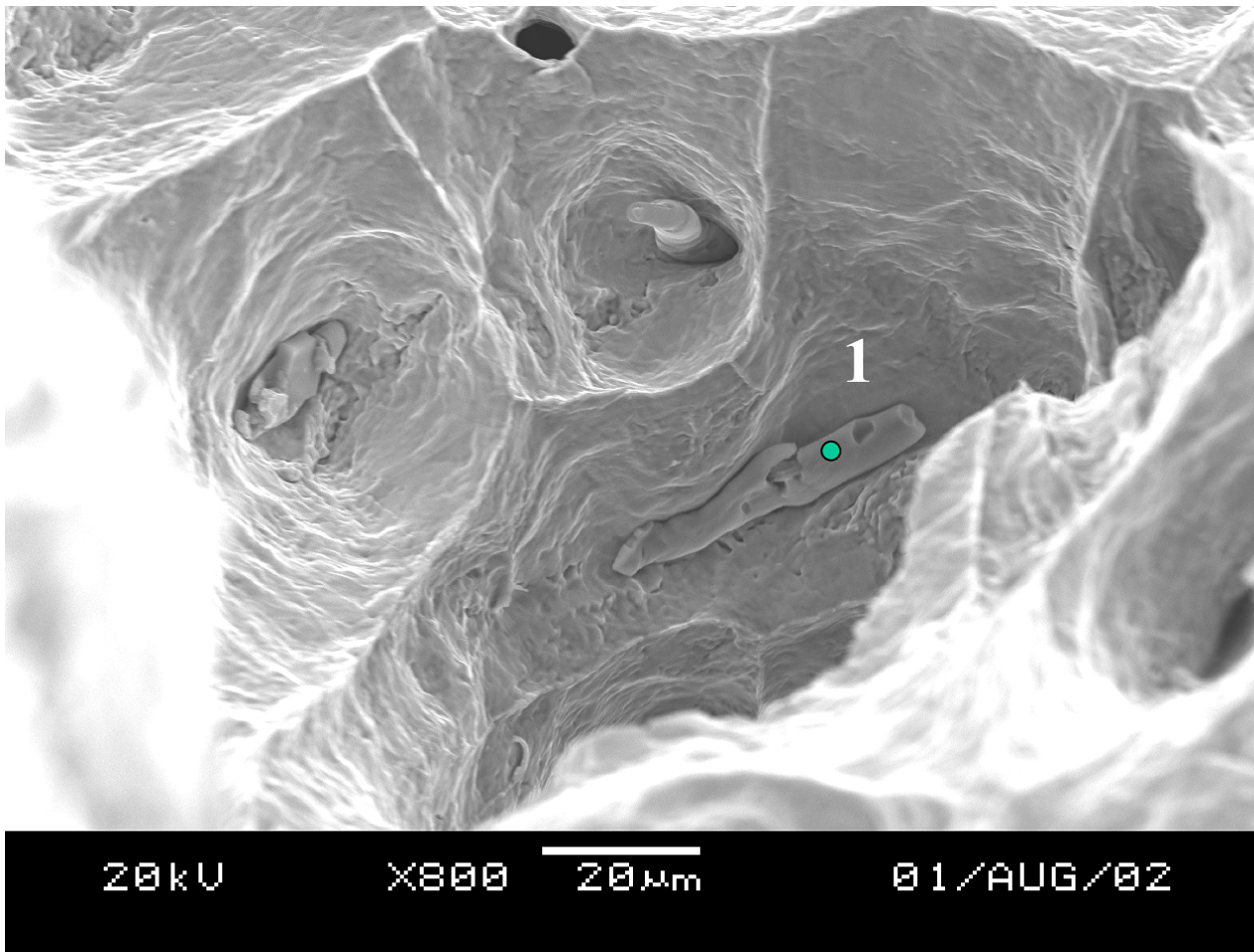
## Fracture Surface 2B-2



- **Magnification, 50X.**
- **Ductile specimen at 2150 °F.**
- **Fracture surface is more ductile than 2B-1 sample.**
- **Variable surface height due to crack propagation character.**



## Fracture Surface 2B-2

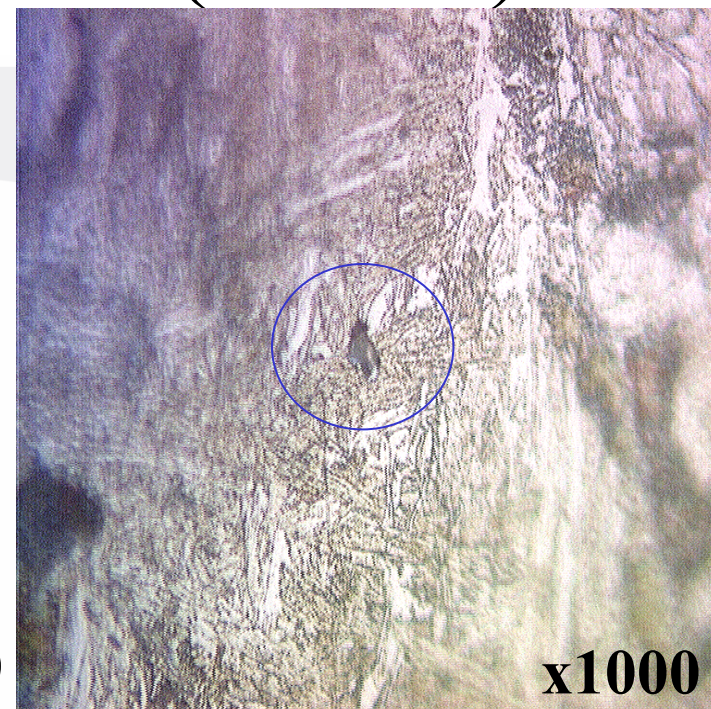
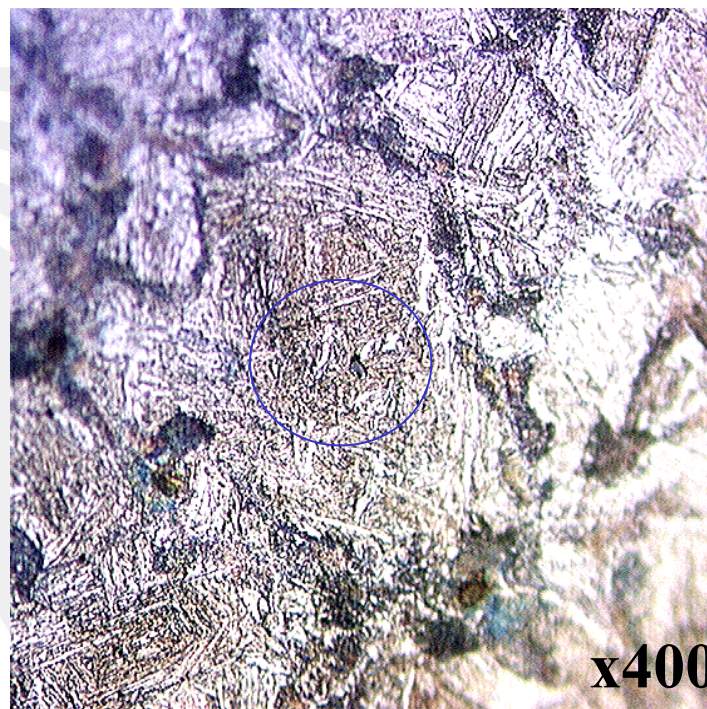
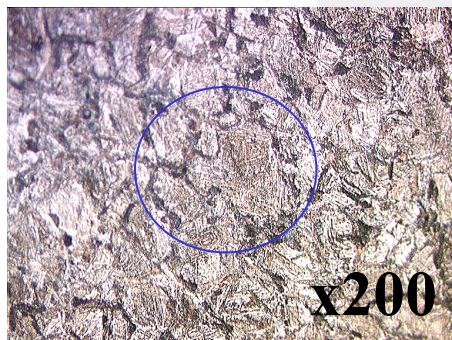
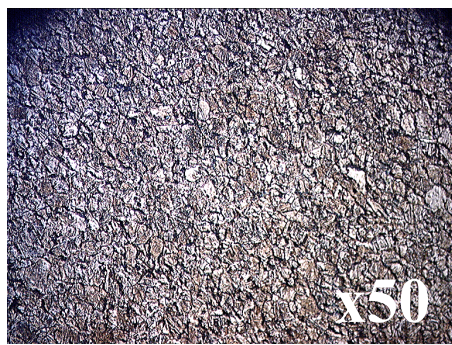


- Magnification, 800X.
- EDS analysis inconclusive.
- Possible elongated inclusion normal to principle strain axis visible.
- Typical cause of partial “transverse” behavior.





# #1 As-Received A Center (Low S)

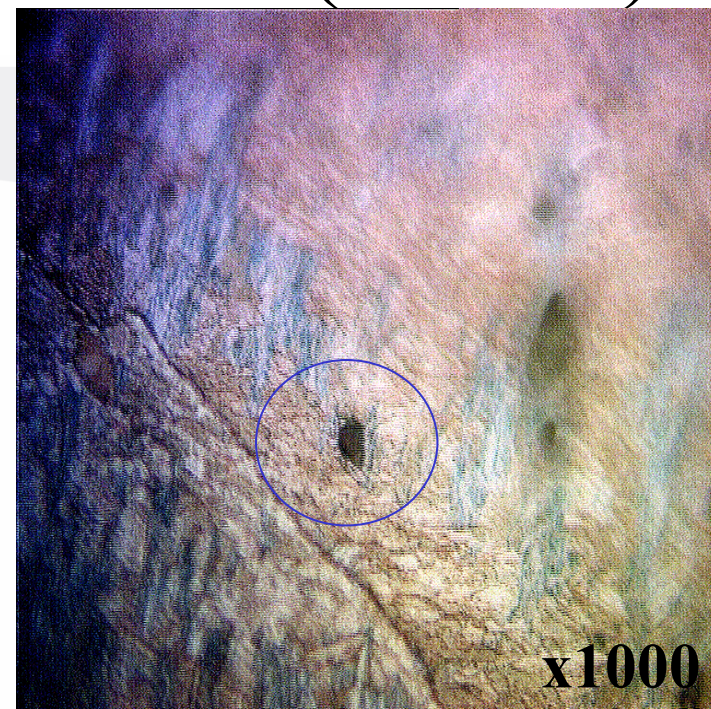
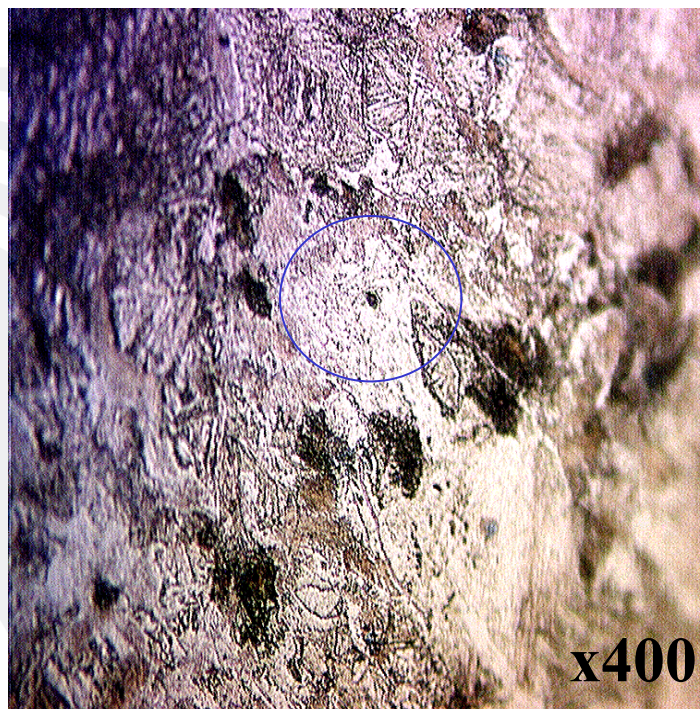
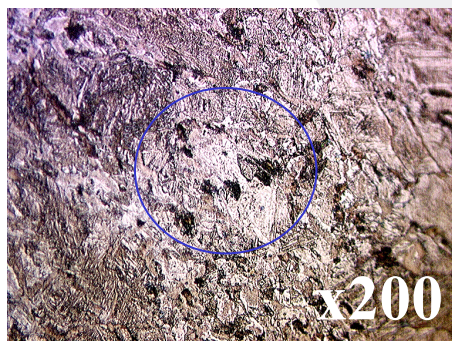
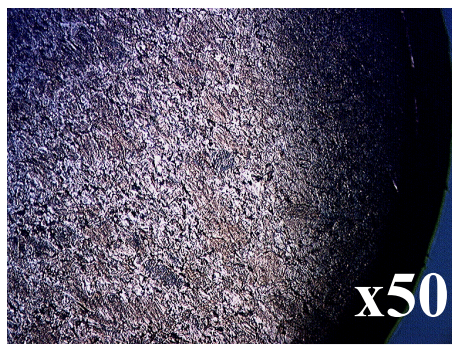


- Precipitates, presumably tempered carbides, formed at prior  $\gamma$ -Fe G.B.s
- Lower S content, expect fewer sulfide inclusions, almost no stringers.
- Equiaxed inclusions forming near center of some prior  $\gamma$ -Fe grains.





# #1 As-Received B Mid Radius (Low S)

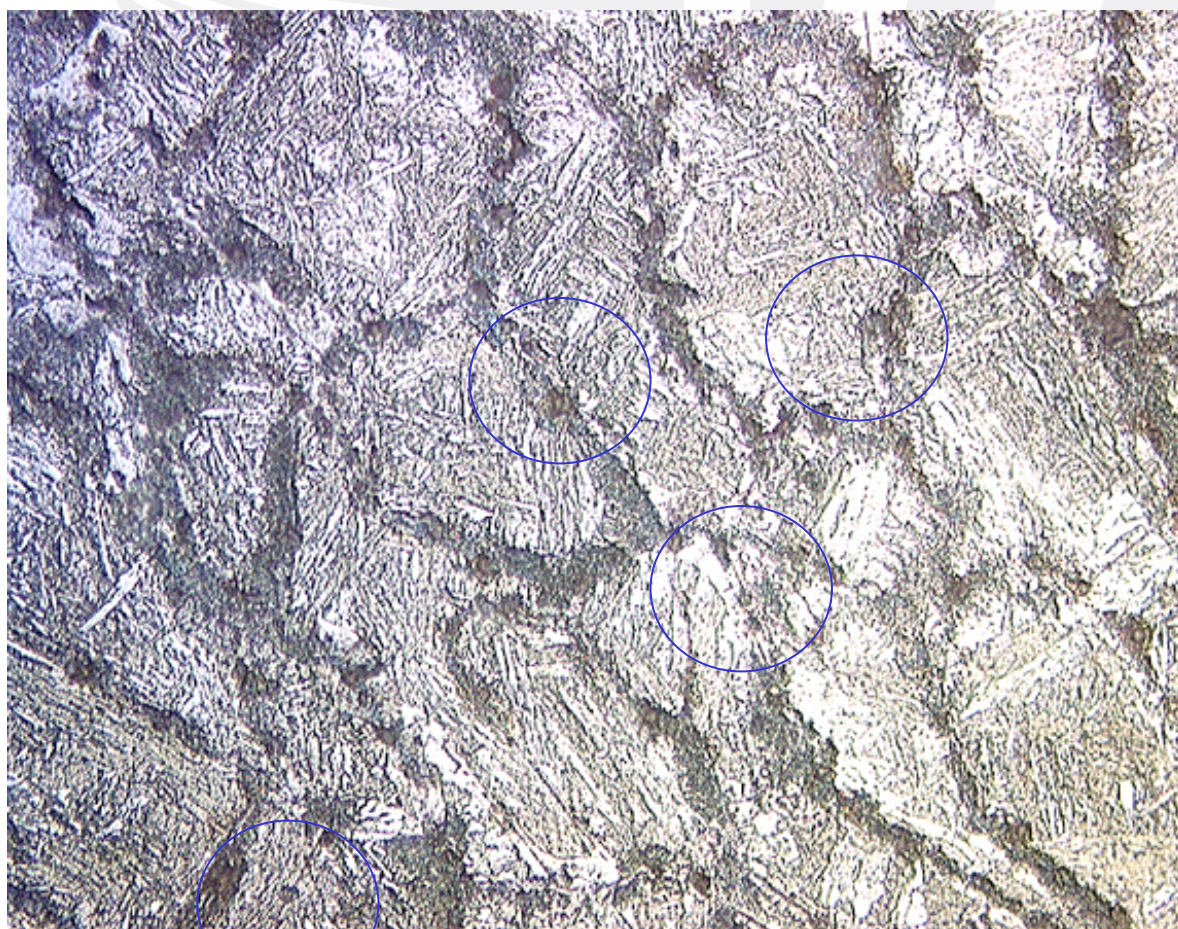


- Precipitates, presumably tempered carbides, formed at prior  $\gamma$ -Fe G.B.s
- Lower S content, expect fewer sulfide inclusions, almost no stringers.
- Equiaxed inclusions forming near center of some prior  $\gamma$ -Fe grains.





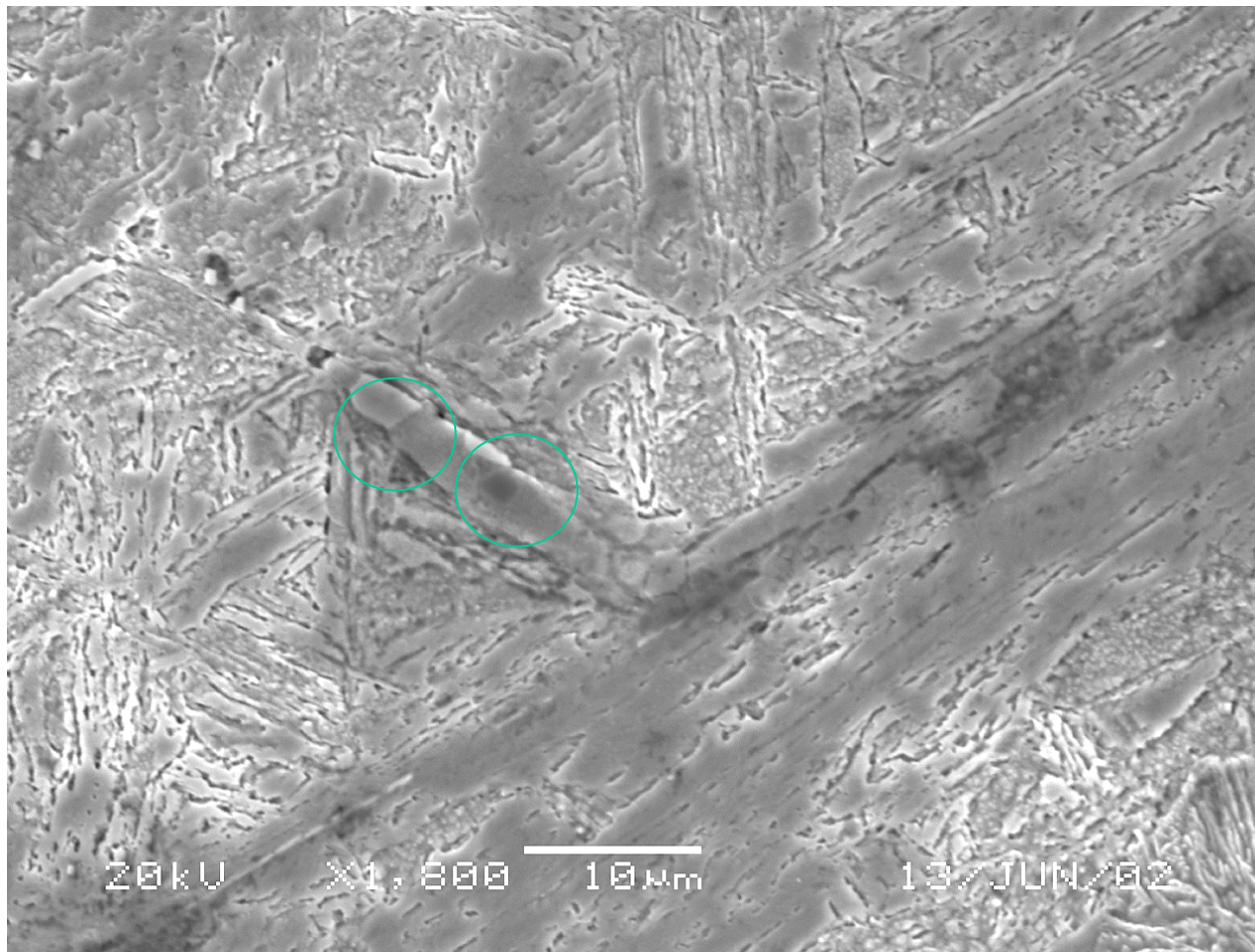
## #2 As-Received Sample B-4



- Magnification, 400X.
- Equiaxed MnS-type inclusions found in both grain centers and at G.B.s
- Assumed Tempered Carbides at G.B.s
- Cut from B-4 test sample



# B4 As Received – 1

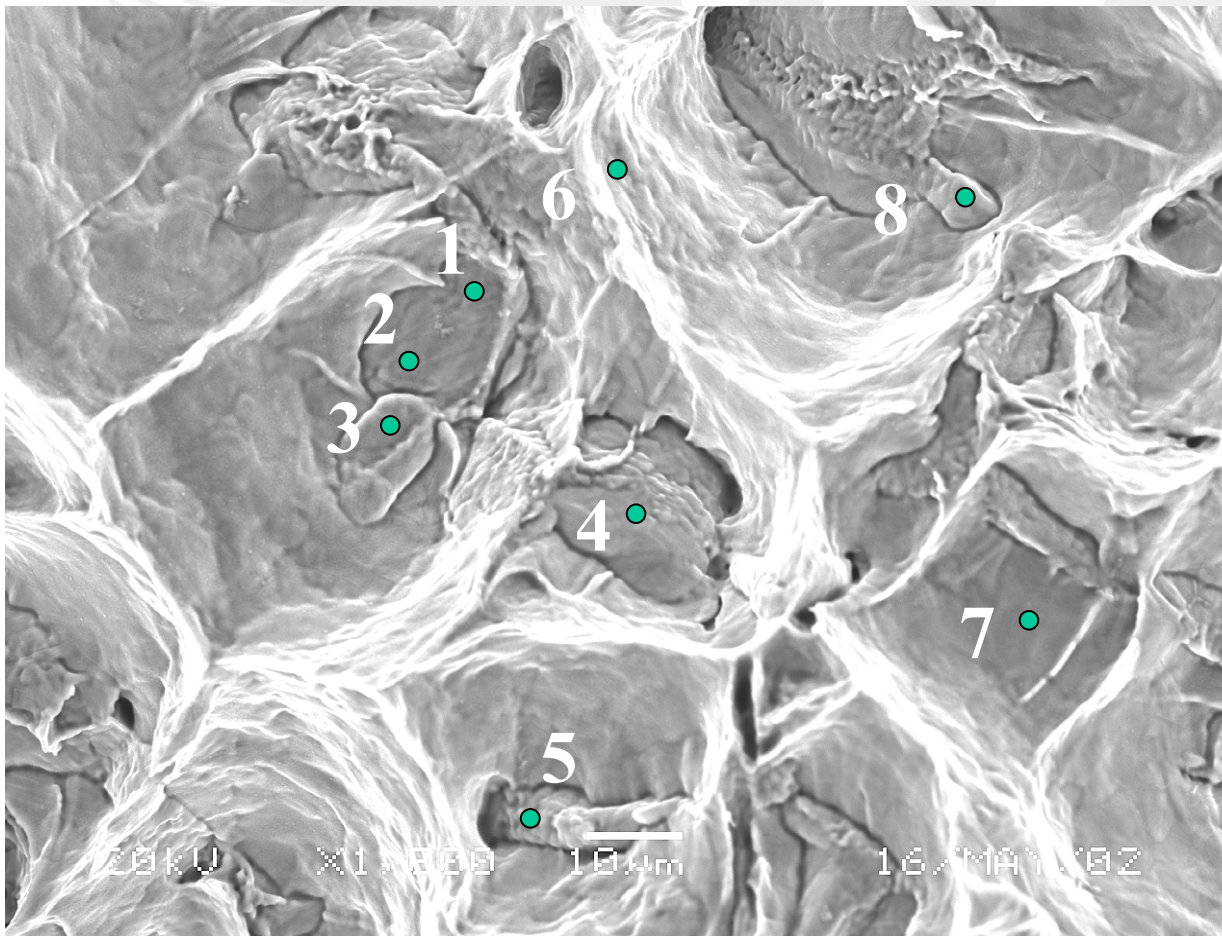


- **Magnification, 1000X.**
- **Incomplete inclusion necking / brittle fracture now observable.**





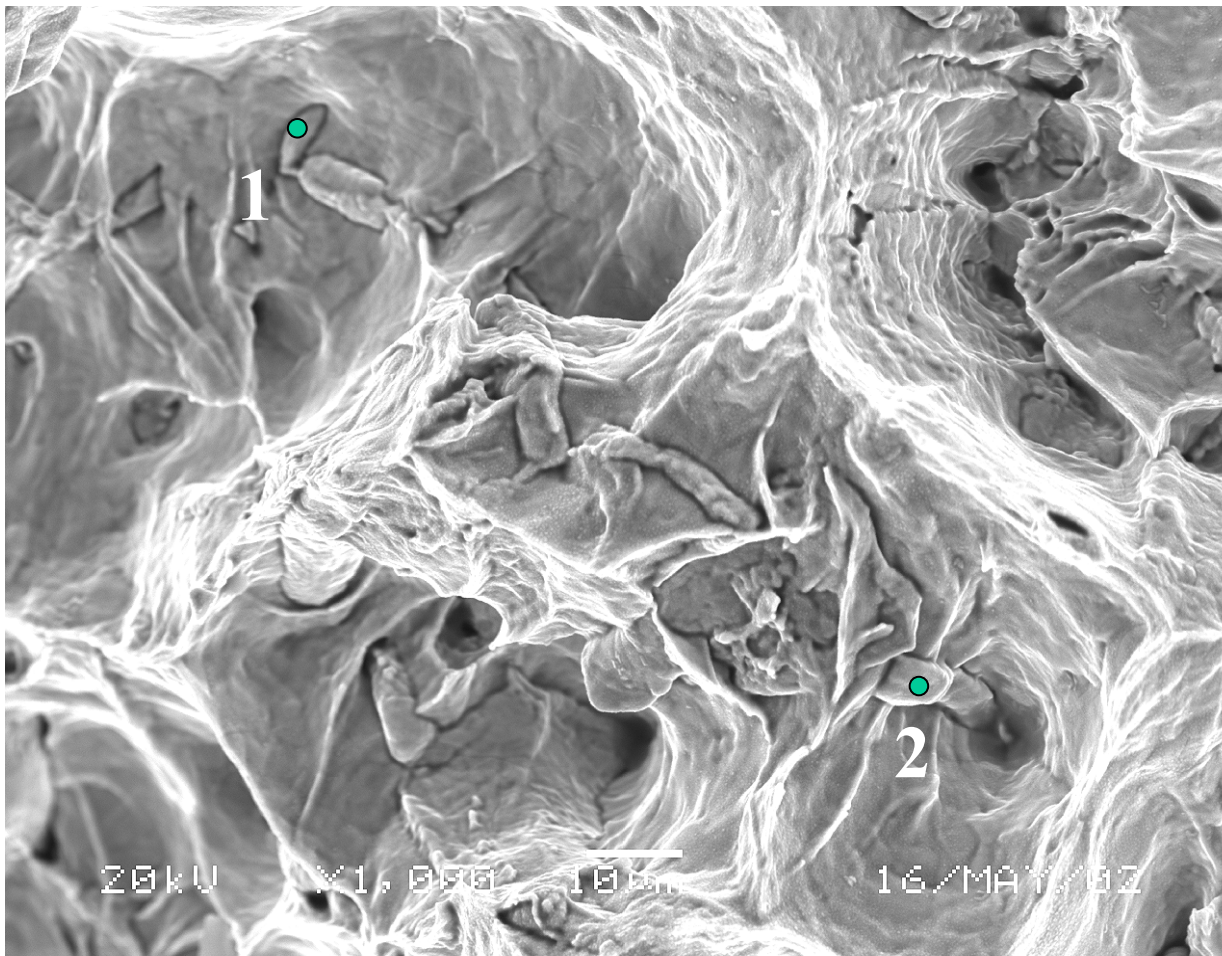
## Fracture Surface B-4



- **Magnification, 1000X.**
- **No inclusions identified; nominal steel chemistry results at each scan point.**



## Fracture Surface B-4



- **Magnification, 1000x.**
- **Low nominal S, hard to identify inclusions.**
- **Nominal steel chemistry found at each scan point.**



# Conclusions

- The high sulfur batch 1 steel was seen to exhibit generally lower %RA and lower TFS values than the low sulfur batch 2 steel for the hot ductility tests.
  - This was assumed to be true primarily because the greater sulfur level allowed for inclusions in the steel of greater size and greater aspect ratio due to rolling to the as-received condition.
  - Elongated inclusions were seen to be especially deleterious to ductility, with inclusions oriented transverse to the principle strain direction being more deleterious than inclusions oriented parallel to or longitudinal with the principle strain direction.





# Conclusions

- The Center material was seen to exhibit generally lower %RA and lower TFS values than the Mid-Radius material.
  - This was assumed to be true primarily because segregation during casting of the steel within interdendritic locales was especially great for the Center material.
  - Therefore, inclusions were more likely to cluster in this region, promoting the formation of so-called “supervoids” and further aiding microvoid coalescence.



# Conclusions

- EDS analysis indicated that many of the MnS inclusions may have had Fe or Cr in solid solution.
  - “Chromium hardening” from solid solution strengthening was noted as likely hardening MnS inclusions significantly. The increase in MnS hardness was said to increase the likelihood of inclusion-matrix decohesion by locally resisting applied strain and raising the local stress level at the interface.
  - Also, the presence of dissolved Fe in MnS inclusions may indicate that FeS is present in the inclusions. FeS is known to have a much lower melting temperature than MnS, and therefore this low melting constituent was said likely to weaken the inclusions and therefore the steel at elevated temperatures approaching 988 °C, or about 1810 °F.



# Conclusions

- 1800 °F was the temperature at which all of the samples began to exhibit increasing ductility with increasing temperature. Below this temperature down to 1500 °F the ductility for all of the samples was seen to be about constant. However, above 1800 °F, some of the samples exhibited unexpected loss of ductility.
  - The level of the loss of ductility was such that %RA and TFS values in these samples approached the constant %RA and TFS values seen at or below 1800 °F. Thus it was seen that the increase in ductility of the steel with increasing temperature was negated for these samples. No further correlation was able to be made between the occurrence of ductility loss and fracture temperature, source location in the cast steel or nominal steel sulfur content level.
  - However, plots of average values of %RA and TFS for material from the same groups (1A, 2A, 3A and 1B, 2B and 3B) reduced some of the variability of the data. This suggests that more testing may be required to achieve data of statistical significance and validate the behaviors herein described.





# Conclusions

- Diffusion of Mn into inclusions at elevated temperatures should compete with entrapment of Fe at inclusions for steel with fast cooling rates. The more stable MnS inclusion should form preferentially with Fe dissolved in solid solution.
- Inclusion orientation was not isolated for these tests. It is likely that the loss of ductility in many of the samples was likely due to variability in inclusion orientation in the test specimens.
- Oxidation of the specimens was not prevented for all of the samples tested. Either the IBT at about 2200 °F or vacancy nucleation and injection into the sample interiors may have promoted brittle fracture of the samples. However, it is believed that these processes are negligible.
- The short soak time prior to test specimen strain to fracture was not believed to significantly affect the shape of inclusions in the steel. Therefore, globularization heat treatments at temperatures above 1150 °C as described for some steels in Chapter II were not thought to apply for the test specimens.



## Selected References

- [2] Baker, T.J., "Use of Scanning Electron Microscopy in Studying Sulphide Morphology on Fracture Surfaces," Proceedings of an International Symposium on Sulfide Inclusions in Steel, pp. 135-157, American Society for Metals, Port Chester, New York, November 1974.
- [12] Chawla, K.K., Composite Materials Science and Engineering, Springer-Verlag, New York, 1997
- [19] Flemings, M.C., Kattamis, T.Z., Mehrabian, R., and Murty, Y.V., "Behavior of Sulfide Inclusions During Thermomechanical Processing of AISI 4340 Steel," Metallurgical Transactions, Vol. 8A, pp. 1275-1281, August 1977.
- [26] Garner, W.E., Chemistry of the Solid State, Butterworths Scientific Publications London, 1955.
- [32] Ignatowicz, S., Pearson, J. and Turkdogan, E.T., "The Solubility of Sulphur in Iron and Iron-Manganese," Journal of the Iron and Steel Institute, P. 349-354, August 1955.
- [37] Kiessling, R., Non-Metallic Inclusions in Steel, Part III and IV, The Metals Society, London, 1968 & 1968 –1976.

# Any Questions?







# Fractographs

- **Magnification about 5X.**
- **Batch 1: Expect to have higher S, P, Si and Al; Lower Fe**
  - 1A Center
  - 1B Mid Radius
  - 2A Center
  - 2B Mid Radius
- **Batch 2: Baseline batch**
  - A Center
  - B Mid Radius

# Fractographs—Remarks

- **Increased ductility with increased temperature as expected.**
- **Unexpected brittle fracture dips across all test temperatures.**
  - Unexpected dip in %RA and  $\epsilon_f$  attributed to morphology of inclusions.
  - Directionality in macroscopic fracture surface topology interpreted as oxidation of void pipes.
- **Oxidation of fracture surface and shear lip.**
  - Excess  $O_2$  in test chamber oxidized sample; blue surfaces.
  - A few were not oxidized; silver fracture surface characteristic of  $N_2$  atmosphere properly established in test chamber.
  - Oxidation of surface assumed negligible effect on mechanical properties.

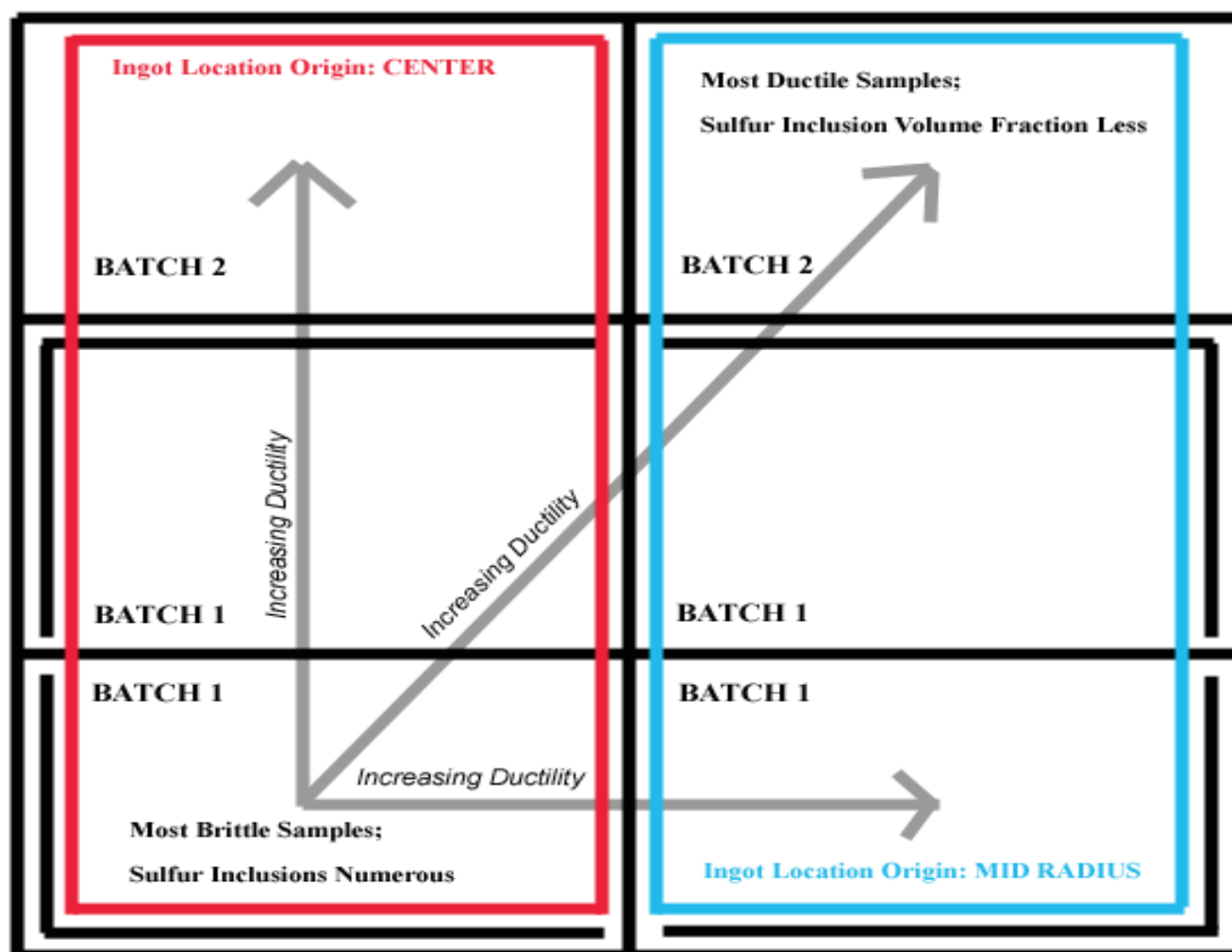
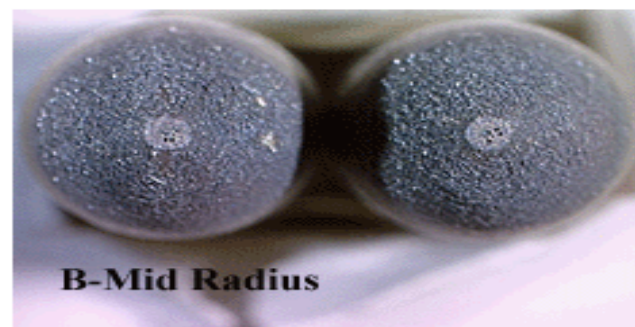
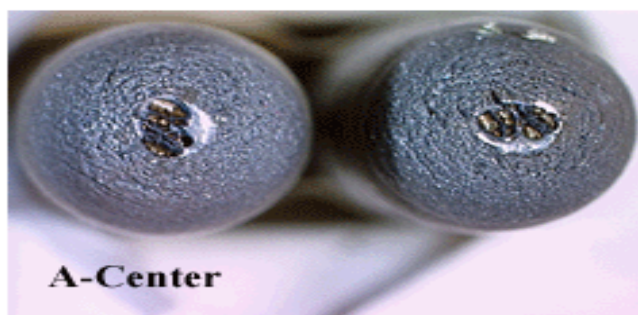


**Figure 5.16: Description of Fractograph Layout**





**1-A-Center (Bad Sample)**

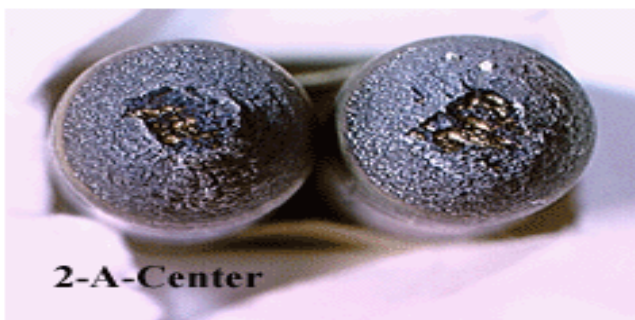
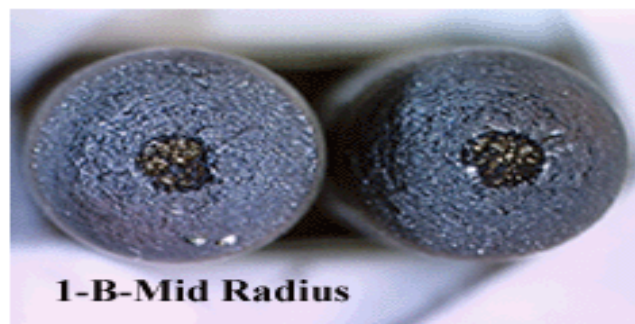


**Figure 5.1: Fractographs, Comparison of Run 1, 2200 F**

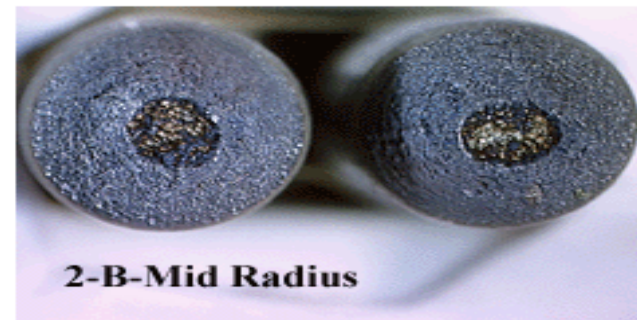
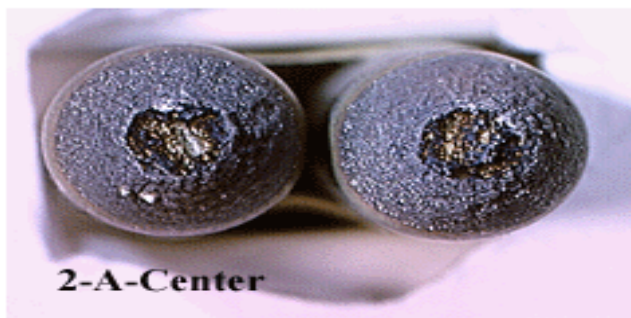
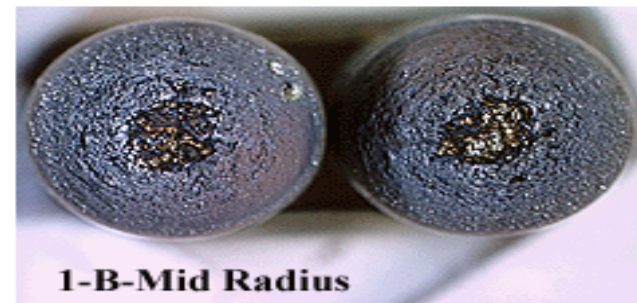
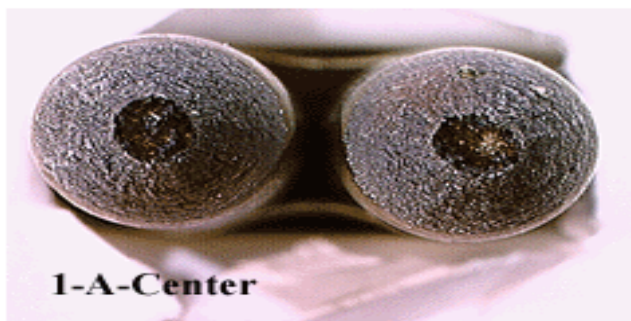
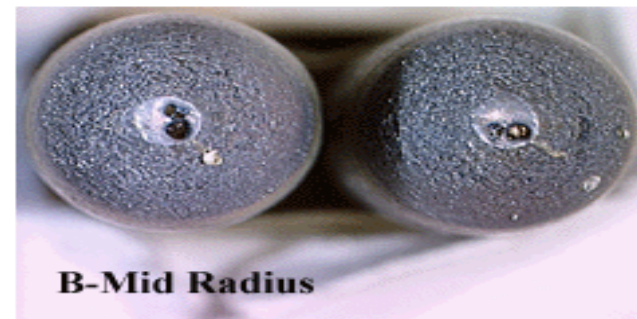
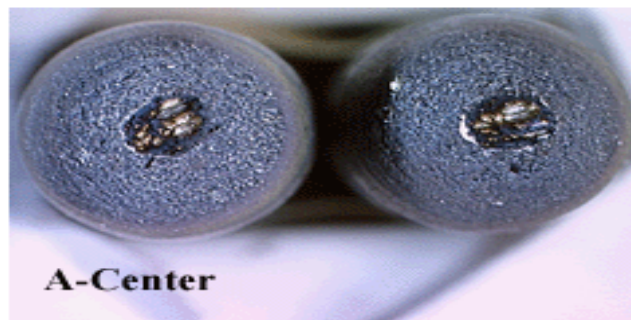


**Figure 5.2: Fractographs, Comparison of Run 2, 2150 F**



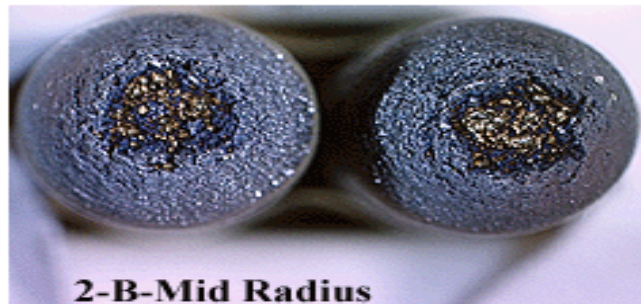
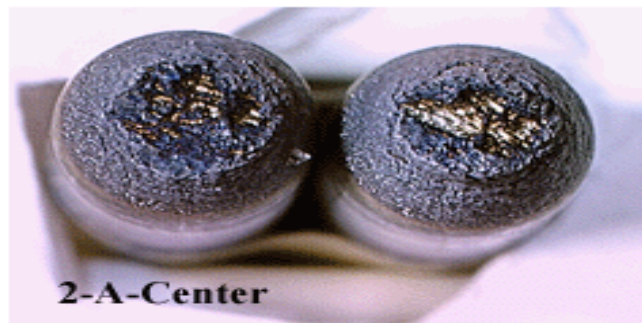
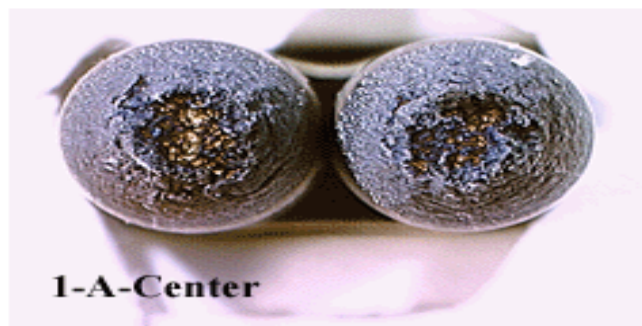
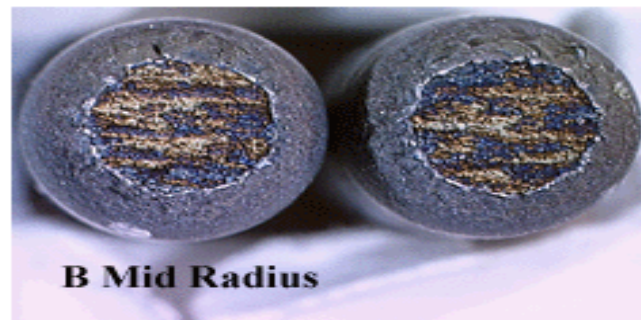
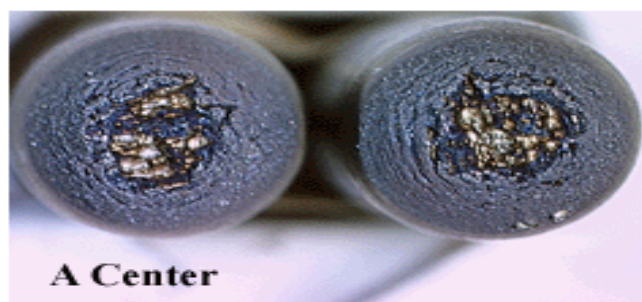


**Figure 5.4 Fractographs, Comparison of Run 4, 2050 F**



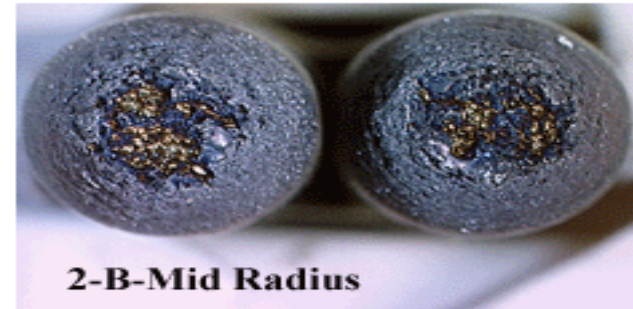
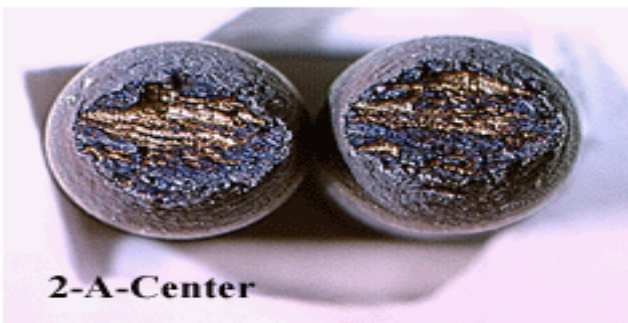
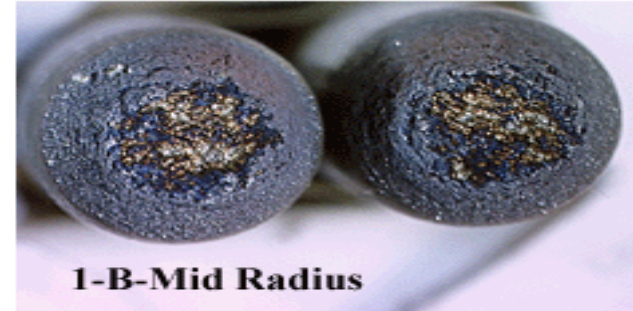
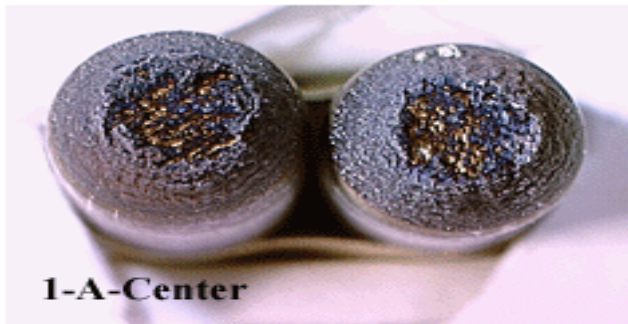
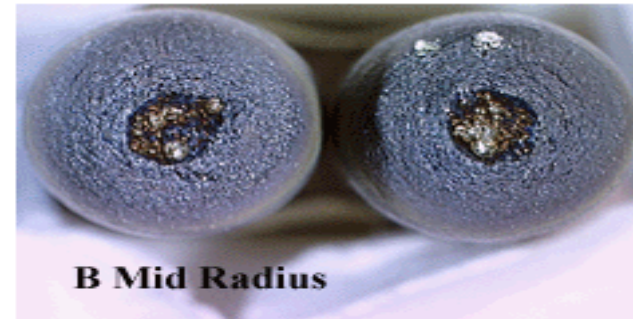
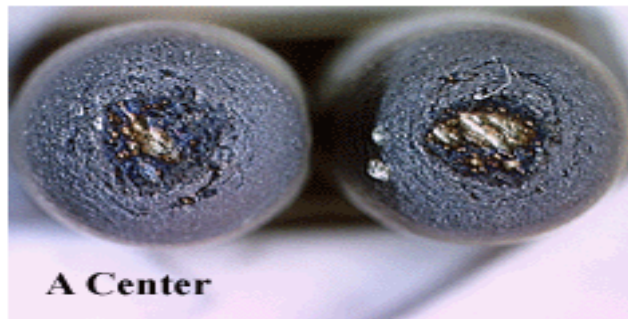


**Figure 5.5: Fractographs, Comparison of Run 5, 2000 F**

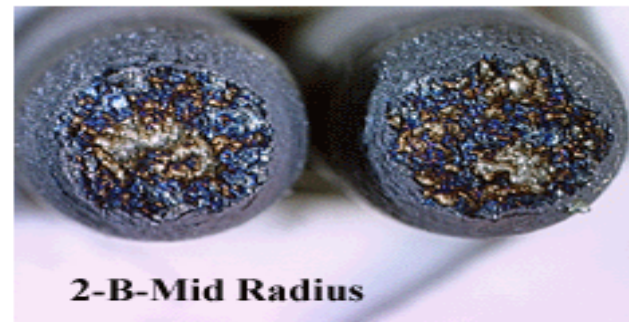
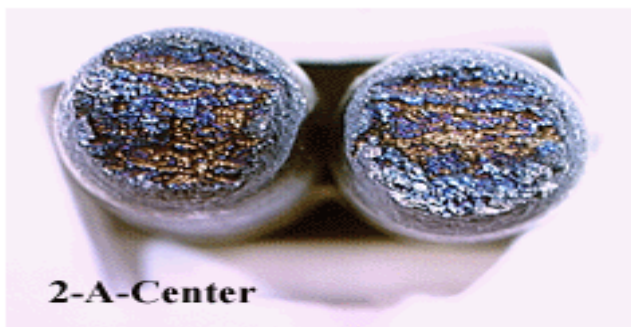
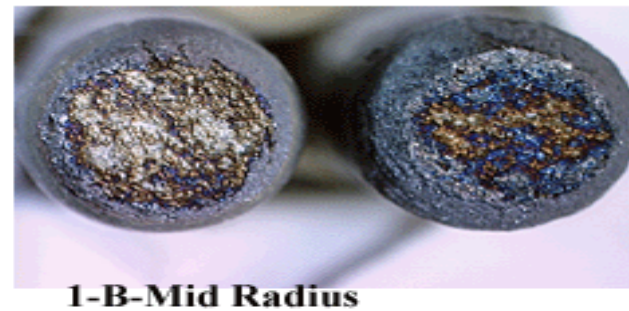
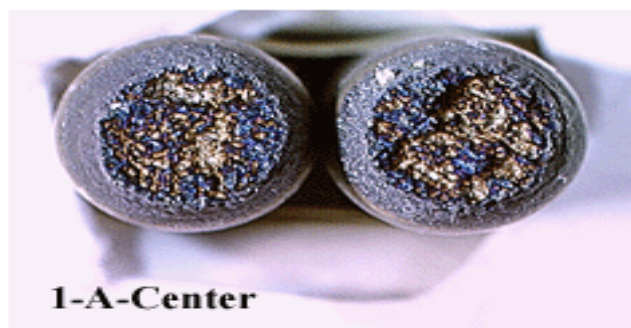
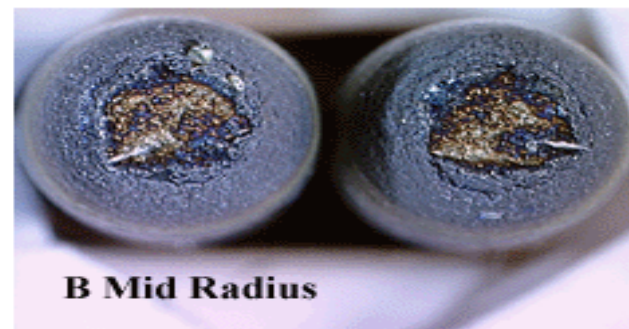
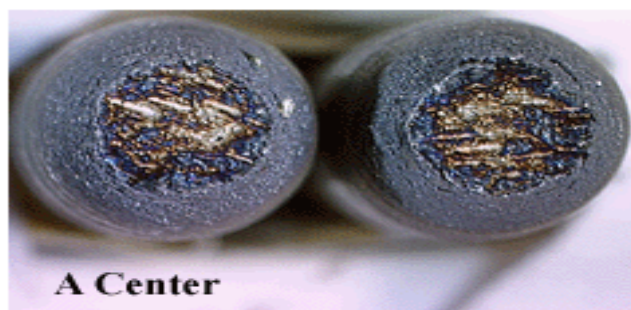
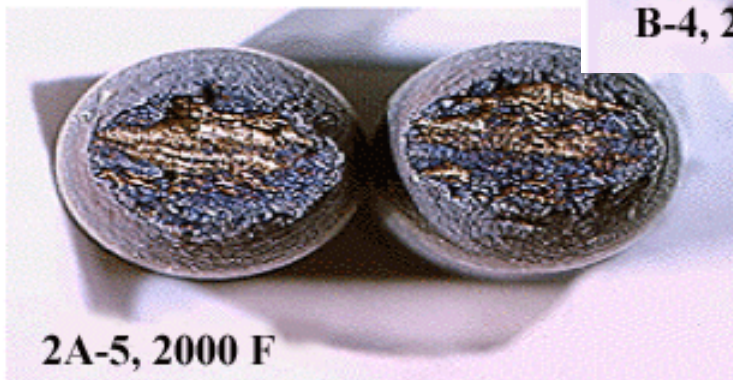
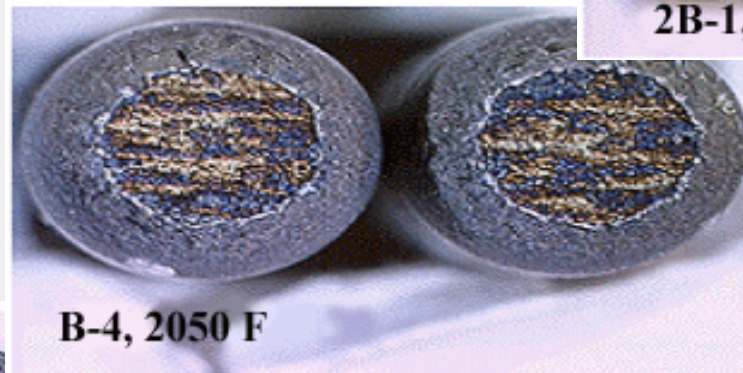
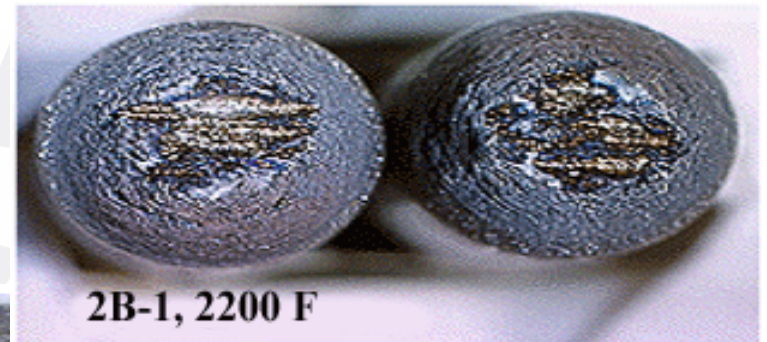


**Figure 5.11: Fractographs, Comparison of Run 11, 1700 F**



# Selection of Samples for S.E.M.

- Fractographs of fracture surfaces confirm directionality.







# Future Work

- **Additional hot workability tests over temperature range to differentiate transverse and longitudinal samples.**
- **Additional S.E.M. and E.D.S. analysis to compare and contrast transverse and longitudinal samples.**
- **Additional Light Microscopy and S.E.M. of as-received material to compare with fracture surfaces.**
- **Further identification of inclusion chemistries.**
- **Continued research of applicable literature.**



# End

